Adenosine Monophosphate-Activated Protein Kinase Inhibits Vascular Smooth Muscle Growth Associated With Vasculoproliferative Disorders

Joshua Stone

June 2013

Director of Dissertation: David A. Tulis, Ph.D., F.A.H.A.

Major Department: Department of Physiology

Abstract

Vascular growth disorders are the major contributing factor to cardiovascular disease, the leading cause of morbidity and mortality worldwide. Aberrant vascular smooth muscle cell (VSMC) growth is a primary etiology foundational to the pathophysiology of this disorder. Recent findings support growth control of VSM by the metabolic sensor adenosine monophosphate-activated protein kinase (AMPK). Therefore, the aim of this project was to test our hypothesis that AMPK has ability to inhibit VSM growth *in vivo* by reducing neointima formation in rat carotid arteries following injury and *in vitro* by promoting VSMC cytostasis in rat thoracic aorta VSMCs. Our data reveal that local or systemic pre-treatment with the AMPK agonist AICAR significantly increases VSM AMPK activity and inhibits neointima formation in rat

carotids following balloon injury. In cultured VSMCs AICAR also induced AMPK signaling and elicited cytostatic growth arrest via protein phosphatase 2A and cyclin-dependent kinase (CDK) inhibitor p21-mediated reduction of G_0/G_1 and S-phase cell cycling. Additionally, data reveal that phosphorylation of microfilament-associated vasodilator-activated serum phosphoprotein (VASP) by AMPK reduces pro-migratory events including microfilament elongation, actin strain-induced autophosphorylation of focal adhesion kinase (FAK), and focal adhesion turnover. Furthermore, AMPK reduced extracellular matrix proteolysis by matrix metalloproteinase (MMP)-9. Finally, evidence is provided for a positive signaling nexus between AMPK and cyclic adenosine monophosphate (cAMP)-dependent protein kinase (PKA) whereby these two systems cooperatively enhance the cytostatic actions of AMPK. Altogether, these results provide compelling evidence that AMPK regulates cytoskeletal/focal adhesion dynamics and cell cycle progression in an effort to reduce VSM growth in both in vitro and in vivo settings. These data increase our understanding of the role of this important metabolic regulator within VSMCs and provide support for its continued investigation in the metabolically-directed treatment of vasculoproliferative disorders.

Adenosine Monophosphate-Activated Protein Kinase Inhibits Vascular Smooth Muscle Growth Associated With Vasculoproliferative Disorders

A Dissertation

Presented To the Faculty of the Department of Physiology

East Carolina University

In Partial Fulfillment of the Requirements for the Degree

Doctorate of Philosophy in Physiology

by

Joshua D. Stone

July, 2013

Adenosine Monophosphate-Activated Protein Kinase Inhibits Vascular Smooth Muscle Growth Associated With Vasculoproliferative Disorders

by

Joshua Stone

APPROVED BY:

DIRECTOR OF DISSERTATION: _____
(David Tulis, Ph.D.)

COMMITTEE MEMBER: _____
(Stefan Clemens, Ph.D.)

COMMITTEE MEMBER: _____
(Christopher Geyer, Ph.D.)

COMMITTEE MEMBER: _____
(Darrell Neufer, Ph.D.)

COMMITTEE MEMBER: _____
(Carol Witczak, Ph.D.)

COMMITTEE MEMBER: _____
(Michael Van Scott, Ph.D.)

CHAIR OF THE DEPARTMENT
OF PHYSIOLOGY: _____
(Robert Lust, Ph.D.)

DEAN OF THE
GRADUATE SCHOOL: _____
(Paul Gemperline, Ph.D.)

Dedication

I dedicate this dissertation to my loving and supportive wife, Missy, and to my adorable kids, Alina and Levi. I love you all more than you could ever know! Thank you for being my biggest fans!

TABLE OF CONTENTS

LIST OF FIGURES

Adenosine Monophosphate-Activated Protein Kinase Inhibits Vascular Smooth Muscle Growth Associated With Vasculoproliferative Disorders

Chapter 1: Background and Significance

Cardiovascular disease (CVD) is the number one cause of fatality worldwide and accounts for greater than half of diagnosed noncomunicable diseases (28, 54). One in three deaths in America is a result of CVD with nearly 55% of all deaths having CV-related etiologies (28). CVD is a continuum of diseases which involve either the heart or the vasculature or both. The disease etiology is quite diverse; however, hypertension and atherosclerosis are the primary causative factors (81). The primary risk factors of CVD, which together promote the progression and complication of the disease include obesity, dyslipidemia, diabetes mellitus, metabolic syndrome, chronic kidney disease, and smoking (28, 54).

Although myocardial infarct (MI) and/or heart failure (HF) are primary clinical foci, according to the American Heart Association over 50% of CVDs are strictly vascular in origin (81). Vascular disease can be coronary, cerebrovascular, and/or peripheral in nature; however, all have the same pathophysiology which includes aberrant vascular growth and fibrosis. Abnormal vascular growth provides the primary mechanism underlying numerous vessel pathologies including atherosclerosis, pressure- and/or flow-mediated hypertrophy, stent-induced hyperplasia, and iatrogenic restenosis after intervention (44, 62, 118). Un-diagnosed and/or un-treated progression of vascular growth within a lipid-rich environment leads to plaque formation and luminal narrowing,

vessel stenosis, and ischemia in downstream tissues.

Aberrant vascular smooth muscle (VSM) growth is a pivotal mechanistic underpinning for these pathologies. While the arterial wall contains a heterogenous population of VSM cells (VSMCs) (34, 71, 79), under homeostatic conditions VSMCs maintain a cytostatic and contractile phenotype. The transformation of normally quiescent VSMCs to an activated state is initiated by mitogenic factors and/or mechanical injury to the vessel. These transformative events induce inflammation, which initiates the transcription and secretion of numerous chemokines thus further exacerbating and promoting inflammation, and VSMC migration, proliferation, and secretion of matrix proteins including collagens. These events lay the foundation for deleterious luminal narrowing and vessel stenosis associated with atherosclerosis, vessel hypertrophy, and restenosis following injury or clinical intervention (44, 62, 77, 82). Despite a plethora of studies aimed at reducing "phenotypic switching" of activated VSMCs, abnormal VSM growth remains a critical contributor to vascular pathophysiology with no absolute clinically-effective treatment identified to date. Therefore, given the current clinical and economic burden of vascular diseases, advanced therapeutic approaches to curb vascular growth are much needed.

AMPK: Adenosine monophosphate-activated protein kinase is a ubiquitously expressed heterotrimeric Serine (Ser)/Threonine (Thr) kinase consisting of a catalytic α-subunit and two regulatory subunits β and γ (36, 66, 84, 87). The kinase responds to a rise in the AMP:ATP ratio under metabolic challenge as well as to chemical and physical stresses. AMP binding is suggested to aid in partial activation of the kinase

causing a conformational change of the protein revealing the activation site for phosphorylation as well as providing significant protection from protein phosphatase deactivation (87). For full catalytic activity of the kinase, upstream phosphorylation of αT172 is required (84, 87). The tumor suppressor protein LKB1 was first described as the AMPK kinase (AMPKK); however, other AMPKKs have recently been described including calcium-dependent CaMKK and the TGFβ activated kinase TAK1. AMPK can also be activated hormonally by leptin or adiponectin (36, 66, 84, 87). Alternate alpha moieties, such as Ser 173 (19) or 485 (42), have been suggested to serve inhibitory functions on AMPK activity; however, these findings are tissue-dependent and their specific function remains unclear.

Actions of AMPK: Upon activation of AMPK, energy producing pathways are upregulated while energy consuming pathways are shut off or rendered minimally active (36, 66, 84, 87). AMPK also phosphorylates and inhibits many key metabolic enzymes such as glycogen synthase, HMG-CoA reductase, and acetyl CoA carboxylase (36, 84, 87). In a traditional sense AMPK responds to stimuli by inhibiting ATP-depleting processes such as cholesterol and protein synthesis while promoting carbohydrate and lipid metabolism, thus increasing ATP synthesis and restoring energy homeostasis within the cell (84, 87). However, more recent studies suggest that AMPK offers significant cardio- and vascular-protective roles by inhibiting cardiac and smooth muscle reactive oxygen species (ROS), reducing fibrosis, and enhancing vascular relaxation by increasing endothelial nitric oxide synthase (eNOS) activity and NO production (23, 83). Moreover, recent reports suggest that AMPK plays a significant role in cellular growth

arrest (23, 35, 61, 64, 99), making it an ideal candidate for studies targeted at reducing uncontrolled VSM growth.

AMPK and Vascular Growth: In intact blood vessels the progression of growth disorders culminates from the activation of VSMCs within the medial wall. This phenotypic activation of VSMCs promotes their *en*luminal migration, proliferation, and matrix deposition with ensuing neointimal development. Given the ability of AMPK to regulate synthetic processes within the cell, it is logical to think that AMPK could regulate specific energy consuming pathways within VSMCs that promote cell migration and proliferation.

Recent reports suggest that AMPK plays a significant role in cellular growth arrest (23, 35, 61, 64, 99). In particular, AMPK has been implicated in the inhibition of G_0/G_1 cell cycle progression and cytostasis in commercial human VSMCs (43). It is suggested that AMPK can inhibit neointima formation in rat femoral arteries following injury (67). A recent comprehensive study in mouse femoral arteries (97) proposed that AMPKα2 is the predominant isoform responsible for these growth inhibitory responses. However, since AMPK possesses two catalytic isoforms, α1 and α2, and AMPKα1 is the predominant isoform in VSM (84), the exact role of the two isoforms under physiologic and stimulated conditions remains unclear. Additionally, we recently reported that AMPK has capacity to communicate with protein kinase A in growth inhibition of primary VSMCs (99).

The physical migration of cells along a substrate is dependent upon highly dynamic actin cytoskeletal and focal adhesion regulation (4, 89). It has been reported that AMPK

has the capacity to phosphorylate and de-activate actin-associated vasodilator-activated serum phosphoprotein (VASP) (9) and to increase focal adhesion integrity and actin bundling (65). Together, by inhibiting the microfilament assembly necessary to promote cell extension and increasing the anchoring of a cell to its substrate, these data represent a potential mechanism by which AMPK could inhibit VSMC migration. It is noteworthy that many potential mechanisms of AMPK-mediated anti-migration may exist; however, this area of investigation within VSMCs and vascular growth remains fairly unexplored. Therefore, our initial investigations focused on the role of AMPK in regulating the actin cytoskeleton and focal adhesion contacts.

While these early findings lend support for anti-growth properties of AMPK within the vasculature, the specific mechanisms involved particularly related to proliferation and migration remains elusive; however, these justify further investigation into AMPK as a potential therapeutic target for use in reducing VSM growth disorders. Given the cytostatic (anti-proliferative and anti-migratory) capacities of AMPK, it makes sense that AMPK may play a major role in the reduction of VSM growth. Of these, specific mechanisms employed by AMPK to inhibit VSMC cell cycling and chemotaxis are especially intriguing yet are largely unexplored and possess critical basic science and clinical importance.

Data presented here lend support for our hypothesis that AMPK inhibits vascular remodeling by inhibiting cell migration in an actin cytoskeleton-associated fashion, and cell growth in a cell cycle regulatory fashion. Here we propose mechanisms employed by AMPK in an effort to reduce VSMC growth and that induction of these signaling events effectively reduce the intimal remodeling of rat carotid arteries following balloon

injury. In brief, our findings show that AMPK significantly reduces neointimal development through cytostatic inhibition of VSMC proliferation and migration. Mechanistic data support roles for AMPK in the stabilization of the actin cytoskeleton and in the enhancement of focal adhesion and ECM stability. Additionally, we provide data suggesting AMPK inhibits VSMC proliferation through cell cycle inhibition. Moreover, we provide early data that suggest both the anti-proliferative and anti-migratory actions of AMPK operate through inhibition of VASP. These findings provide strong evidence for AMPK as a physiological regulator of VSM growth and offer support for its continued study.

Chapter 2: Materials and Methods

This investigation was approved by the East Carolina University Animal Care and Use Committee and conformed to the Guide for the Care and Use of Laboratory Animals (U.S. National Institutes of Health, Publication No. 85-23, revised 1996).

Materials

AICAR was purchased from Toronto Research Company (North York, Ontario) and Invitrogen (Carlsbad, California), Compound C was purchased from Invitrogen, A-769662 was purchased from Tocris (Minneapolis, MN), forskolin and PKI were purchased from Enzo Life Sciences (Farmingdale, New York), and IBMX was purchased from Calbiochem (Darmstadt, Germany). Recombinant TGFβ1 was purchased from R&D Systems (Minneapolis, Minnesota). All primary antibodies were purchased from Abcam (Cambridge, Massachusetts), ECM Biosciences (Versailles, Kentucky), or Cell Signaling (Danvers, Massachusetts), were diluted 1:1000 for In-Cell and chemiluminscent Western blotting, or 1:500 for immunofluorescence detected by flow cytometry and were targeted against the following: AMPK, $pAMPK_{Thr172}$, $pAMPK_{Ser485}$; ACC, $pACC_{Ser80}$; PKA, $pPKA_{Thr197}$; VASP, $pVASP_{Ser157,}$ $pVASP_{Thr278}$; FAK, $pFAK_{Tyr397}$, paxillin; Smad2, $pSmad2_{Thr8,}$ Smad3, $pSmad3_{Ser423}$, Smad7; cyclin D, cyclin E, CDK2, CDK4, CDK6, p21, p27; α-tubulin, and β-actin. Antibodies were diluted in IRDye blocking buffer (Rockland; Gilbertsville, Pennsylvania) for In-Cell Western blotting or 1% bovine serum albumen (BSA) in PBS (Gemini; Stoneham, MA) for immunofluorescence. IRDye secondary antibodies (1:1000; Rockland) and FITC- or

TxRed-conjugated secondary antibodies (1:10000; Rockland) were used for protein detection while Draq 5 (1:10000; Cell Signaling) and Sapphire 700 (1:1000; Li-Cor; Lincoln, Nebraska) were used for DNA staining and protein normalization. Propidium iodide (PI) and RNAse for cell cycle analysis were purchased from Invitrogen. AlexaFluor-conjugated deoxyribonuclease I or phalloidin stains for G-actin and F-actin were purchased from Invitrogen.

Methods

Rat carotid artery balloon injury

Experimental balloon injury was performed on the left carotid artery of male Sprague Dawley rats (500 g) as we have previously described (109, 111). Briefly, animals were anesthetized (ketamine (90 mg/ml)/xylazine (10 mg/ml); 1.0 mL/kg body weight, intraperitoneal) and a Fogarty 2F embolectomy catheter (Edwards Lifesciences Corporation, Irvine, CA) was introduced through an arteriotomy site and advanced through the left carotid artery (LCA), inflated, and withdrawn with rotation three times to achieve arterial injury. The exposed portion of the LCA was treated with either 0.5 mg/kg bw AICAR or A769662 in 1 mL pluronic gel or equal amounts vehicle in pluronic gel and the tissues were closed and the animals given meloxicam (1 mL/kg, subcutaneous) for pain.

Tissue Processing and Staining

Two weeks following surgery animals were anesthetized and euthanized by pneumothorax and exsanguination. Tissues were perfusion-fixed, paraffin-embedded,

and standard staining techniques were utilized to analyze vessel growth as we have previously described (109). Briefly, neointimal (NI) and medial wall (MW) areas were measured and their ratios were calculated (as NI/MW) as a standard measure of remodeling (109). Also, perimeters of the internal and external elastic laminae were measured to obtain vessel circumferences (56). Additionally, a small cohort of animals was euthanized at varying times, and carotids were excised and homogenized for protein analysis as described (112).

Cell culture

Primary VSMCs were isolated from thoracic aortae of male Sprague-Dawley rats (100-125 grams; Charles River Labs) by collagenase and elastase digestion and characterized morphologically as previously described (20). VSMCs were cultured in Dulbecco's Modified Eagles Medium (DMEM) supplemented with Fetal Bovine Serum (FBS, 0.5-10%), 2 mM L-glutamine, and 1:500 dilution of 50 ug/mL Primocin at 37 °C in 95% air/5% CO_2. Cells were serially split and used through passage 6 (12, 47, 99). For all assays, n is calculated as at least 3 separate trials each with at least 3 wells (or reads) per assay from serially-split clonal cells.

Protein detection

VSMCs were seeded in 96-well plates and, once confluent, were treated with specified agents. After treatment, cells were formalin-fixed and protein phosphorylation was determined by In-Cell Western analysis as recently described (1, 48, 99). Briefly, fixed cells were permeabilized with 0.1% Triton-X, blocked with IRDye blocking buffer

and treated with rabbit anti-rat primary antibodies (1 h; RT). Target proteins were IR-labeled and DNA was stained for protein normalization. Fluorescence was detected and analyzed using Li-Cor Odyssey Infrared Imaging System and software. Traditional Western blots were performed on primary cell lysates as previously described (49, 63, 113) in order to confirm AMPK activation and to complement In-Cell Western data.

Assessment of Kinase activity

VSMCs were seeded in 96-well plates and, once confluent, were treated with specified pharmacologic agents. After treatment, cells were formalin-fixed, and protein phosphorylation was determined by In-Cell Western analysis as recently described (2, 47). Briefly, fixed cells were permeabilized with 0.1% Triton-X, blocked with IRDye blocking buffer and treated with rabbit anti-rat primary antibodies for 1 hour at RT. Target proteins were IR-labeled and DNA was stained for protein normalization. Fluorescence was detected and analyzed using Li-Cor Odyssey Infrared Imaging System and software. Additionally, traditional Western blots were performed on primary cell lysates as previously described (63, 113) to verify In-Cell Western data for select experiments. For specific activity, treated cells were lysed in buffer (50mM Tris, pH 6.8; 1% SDS; 0.1% Triton; protease inhibitor cocktail (Thermo); phosphate inhibitor cocktail (Thermo)), and added to wells of a 96-well microtiter plate. ELISA-based activity assays were performed per manufacturer's instructions. Briefly, for AMPK (MBL International, Woburn, Massachusetts), activity was assessed using a mouse insulin receptor substrate phospho-serine 789 reporter with HRP chemiluminescence at 450nm (58, 106). For PKA (Enzo Life Sciences), activity was measured by

tetramethylbenzidine substrate color development proportional to PKA phosphotransferase activity and measured at 450 nm as described (13).

Phosphatase Activity

Cells were harvested in phosphatase inhibitor-free buffer, prepared according to manufacturer's suggestion (Invitrogen), and added to wells of microtiter plates containing 6,8-difluoro-4methyl-umbelliferyl phosphate substrate. When activated by phosphatases, DiFMU was generated in proportion to phosphatase activity, which was read at 450 nm. For specific (PP-2A and PP-2C) phosphatase activities, additional components were added to the buffer per manufacturer's directions that allowed for activity analyses of specific phosphatases within the lysate (50, 72).

MMP activity analysis

MMP activity was assessed by matrix gel zymography (55). Briefly, conditioned media was electrophoresed in a 10% zymogram gel containing 1mg/mL gelatin. The gel then underwent a series of washings at RT for 2 hrs followed by an overnight incubation at 37°C in renaturing buffer. The gel was then stained with Coomassie blue and visualized using an Epson Perfection V750 Pro scanner. Proteolytic activity was assessed as the density of a white band (indicative of enzymatic digestion) on a dark blue field. Additionally, expression of tissue inhibitor of MMP (TIMP) was analyzed from the conditioned media of treated cells by traditional Western blot as we have described previously (63, 113).

Immunocytochemistry:

VSMCs were seeded on glass coverslips and allowed to adhere. Cells were treated for 1-48 hrs with select pharmacologic agents, formalin-fixed, permeabilized (0.1% Triton-X), and blocked with 3% BSA in PBS + 0.1% Tween-20 (PBST). Protein IgG reactions were carried out using selective primary antibodies followed by counterstaining with fluorescently-tagged secondary antibodies (FITC and TxRed). Fluorescently-tagged phalloidin and deoxyribonuclease I were used to detect F- and G-actin, respectively.

Immunofluorescence:

Confluent VSMCs were treated with select pharmacologic agents for 1-24 hours then trypsinized, fixed with 4% formalin, washed with PBS, permeabilized with 0.1% Triton-X in PBS, washed, and blocked with 1% BSA in PBS. Select proteins were detected by primary/secondary conjugation in 1% BSA and analyzed by flow cytometry. Fluorescently-tagged phalloidin and deoxyribonuclease I were used to detect F- and G-actin, respectively analyzed by flow cytometry (Accuri C6 Flow Cytometer) using CFlow Plus software (Accuri) (100).

Cell cycle analysis

Cells were plated in 12-well plates at 80,000 cells/well in complete media until ~50% confluent. Cells were quiesced in 0.5% FBS for 24 hours followed by treatment in complete growth media (DMEM, 10% FBS, Primocin) containing select pharmacologic agents for 24 hours. Cells were trypsinized and stained with propidium iodide (PI;

Invitrogen) per manufacturer's recommendations (47, 99). The fraction of cells present in each phase of the cell cycle was assessed by flow cytometry (C6, Accuri).

Cell proliferation and viability analyses

VSMCs were plated in 6-well plates at 180,000 cells/well in complete media until ~50% confluent. Cells were quiesced in 0.5% FBS for 24 hours followed by treatment in complete growth media for 48 hours as described. Cells were trypsinized and proliferation and viability were assessed through automated cell counting with trypan blue exclusion staining (ViCell, Beckman Coulter).

Cell migration analyses

Following protocols previously described with minor modifications (47, 59), VSMCs were seeded at 180,000 cells/ml in the upper chamber of a Fluorblok transwell system (BD) in complete media and allowed to adhere. Cells were then treated for 1 hour following staining with Cell Tracker Green (10 uM; Invitrogen). Serum-free media was applied to the upper chamber containing the same original treatment and 10 ng PDGFβ was applied to the bottom chamber as a chemoattractant (124). Cell migration was assessed from time 0 through 18 hours by bottom-read fluorescence at 525 nm (Tecan Infinite M200) with each time point random fluorescent units (RFU) normalized to time=0 RFU for each respective condition. Net migration was calculated as a fold change of the total migration for each condition over total control (vehicle) migration at 18 hours. Additionally, using a wounding assay cells were grown to confluence in 6-well plates and select pharmacologic agents were added to the growth media for 1 hour. Following

treatment cells were wounded with a 2mm blade and the rate of wound healing was assessed by photomicrography through 24 hours.

Anti-VASP Lv-shRNA transduction

Lv-shRNA (SMART vector 2.0) directed against the full length VASP or non-targeting controls (NTC; Dharmacon Research, Lafayette, CO) were utilized to reduce expression of endogenous VASP. Transduction efficiencies and appropriate multiplicity of infection (MOI) were determined per manufacturer's guidelines. Rat VSMCs were plated in 96-well plates at 40% confluence and switched to 0.5% serum following adherence. Cells were treated with Lv-shRNA SMART vector 2.0 against full length VASP (MOI 0.3-5) or NTC controls for 24 hours in transduction media lacking antibiotic. Media was changed after 24 hours to high glucose-DMEM, 15% FBS and penicillin/streptomycin mix, and on day 3 cells were expanded to 24-well plates and VASP mutants were selected by Puromycin resistance for 24 hours. Stable cell lines were established and used as needed for verification of VASP deficiency and cell growth assays.

Statistical analyses

Data were analyzed using Excel 2011 (Microsoft) and Sigma Plot 11.2 (SPSS, Inc.). All data sets were tested for normal distribution and met the homogeneity prerequisites for analysis of variance (ANOVA). One-way ANOVA and Tukey's post-hoc multiple comparison tests were used to detect changes between individual groups. Two-way ANOVA with multiple comparisons and Tukey's post-hoc tests were used for protein

phosphatase analysis, migration, and cell cycle analysis to detect significance among groups. Data are expressed as mean ± standard error of the mean (SEM), with a $p < 0.05$ considered statistically significant.

Chapter 3: AMP-Activated Protein Kinase Inhibits Vascular Smooth Muscle Cell Proliferation and Migration and Vascular Remodeling Following Injury

Joshua D. Stone, Avinash Narine, Patti R. Shaver, Jonathan C. Fox,

Jackson R. Vuncannon, David A. Tulis

Published:

Am J Physiol Heart Circ Physiol. 2013 Feb 1;304(3):H369-81.

Abstract

Vascular smooth muscle cell (VSMC) activation promotes a synthetic phenotype that underlies many vessel growth disorders. In this regard it has been suggested that the metabolic sensor adenosine monophosphate-activated protein kinase (AMPK) has significant anti-growth and anti-metastatic properties and may serve as a viable therapeutic target. In the current study we hypothesized that AMPK reduces neointima formation following balloon injury and that this occurs through reduction in VSMC proliferation and migration. Data reveal that local or systemic dosing with the AMPK agonist AICAR significantly increased AMPK activity *in vivo* and inhibited neointima formation in rat carotid arteries 2 weeks after injury. In rat primary VSMCs AICAR inhibited migration and induced cytostatic growth arrest through increased protein phosphatase 2A-mediated inhibition of mitosis-promoting cyclin B. AICAR also significantly enhanced AMPK-specific Thr278 phosphorylation of the actin anti-capping vasodilator-activated serum phosphoprotein (VASP), increased G:F actin ratios and stress fiber formation, and abrogated PDGF-stimulated Ser397 autophosphorylation of focal adhesion kinase, pro-migratory cytoplasmic accumulation of paxillin, and extracellular matrix proteolysis by MMP-9. Together, these results provide compelling evidence that AMPK serves to inhibit VSM migration and proliferation through regulation of cytoskeletal/focal adhesion/ECM stability, increasing our knowledge of this important metabolic regulator and providing support for its continued investigation in the treatment of vascular growth disorders.

Introduction

Abnormal vascular smooth muscle (VSM) growth is a key mechanistic underpinning for many vasculopathies including atherosclerosis, vessel hypertrophy, and restenosis following injury or clinical intervention (44, 62, 77). In intact blood vessels the progression of growth disorders culminates from the activation of VSMCs within the medial wall, thus promoting their luminal migration, proliferation, and matrix deposition and ensuing neointimal development. The physical migration of cells along a substrate is dependent upon highly dynamic actin cytoskeletal and focal adhesion turnover (4, 89). Adenosine monophosphate-activated protein kinase (AMPK) is a key metabolic sensor that responds to cellular energy deprivation and/or chemical and physical stresses. It has been reported that AMPK has capacity to phosphorylate and de-activate actin-associated vasodilator-activated serum phosphoprotein (VASP) (9) and to increase focal adhesion integrity and actin bundling (65). Therefore, given the anti-growth and potential anti-migratory capacities of AMPK, it makes sense that AMPK may play major roles in the reduction of VSM growth. This warrants further investigation in order to gain insights into the mechanisms employed by AMPK to control VSM growth.

The purpose of this study therefore was to examine our hypothesis that AMPK inhibits VSM growth by inhibiting cellular migration and cell cycle progression and actin cytoskeletal and focal adhesion dynamics. We propose that these mechanisms are employed by AMPK in an effort to reduce VSM growth and that induction of these signaling events will effectively reduce neointima formation of rat carotid arteries following balloon injury. In summary, novel findings show that AMPK significantly reduces neointimal development through cytostatic inhibition of VSMC proliferation and

reduction in migration. Mechanistic data support roles for AMPK in the stabilization of the actin cytoskeleton and in the enhancement of focal adhesion and ECM stability. These findings provide strong evidence for AMPK as a physiological regulator of VSM growth and offer support for its continued study.

Results

Systemic and local AICAR inhibit vascular remodeling

Previous work by our lab established both systemic pre-treatment (114) and localized dosing (115, 116) of pharmacologic agents concomitant with the rat carotid artery model of vascular injury (109, 113-115). In similar fashion, in the current study we assessed the effects of systemic pre-treatment as well as localized delivery of the well-characterized AMP-mimetic AICAR (14, 67, 99, 103, 121) (0.5 g/kg BW systemic; 1 mg local) on vascular remodeling in rat balloon-injured carotid arteries. Additionally, we utilized the direct, non-metabolic AMPK-activating small molecule A-769662 (30, 37, 73, 92) (1 mg) with localized delivery to verify specificity of AICAR-mediated AMPK effects. First, in order to verify these treatment regimens on uninjured vessels, daily intraperitoneal dosing with AICAR for 2 days or localized perivascular delivery of AICAR or A-769662 each significantly induced AMPK activity assessed by Thr172 phosphorylation (17) in carotid artery lysates compared to vehicle (NaCl or DMSO)-treated control vessels (Fig. 3.1).

Figure 3.1

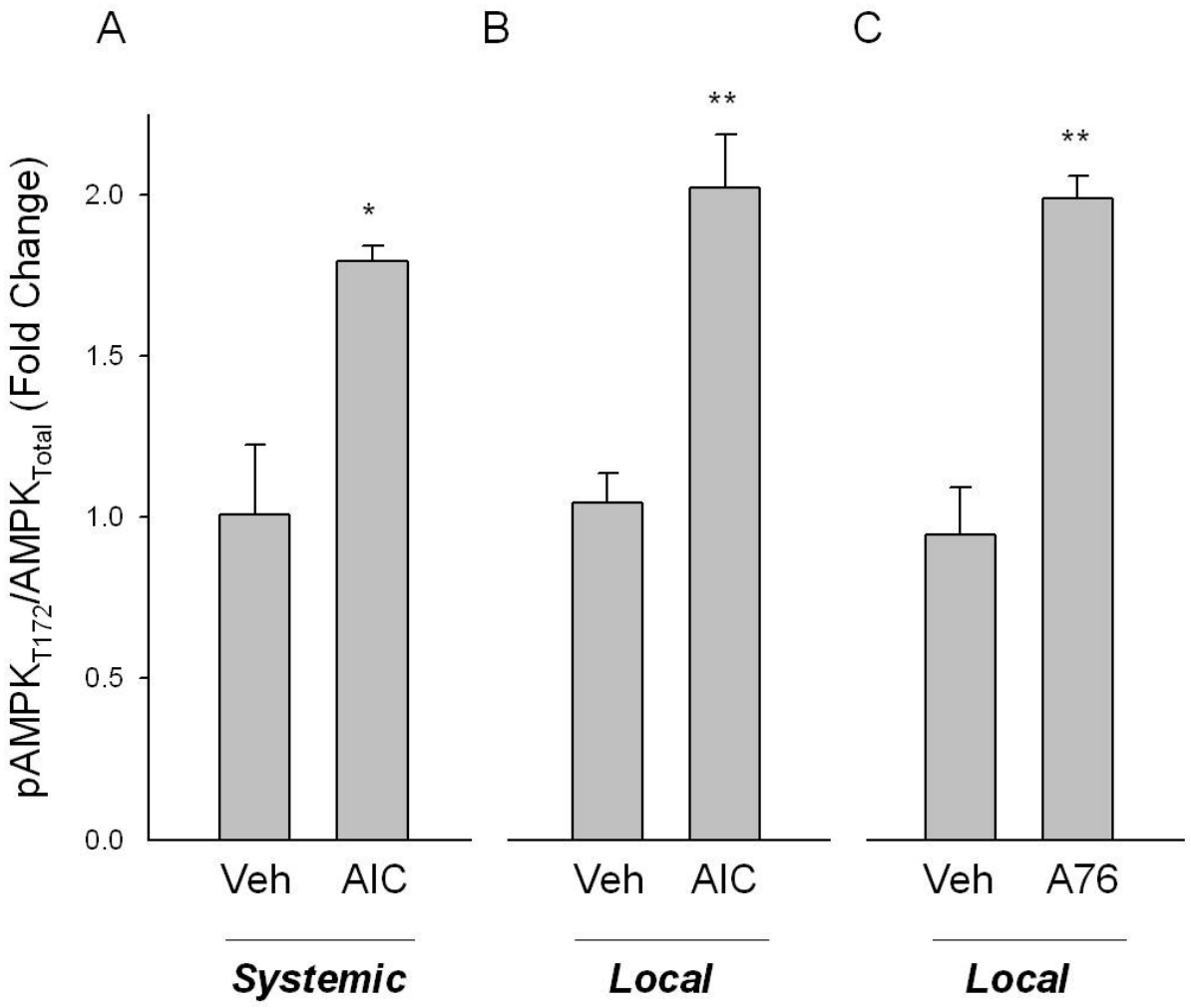

Figure 3.1. AICAR or A-769662 activates AMPK in rat carotid arteries. Male Sprague Dawley rats were treated with AICAR either systemically **(**0.5 g/kg BW intraperitoneal injection, 1x/day for 2 days) or locally (1 mg in Pluronic gel) on uninjured left carotid arteries for 24 hours. Carotid arteries were harvested and tissues homogenized and probed for pAMPK-Thr 172 and total AMPK. In both treatment regimens AICAR significantly induced AMPK activity as assessed by Thr172 phosphorylation (A and B). Additionally, localized treatment with the small molecule A-769662 significantly increased pAMPK Thr172 (C). Data are presented as mean pAMPK-Thr172/total AMPK (+/- SEM) as a marker of AMPK activity over 3 separate experiments. P values less than 0.05 were considered statistically significant. *= $p<0.05$ compared to vehicle (Veh) control; ** = $p<0.005$ compared to Veh.

Two weeks after balloon injury both AICAR and A-769662 significantly reduced neointima formation compared to vehicle-treated controls using both systemic (Figs. 3.2A, 3.2D) and localized (Figs. 3.2B, 3.2C, 3.2E, 3.2F) dosing regimens. Notably, comparable levels of growth inhibition were observed between localized AICAR and A-769662. Vessel circumferences, measured as internal and external elastic lamina lengths, were obtained to rule out anatomical vessel distension as contributor of the observed remodeling but were found not to be significantly different in any treatment group compared to vehicle controls (data not shown).

Figure 3.2

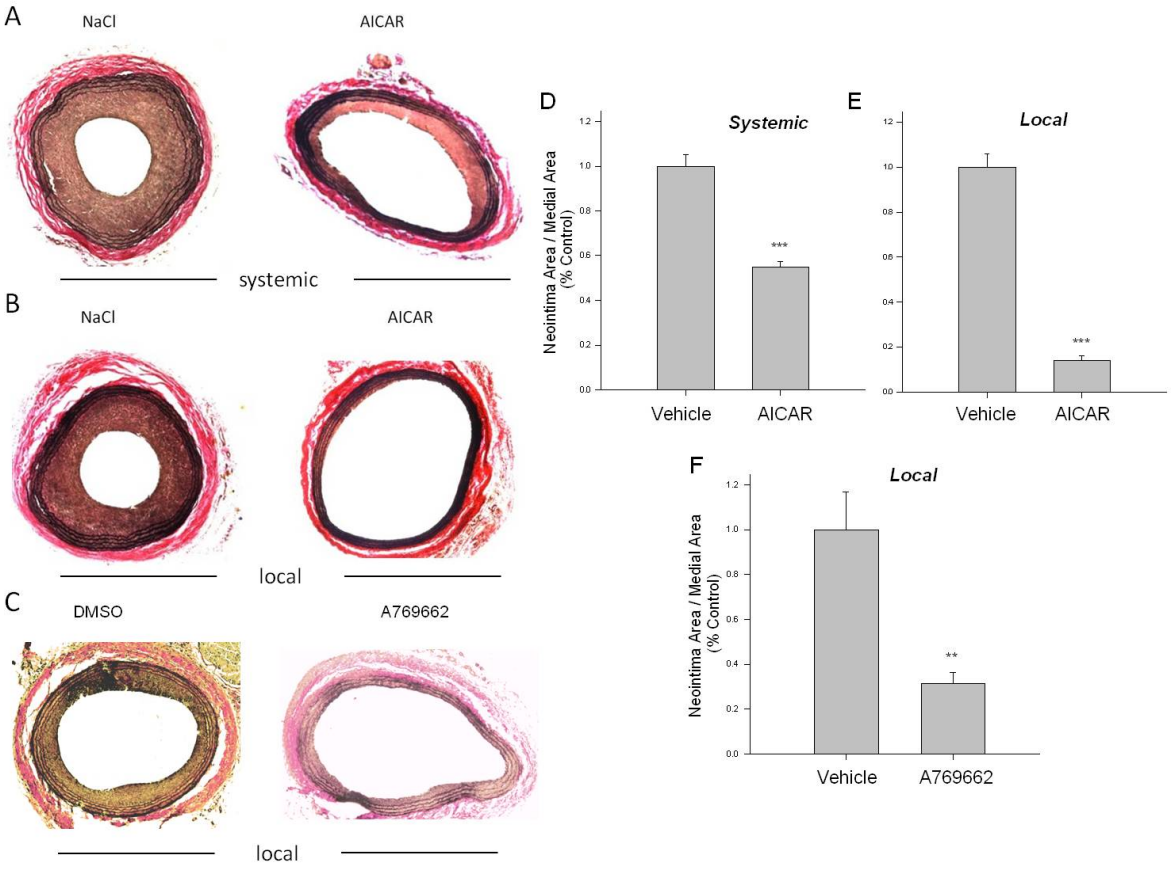

Figure 3.2. AMPK inhibits neointima formation 2 weeks after carotid artery balloon injury. Rats were given systemic AICAR (0.5 g/kg BW IP) every 24 hours for 2 days prior to injury, or LCAs were given local AICAR (1 mg) or A-769662 (1 mg) in Pluronic gel immediately following injury. After 14 days rats were euthanized and carotids were perfusion-fixed, collected and processed for staining. (A) Representative photomicrographs of balloon-injured, perfusion-fixed Verhoeff-Van Gieson-stained left carotid arteries of systemically dosed rats 14 days post-injury. (B and C) Representative photomicrographs of carotid arteries as with (A), but using localized delivery of AICAR (B) or A-769662 (C) on the injured vessel. (D - F) Neointimal area/medial area for vehicle-, AICAR-, or A-7679662-treated carotid arteries 14 days following injury. Both systemic (D) and local (E) AICAR and local A-769662 (F) significantly reduced neointimal growth compared to vehicle-treated vessels. Data are presented as mean +/- SEM for 6-8 separate experiments per cohort. P values less than 0.05 were considered statistically significant. ** = $p<0.005$ compared to Vehicle; *** = $p<0.001$ compared to Vehicle.

AICAR increases AMPK activity in primary VSMCs

In rat primary VSMCs AICAR (1 mM) significantly enhanced Thr172 phosphorylation of AMPK at 1 hour (14, 29, 99, 121) which continued through 24 hours (Fig. 3.3A). This activating phosphorylation was completely reversed by the AMPK inhibitor Compound C (CC, 10 uM) at both time points (14, 97, 99, 103), yet CC alone did not alter basal (untreated) Thr172 phosphorylation levels. In addition, an AMPK-specific activity assay verified that the observed increases in Thr172 phosphorylation correlate with increased activity at both 1 and 24 hours (Fig. 3.3B). Again, CC alone had no impact on basal AMPK activity.

Figure 3.3

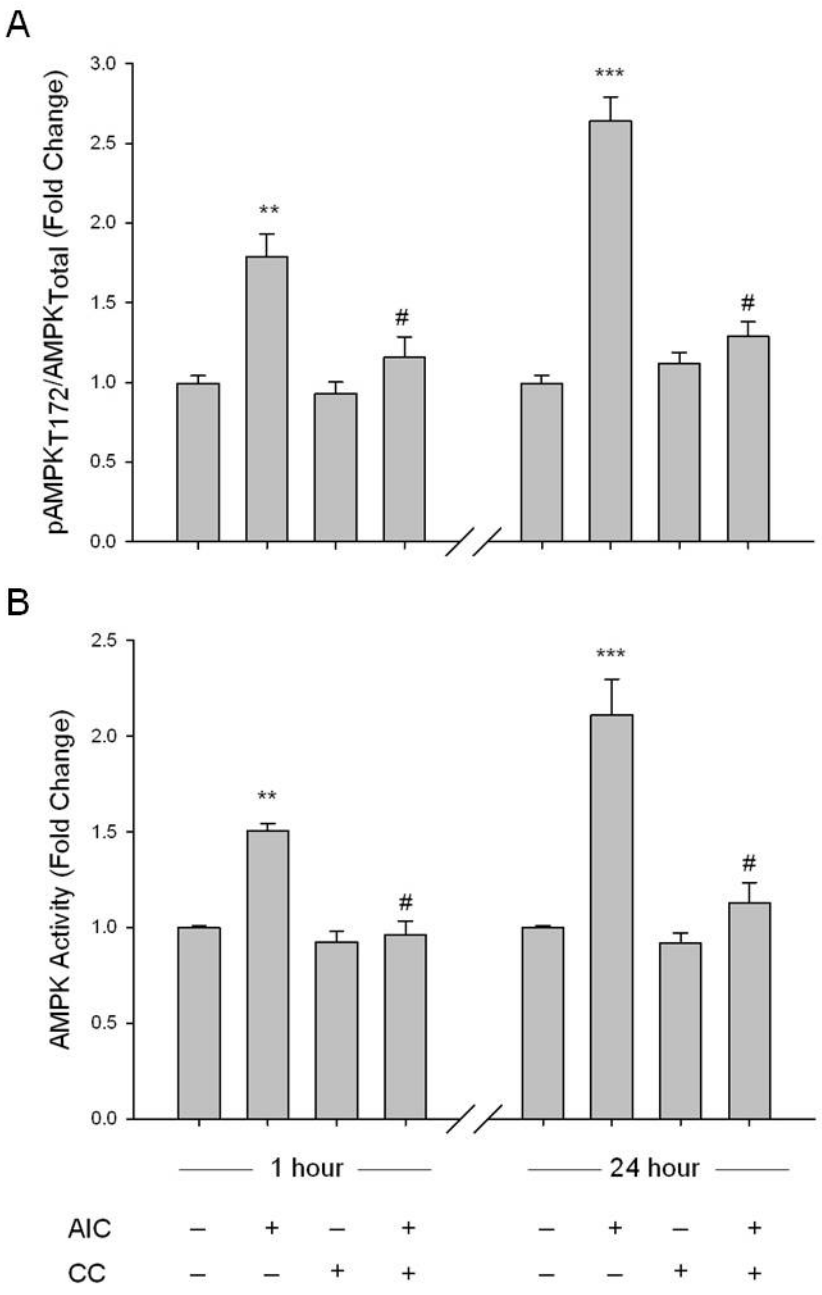

Figure 3.3. AICAR increases AMPK signaling in rat primary VSMCs. Cells were treated with AICAR (1 mM, 60 min) and/or the AMPK inhibitor Compound C (CC; 10 uM, 60 min) and AMPK-Thr172

phosphorylation (A) and AMPK activity (B) were measured respectively by In-Cell Western analysis and an AMPK-specific activity assay. AICAR significantly increased phosphorylation of both AMPK-Thr172 (A) and AMPK activity (B) after 1 hour and 24 hours, both fully reversible by CC. CC alone exerted no effect on basal AMPK-Thr172 phosphorylation or AMPK activity. Data are presented at pAMPK-Thr 172/total AMPK and normalized to DNA content (Draq 5/Sapphire 7) or absorbance at 540 nm for activity, and within each study n = 5-7. P values less than 0.05 were considered statistically significant. ** = $p<0.005$ compared to control; *** = $p<0.001$ compared to control; # = $p<0.05$ compared to respective activator treatment.

AMPK inhibits VSMC proliferation

In rat primary VSMCs AICAR (1 mM) significantly inhibited viable cell numbers after 48 hours, and CC largely reversed this anti-proliferative effect (Fig. 3.4A). Interestingly, CC alone significantly reduced cell numbers compared with vehicle controls. Notably, using trypan blue exclusion changes in cell viability were not observed in any treatment group and overall viability ranged between 85% and 90% after 24 hours (data not shown). Using flow cytometry, AICAR significantly reduced G_2/M cell populations and significantly increased S phase cell populations after 24 hours compared to vehicle-treated cells, and the changes in the S and G_2/M phases were fully reversed with concomitant CC (Fig. 3.4B). AICAR also induced a non-significant increase in G_0/G_1 cell populations which correspond well with the decrease in G_2/M cell populations. Interestingly, CC alone significantly reduced cell numbers after 48 hours and non-significantly reduced cells in G_2/M after 24 hours.

Figure 3.4

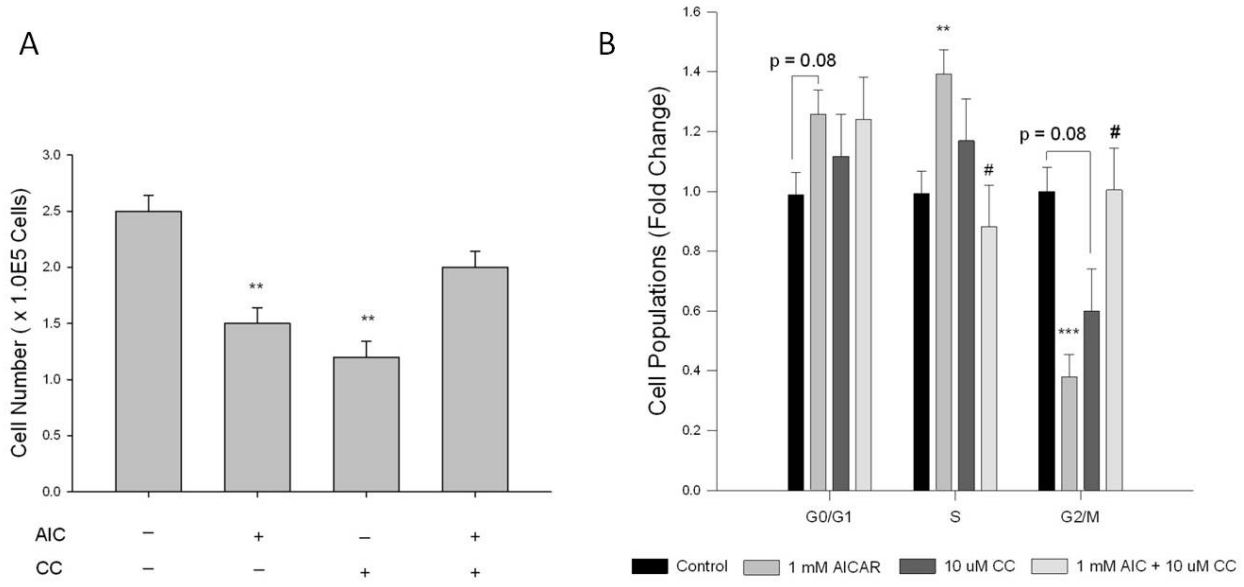

Figure 3.4. AMPK induces cell cycle arrest and inhibits VSMC proliferation. Cells were treated with AICAR **(**1 mM) and/or Compound C (CC; 10 uM) following overnight quiescence in 0.5% serum. (A) Cell numbers were quantified after 48 hours by automated cell counting and trypan blue exclusion and (B) cell cycle progression after 24 hours was analyzed by flow cytometry using propidium iodide. AICAR significantly reduced cell numbers and inhibited cell cycle progression revealed by increased G_0/G_1 and S and reduced G_2/M cell numbers. Of note, CC alone significantly reduced cell numbers compared with vehicle controls (A) and significantly reduced cell numbers in G_2/M. Trypan blue exclusion failed to detect any differences in cell viability in any treatment group (data not shown). P values less than 0.05 were considered statistically significant after multiple comparisons and two-way ANOVA. ** = $p<0.005$ compared to control; *** = $p<0.001$ compared to control; # = $p<0.05$ compared to respective activator treatment.

It has been suggested that protein phosphatase-2A (PP-2A) has ability to inhibit G_2/M cell cycle progression by inhibiting the cdc/cyclin B complex (45). In our study using a PP-2A-specific activity assay in primary VSMCs, data show that AMPK promotes PP-2A activity (1 mM AICAR; 24 hours) in a CC-reversible fashion (Fig. 3.5A). Concomitantly cells treated with AICAR over 24 hours showed significant reductions of cyclin B in nuclear fractions compared to controls, which was fully reversed by CC (Fig. 3.5B).

Figure 3.5

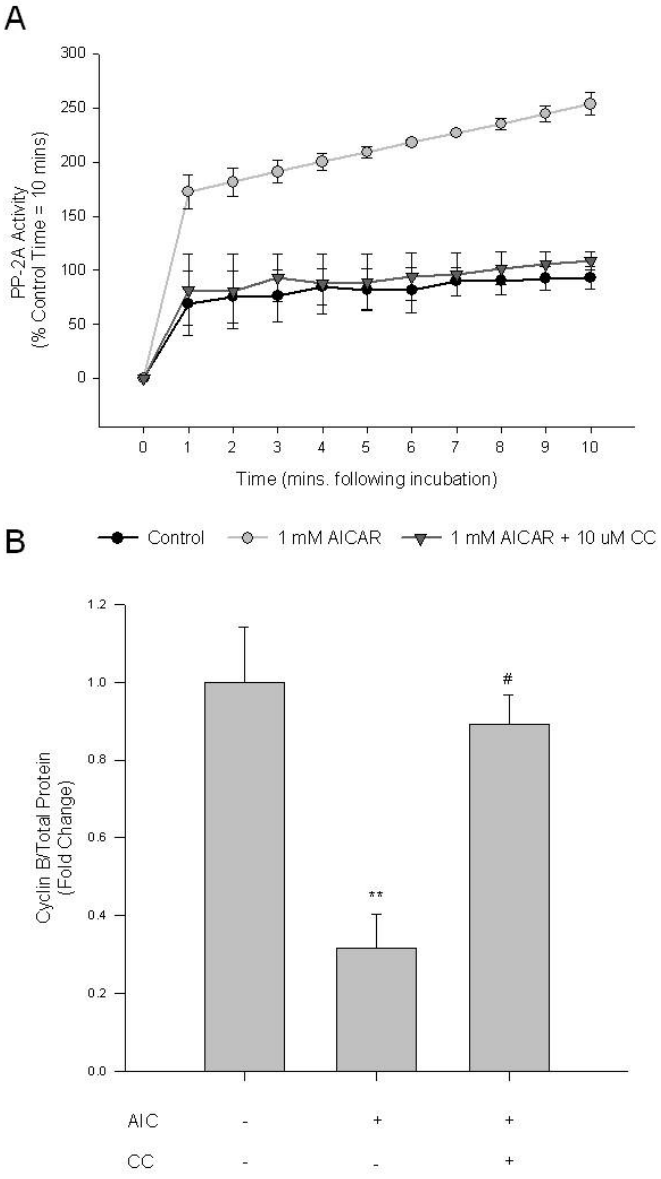

Figure 3.5. AMPK promotes protein phosphatase-2A activity and reduces cell cyclin B expression. Cell lysates were prepared from cells treated with AICAR **(**1 mM) and/or Compound C (CC; 10 uM) for 24 hours. Phosphatase activity of diluted (1:10) lysate samples were measured by DiFMUP fluorescence at 452 nm after 10 minutes of incubation in the dark. Activity analysis revealed that AICAR induced global Ser/Thr phosphatase activity compared to control (data not shown). (A) With addition of $NiCl_2$ (1 mM) to the reaction buffer, PP-2A-specific activity was measured and results revealed that AICAR significantly elevated PP-2A activity which was reversed by CC. Treated cells underwent fractionation so that nuclear lysates could be electrophoresed and probed for cdc2/cyclin B expression. (B) Cyclin B expression was significantly decreased in AICAR-treated cells in a CC-reversible fashion compared to controls. Two-way ANOVA with Tukey's post-hoc testing was used for multiple comparisons across time points as well as within each treatment group for phosphatase activity and one-way ANOVA detected differences among groups for protein analysis. P values less than 0.05 across time within each group were considered statistically significant. ** = $p<0.005$ compared to control; # = $p<0.05$ compared to respective activator treatment.

AMPK inhibits VSMC migration

Using a transwell chemotaxis assay, AICAR (1 mM) significantly inhibited PDGF-β (20 ng/ml)-induced VSMC migration over 18 hours (Fig. 3.6A). While CC alone exerted no effect on basal levels of migration, AICAR-mediated inhibition of migration was partially reversed in the presence of CC and, per a 2-way ANOVA, was not statistically different from vehicle controls ($p=0.412$). In complement, a wound-healing assay on serum-stimulated confluent VSMCs showed that AICAR (1 mM) significantly reduced migration (as shown by increased wound width) over a 24 hour period (Figs. 3.6B and 3.6C).

Figure 3.6

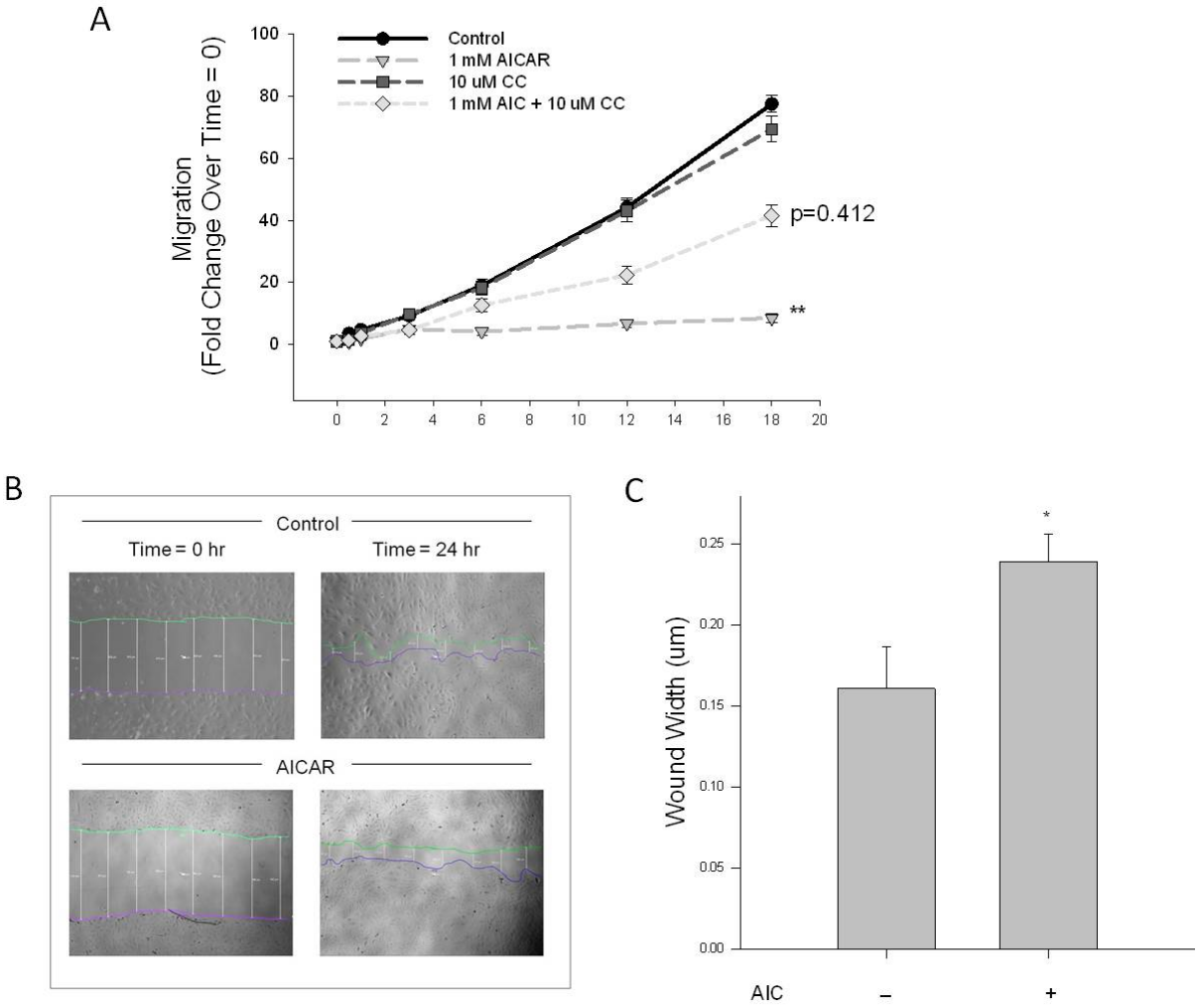
A
Migration
(Fold Change Over Time = 0)
Control
1 mM AICAR
10 uM CC
1 mM AIC + 10 uM CC
p=0.412
**
B
Control
Time = 0 hr
Time = 24 hr
AICAR
C
Wound Width (um)
*
AIC
–
+

Figure 3.6. AMPK inhibits VSMC migration. (A) Cells were labeled with CellTracker Green and treated with AICAR (1 mM) and/or Compound C (10 uM), and PDGF-stimulated (10ng/mL) chemotaxis was determined using a modified Boyden chamber apparatus and bottom-read fluorescence at 525 nm between 0 and 18 hours. AICAR significantly reduced cell migration, which showed a non-significant reversal with simultaneous CC (A). CC alone failed to alter basal migration compared to controls. (B) Cells were grown to confluence in 6-well plates and treated the same as above. A 2 mm blade was used to injure the cell monolayer and photomicrographs were taken from time 0 through 24 hours. Photomicrographs show vehicle- and AICAR-treated cells immediately after scrape injury (time = 0) and after 24 hours. (C) Measurement of the wound width reveals that AMPK significantly inhibits VSMC wound healing after 24 hours. Two-way ANOVA with Tukey's post-hoc testing was used for multiple comparisons across time points as well as within each treatment group. P values less than 0.05 across time within each group were considered statistically significant. *= $p<0.05$ compared to control; ** = $p<0.005$ compared to control.

AMPK promotes actin cytoskeleton stability

Actin-associated VASP acts as an anti-capping protein that promotes actin nucleation and filament elongation required for cell migration (6, 7, 15, 90). Upon site-specific phosphorylation VASP is rendered inactive and actin filaments are capped and polymerization stops, hence phosphorylated VASP can serve as an anti-migratory factor. It has been shown that VASP possesses an AMPK-specific phosphorylation site Thr278 (9). In this study we show that AICAR (1 mM) significantly increases pVASP-Thr278 compared to vehicle controls after 1 hour, and this was completely reversed with CC (10 uM) (Fig. 3.7).

Figure 3.7

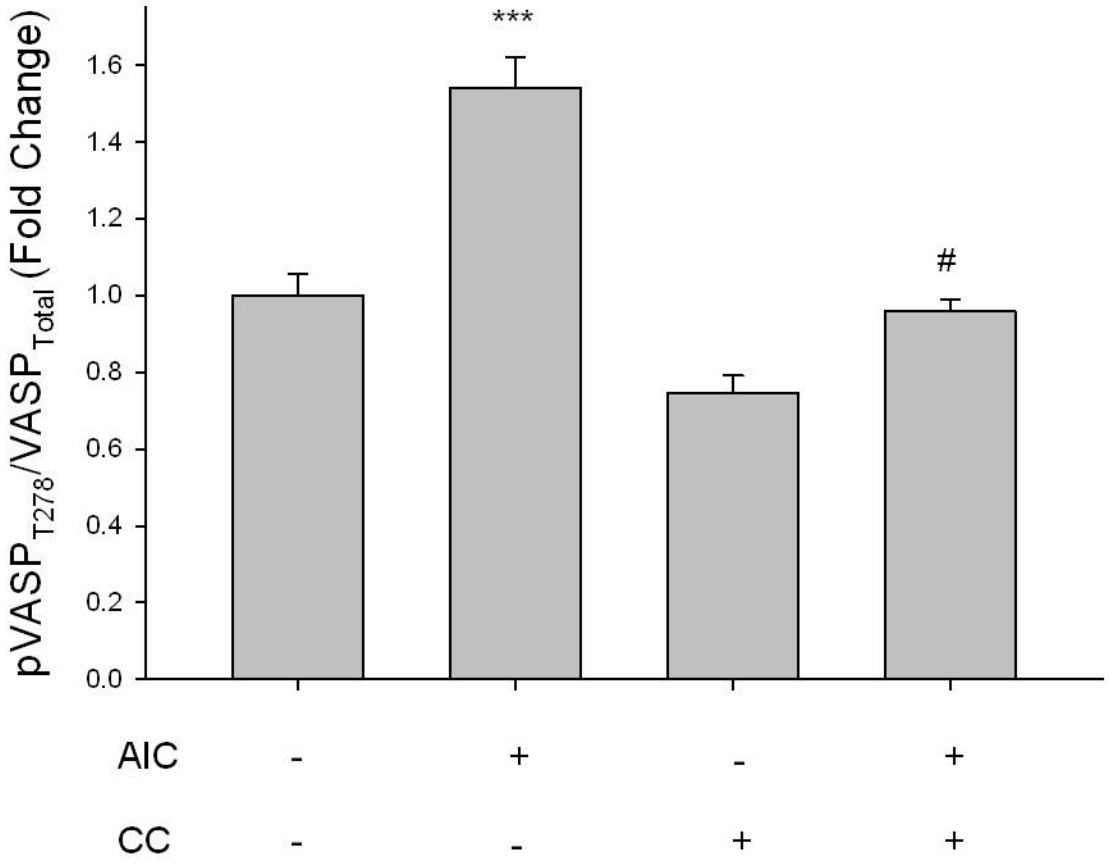

Figure 3.7. AMPK inhibits VASP-mediated actin anti-capping. Cells were treated with AICAR (1 mM, 60 min) and/or Compound C (CC; 10 uM, 60 min), and VASP Thr278 phosphorylation was measured by In-Cell Western analysis. AICAR significantly induced pVASP Thr278, a proposed AMPK-specific site, which was fully reversed by CC. CC alone did not affect basal pVASP Thr278 status. Data are presented at pVASP Thr278/total VASP and normalized to DNA content (Draq 5/Sapphire 7) for 5-7 experiments. P values less than 0.05 were considered statistically significant. *** = $p<0.001$ compared to control; # = $p<0.05$ compared to respective activator treatment.

Of note, CC alone had no effect on VASP-Thr278 phosphorylation. Immunofluorescent flow cytometry for G- and F-actin shows that AICAR significantly increases the G:F-actin ratio after 1 hour (Fig. 3.8A) which continues through 24 hours (Fig. 3.8B). At both times CC fully reversed basal and AICAR-induced G:F ratios. In support, phalloidin staining for F-actin suggests that AICAR significantly increases (~55%; 9 +/- 2 control vs 20 +/- 3 AICAR/field of view) actin bundling and stress fiber formation in primary VSMCs compared to vehicle-treated cells which exhibited an organized parallel arrangement of actin fibers (Fig. 3.8C).

Figure 3.8

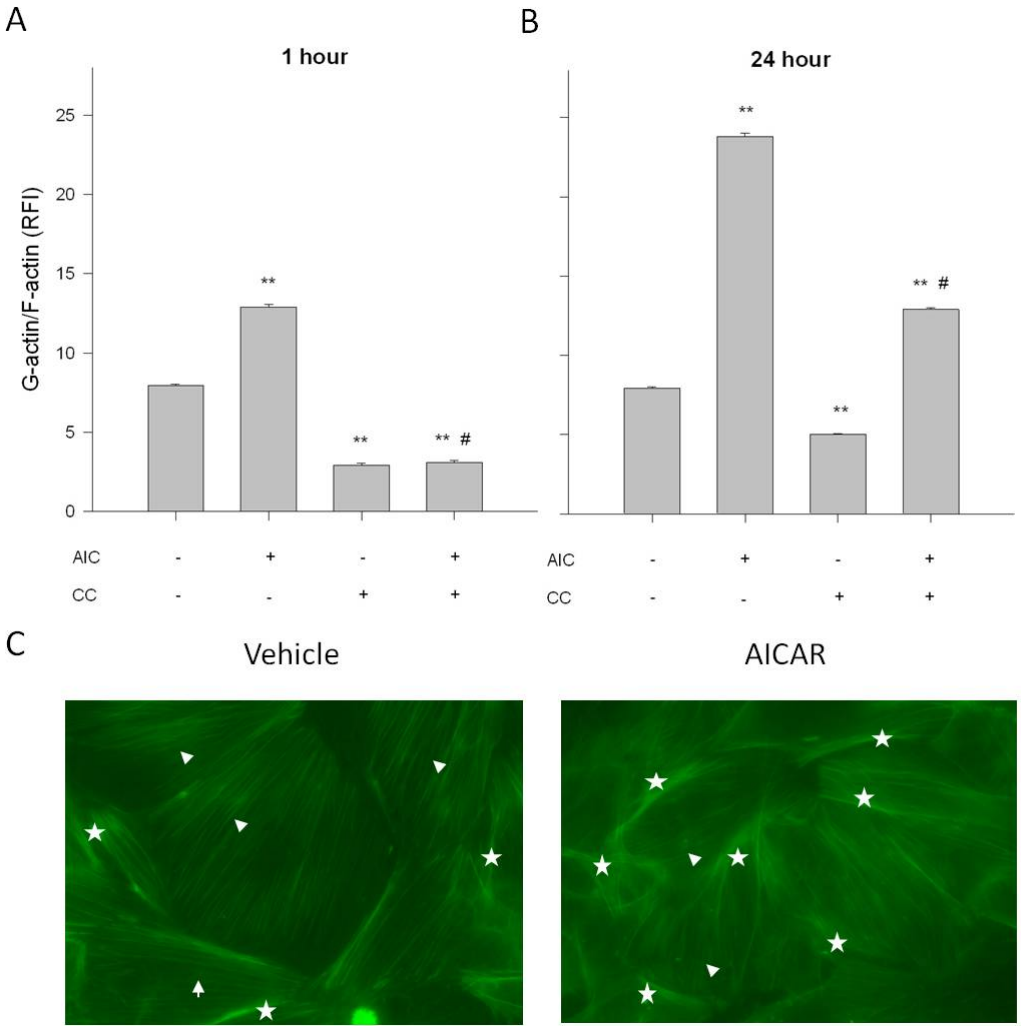

Figure 3.8. AMPK promotes actin de-polymerization and stress fiber formation. Cells were treated with AICAR **(**1 mM, 60 min) and/or Compound C (CC; 10 uM, 60 min) and fixed and stained for F-actin (fluorescently-tagged phalloidin) or G-actin (fluorescently-tagged deoxyribonuclease I), and fluorescence was read by flow cytometry or visualized by fluorescence microscopy. Immunofluorescence reveals that AICAR promotes F-actin disassembly revealed by increased G:F actin in a CC-reversible fashion after (A) 1 hour continuing through (B) 24 hours. Notably, CC alone significantly reduced basal G:F actin compared to vehicle controls at both times. (C) Cells were counterstained for F-actin (fluorescently-tagged phalloidin) and visualized using fluorescent microscopy. Representative photomicrographs reveal that AMPK promotes the disassembly of an organized F-actin array seen in vehicle treated cells (arrowheads) and promotes actin bundling and stress fiber formation (stars). P values less than 0.05 were considered statistically significant. ** = $p<0.005$ compared to control; # = $p<0.05$ compared to respective activator treatment.

AMPK promotes focal adhesion stability

Focal adhesion kinase (FAK) is largely responsible for focal adhesion turnover and the promotion of cell detachment and migration along a substratum (53, 89, 107). In rat primary VSMCs, pFAK-Tyr397, a necessary event for kinase catalytic activity (107), was significantly elevated with addition of PDGF-β (10 ng/mL) after 1 hour, yet AICAR significantly reduced this activated phosphorylation of FAK in the presence of PDGF-β to control levels (Fig. 3.9).

Figure 3.9

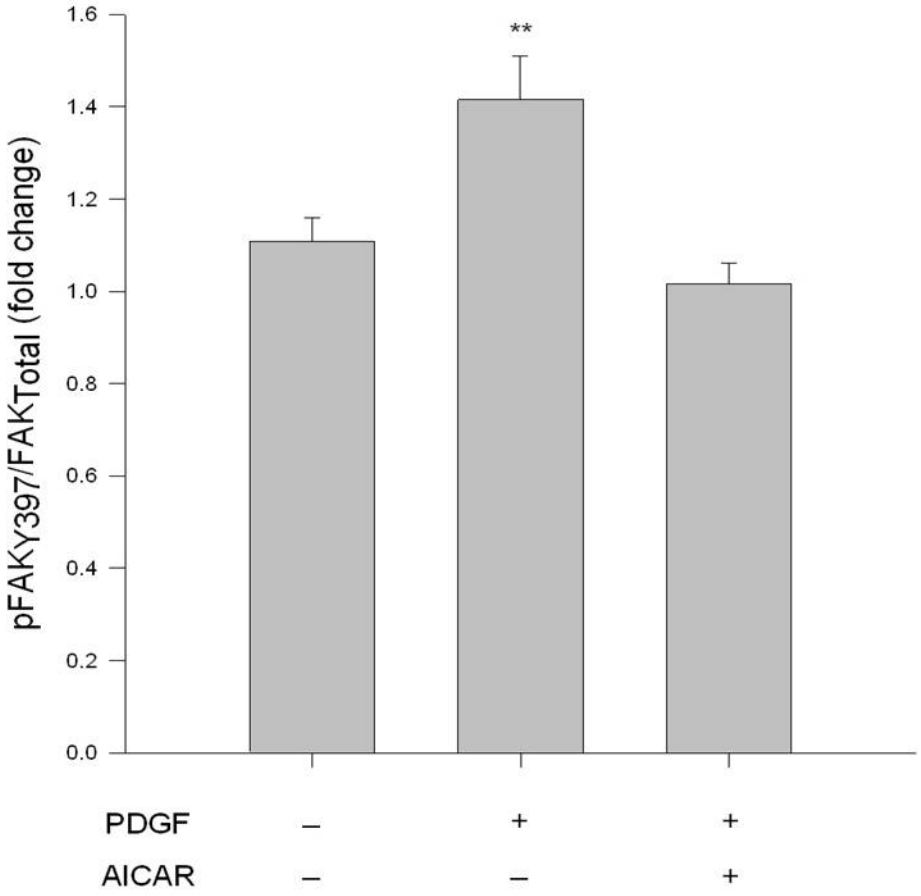

Figure 3.9. AMPK inhibits FAK activity. Cells were treated with PDGFβ (10ng/mL, 60 min) with/without AICAR (1 mM, 60 min), and FAK Tyr397 phosphorylation was measured as an indication of kinase activity. PDGFβ induced significant pFAK Tyr397, which was fully reversed by AICAR. Data are presented at pFAK Tyr397/total FAK and normalized to DNA content (Draq 5/Sapphire 7) for 5-7 separate experiments. P values less than 0.05 were considered statistically significant. ** = $p<0.005$ compared to control.

Another essential component of a functional focal adhesion is paxillin (65, 107). Immunostaining for paxillin on adherent VSMCs shows marked cytoplasmic staining in vehicle-treated cells yet significant nuclear staining in AICAR-treated cells after 24 hours (Fig. 3.10A). Immunofluorescence detected by flow cytometry revealed that total paxillin content was increased after 24 hours compared to controls which was fully reversible in the presence of CC (Fig. 3.10B). Lastly, it has been suggested that paxillin is differentially expressed in each cellular compartment which confers a pro- or anti-migratory signal within the cell (38, 122). In this manner, quantitative data from immunostaining suggest that AICAR promotes nuclear and membranous accumulation of paxillin while preventing cytosolic accumulation after 24 hours compared to vehicle treated cells (Fig. 3.10C).

Figure 3.10

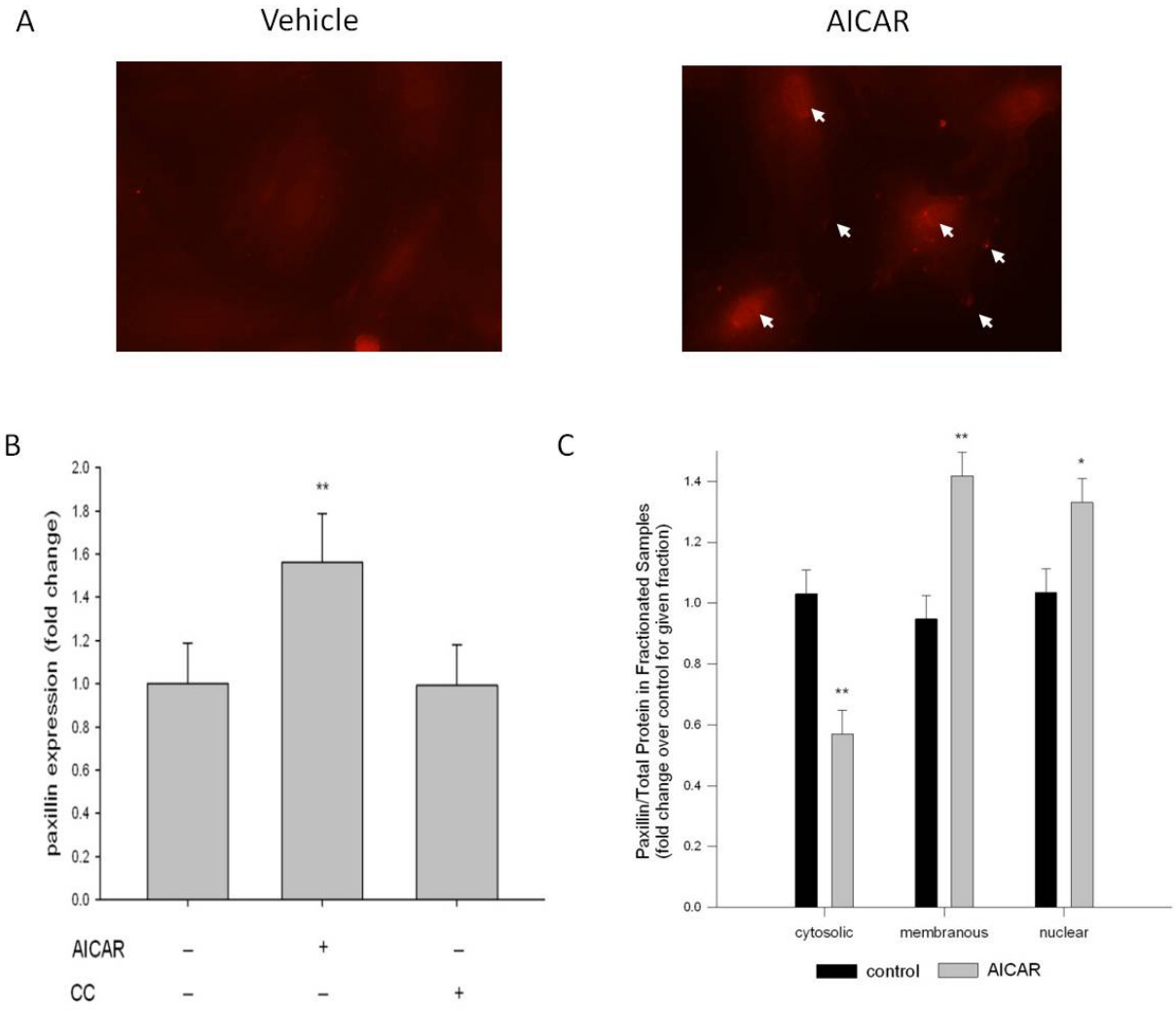

Figure 3.10. AMPK promotes anti-migratory signaling through paxillin. Cells were treated with AICAR **(**1 mM, 60 min), Compound C (CC; 10 uM, 60 min) or a combination of both then either fixed and stained for paxillin or fractionated and probed for paxillin within specific cell compartments. (A) Representative immunofluorescent images suggest widely disperse paxillin staining in vehicle cells while AICAR promotes paxillin accumulation (arrows) within the nucleus and at focal contacts. (B) Protein analysis reveals that AMPK promotes paxillin expression after 24 hours (C) and that this expression is contained within the nuclear and membranous fractions, indicative of anti-migratory signaling via paxillin**.** P values less than 0.05 were considered statistically significant. *= $p<0.05$ compared to control; ** = $p<0.005$ compared to control.

AMPK promotes cell/ECM stability

The extracellular matrix provides a substrate for cellular binding as well as material on which to exert forces necessary for movement. Growth factors and pro-synthetic cytokines promote the production and secretion of matrix metalloproteinases (MMPs) that degrade the extracellular matrix and thus regulate cell motility (68). The gelatinases MMP-2 and MMP-9 are integral to VSMC migration (11, 46, 68). In our study, MMP-specific column zymography on conditioned media from vehicle- or AICAR-treated VSMCs after 24 hours revealed that while no differences were observed in MMP-2 activity between these cohorts (Fig. 3.11A), AICAR significantly reduced MMP-9 activity compared to vehicle controls (Fig. 3.11B). Regarding MMPs, tissue inhibitor of metalloproteinase (TIMP)-1 acts as an extracellular regulator capable of tightly controlling MMP-9 activity. In our study TIMP-1 expression approximately doubled ($p < 0.01$) in conditioned media from AICAR-treated VSMCs compared to vehicle controls after 24 hours (Fig. 3.11D).

Figure 3.11

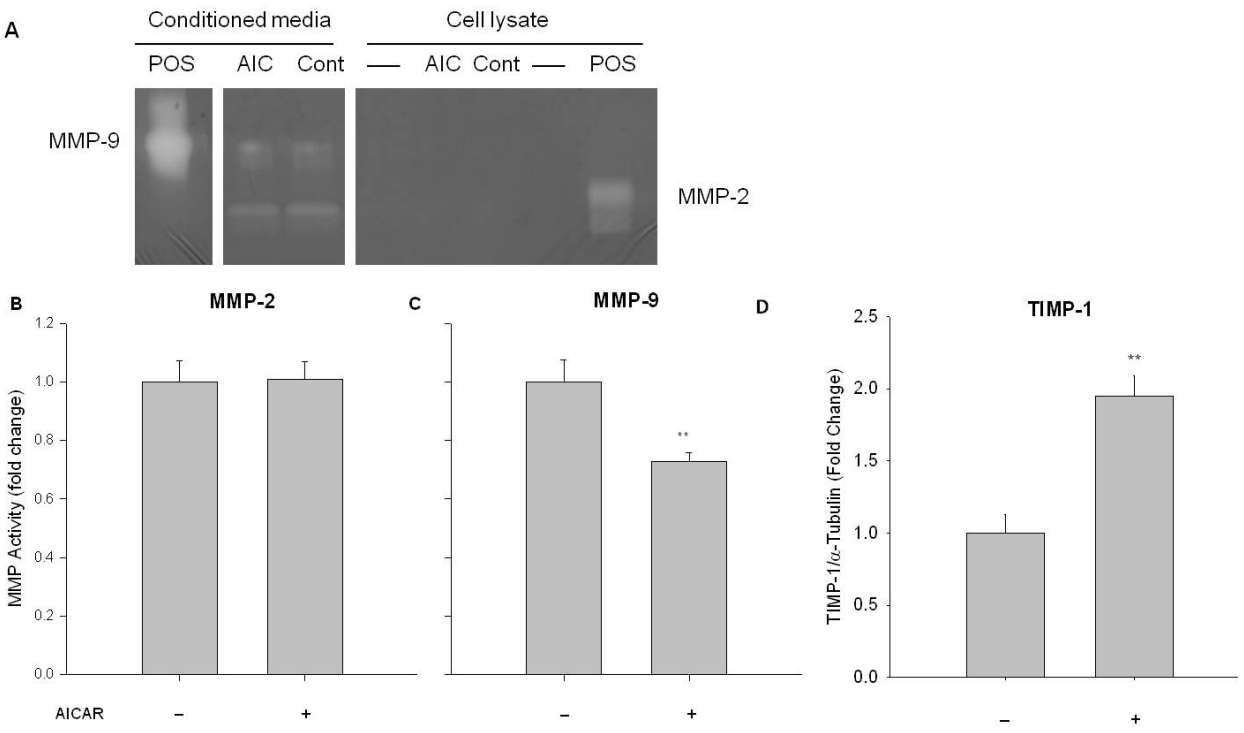

Figure 3.11. AMPK inhibits MMP-9 proteolysis of VSMC extracellular matrix. Cells were treated with either AICAR (1 mM) or Compound C (CC; 10 uM) for 24 hours and conditioned media was collected. Positive controls (POS) are shown on the blot for both MMP-2 and MMP-9. (A) A representative column gel zymogram for MMP activity reveals that while no changes were observed for MMP-2 in the presence of induced AMPK (B), AMPK selectively inhibits MMP-9 activity in conditioned media of AICAR treated cells as compared to controls (C). Gel zymograms were run on the same gels, but images were separated to exclude empty lanes (denoted as dashes in cell lysate columns). (D) Traditional Western blot reveals that AMPK significantly increases expression of the MMP-9 inhibitor TIMP-1 in conditioned media of AICAR-treated cells compared to controls after 24 hours. P values less than 0.05 were considered statistically significant. ** = $p<0.005$ compared to control.

Discussion

Findings in this study support our hypothesis that AMPK has capacity to reduce arterial remodeling via inhibition of VSMC proliferation and migration. Data suggest that AMPK, stimulated via two distinct pharmacologic approaches, operates by provoking cell cycle arrest through a PP-2A/cyclin B mechanism and by preventing cytoskeletal/focal adhesion restructuring necessary for VSMC migration. These findings offer unique insight into AMPK signaling as a novel system with significant therapeutic potential in the remediation of vascular growth disorders. Smooth muscle-mediated vascular remodeling plays a pivotal role in the onset and complication of vasculoproliferative diseases (44, 62, 77); therefore, targeted therapies are of great clinical importance. Data presented here lend strong support for AMPK as a biologically active signaling molecule within VSM capable of curbing cell migration and proliferation and extracellular matrix turnover, all major players in pathologic vascular remodeling.

Using the well established balloon injury model to induce VSMC-mediated vessel remodeling (109, 114, 116), we illustrate here that both systemic dosing and local application of the AMPK agonist AICAR is sufficient at inducing AMPK activity and at markedly reducing neointimal formation (Figs. 3.1, 3.2). The use of AICAR and CC has been established in our lab (99) and by others to respectively promote or inhibit AMPK activity, and both agents have been utilized *in vivo* (25, 67) and *in vitro* (14, 29, 99, 121) in VSM. In an effort to confirm the results observed by treatment with AICAR, we also utilized a specific and non-metabolic agonist of AMPK, the small molecule A-769662. This agent has been documented to directly activate AMPK in cell-free systems, in

intact cells, and *in vivo* without the side effects associated with the more traditional AMPK-activating biguanides (30). Importantly, A-769662 has been recently characterized for use in activating AMPK in vascular cells (73). Specifically, in our current study considering that the rat artery balloon injury model represents an *in vivo* proof-of-concept of our *in vitro* findings using isolated primary VSM cells, we used A-769662 in the *in vivo* model to further validate our findings with AICAR. The results obtained from localized treatment of injured vessels with A-769662 paralleled the results obtained with use of AICAR, thus confirming that the *in vivo* results as well as those obtained *in vitro* could be attributed to AMPK and not off-target drug-specific effects. Results using localized, perivascular delivery of AICAR or A-769662 are noteworthy and represent the first report demonstrating that local delivery of AMPK agonists immediately following intervention are biologically effective. Often, an *a priori* treatment to reduce vessel remodeling is not possible and systemic therapies can suffer from undesired side effects; however, localized delivery of an agent at the time of vascular intervention capable of reducing iatrogenic complications offers high clinical translation.

In order to examine underlying mechanisms of growth suppression by AMPK, in rat primary VSMCs following verification of the biologic activity of AICAR (Fig. 3.3) we show its ability to significantly reduce cell numbers through inhibition of cell cycle progression (Fig. 3.4). Flow cytometry revealed that AICAR exerts cytostasis in the G0/G1 and S phases with concomitant reduction in progression through to the G2/M phase. Of note, no changes in cell viability were observed in any treatment group; therefore, the observed changes in cell number are likely due directly to alterations in cell cycle progression and not from overt cytotoxicity. Additionally, a significant reduction in the

cell numbers of CC-treated cells after 48 hours was observed and is complemented by a non-significant reduction in G2/M cells after 24 hours. It is possible to explain these phenomena by recent findings from collaborating investigators that revealed non-AMPK cytostatic effects of CC alone (74). Also, CC exhibits irreversible inhibitory actions on AMPK (33), and without a functional AMPK system it is plausible to speculate that the metabolic status of the cell could be compromised in such a way that after 48 hours CC may induce cytotoxic effects.

It was previously suggested that AMPK has ability to promote cytostasis by cyclin-dependent kinase inhibition via a p53/p21 pathway in a commercialized human VSM cell line (43) or through a Skp2/$p27^{Kip1}$ pathway in AMPK-deficient mouse VSMCs (97). While intriguing and relevant to the current study, these previous reports seem somewhat contradictory; therefore, in addition to these findings, alternate mechanisms by which AMPK inhibits cell cycle progression are plausible. It has been reported that PP-2A has the ability to disrupt the cdc/cyclin B complex and inhibit G_2/M progression. Since our cell cycle analysis reveals a large increase in S-phase cells, we investigated the hypothesis that PP-2A contributes to the mechanism for AMPK inhibition of VSMC proliferation. Data presented here suggest that AMPK induces PP-2A activity (Fig. 3.5A) and concomitantly reduces cdc2/cyclinB expression after 24 hours (Fig. 3.5B), thus supporting the hypothesis that AMPK works, at least in part, through PP-2A/cyclin B to induce S-phase cytostasis.

In addition to proliferation, VSMC migration is pivotal in the pathophysiology of vessel remodeling. In this study we demonstrate that AMPK plays a key role in the inhibition of VSMC migration using two distinct experimental approaches, a modified

transwell chemotaxis assay and a wounding assay. The physical movement of cells across a substrate is a complex process highly dependent upon the actin cytoskeleton and its interface with focal contacts and the extracellular matrix. We present one of the first reports of how AMPK may act to inhibit VSMC migration, which could offer significant therapeutic insight for the curbing of disease processes that arise from an induction of cell migration. Novel data presented here reveal possible mechanisms by which AMPK inhibits VSMC migration. Actin polymerization and leading edge formation are critical for directional cellular movement; however, AMPK impairs actin polymerization, presumably by inhibiting the anti-capping potential of VASP through direct, site-specific phosphorylation (9). Here we observed significant enhancement of pVASP at the AMPK-sensitive T278 site by AICAR (Fig. 3.7). The resulting impairment of actin polymerization is evidenced by concomitant accumulation of G-actin in the cytosol and increased stress fiber formation in cultured VSMCs (Fig. 3.8). Thus, these data argue convincingly that AMPK hinders cytoskeletal rearrangement necessary for VSMC migration as part of its mechanism of growth retardation.

Unique findings presented here also reveal that AMPK has potential to inhibit focal adhesion turnover necessary for the movement of cells across or through substrata. We show that AICAR treatment impairs FAK activation by inhibiting Tyr397 phosphorylation (Fig. 3.9), a necessary event for kinase activity (107). Upon activation, FAK induces paxillin phosphorylation and targets GTPase activity at the focal adhesion allowing for focal contact release (107). Therefore, inhibition of FAK activity offers another possible mechanism by which AMPK mediates inhibition of migration. Additionally, it has been suggested that paxillin acts as a bi-directional membrane-to-

nucleus signaling molecule and that differential accumulation of paxillin in distinct cellular compartments is indicative of either a pro- or anti-synthetic/migratory event (38, 122). Our data reveal that AICAR prevents cytosolic accumulation of paxillin while promoting nuclear accumulation and membrane stability (Fig. 3.10). Taken together, these data reveal a novel and intriguing anti-migratory signaling network via AMPK-mediated inhibition of FAK and FA/paxillin dissociation, thereby reducing pro-migratory signals and promoting focal adhesion stability and growth suppression.

To more comprehensively address the biophysics of migrating and synthetic VSMCs, we assessed activity of the extracellular matrix (ECM)-degrading gelatinolytic MMPs. Upon activation, VSMCs produce and secrete MMP-2 and MMP-9 that act to degrade the ECM thereby allowing for VSMC expansion/migration and collagen deposition (11, 46, 68). Here we show that AICAR selectively impairs MMP-9 activity and enhances inhibitory TIMP-1 expression (Fig. 3.11), which we suggest promote a more stable FA via reduced extracellular matrix degradation thus increasing FA/substratum connectivity. Combined, these data suggest a novel role for AMPK in the reduction of MMP-9 activity that may play a key role in the inhibition of cellular migration via enhanced FA contacts as well as matrix-based morphological changes in the vessel wall following injury. Based on our findings, a schematic is shown in Figure 12 depicting cellular signaling actions of AMPK in VSM.

Figure 3.12

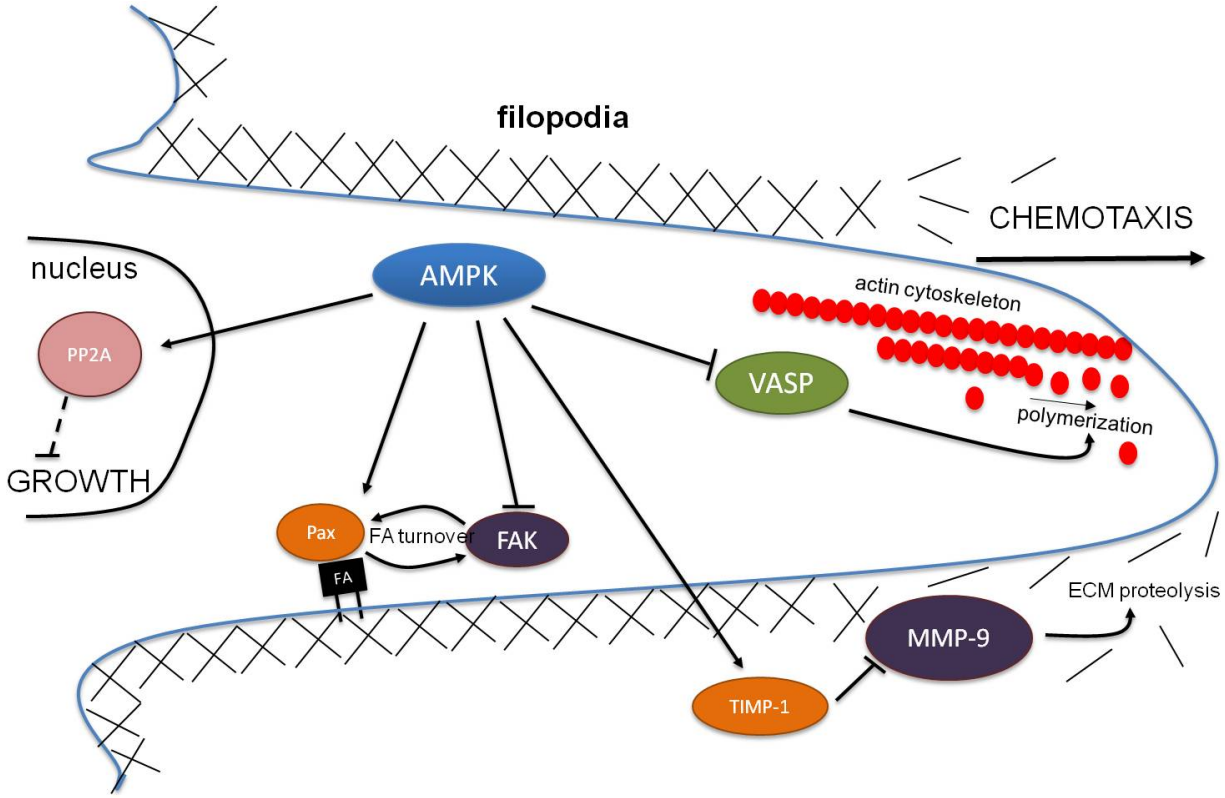

Figure 3.12. Schematic depicting the proposed role of AMPK in the control of VSM growth. In this diagram blunt lines represent proposed inhibitory mechanisms while arrows represent proposed stimulatory mechanisms. Those pathways that were not directly tested in this study but that remain part of our overall hypothesis are presented as dashed lines. Biochemical and functional data described herein suggest that AMPK has ability to inhibit VSMC proliferation by inhibiting cell cycle progression, possibly by increasing PP-2A within the nucleus. Additionally we report that AMPK has ability to inhibit VSMC migration, presumably via inhibition of VASP anti-capping actions on actin polymerization and increasing focal adhesion integrity. Additionally, AMPK shows ability to inhibit extracellular matrix degradation by MMP-9, which we suggest is under control of inhibitory TIMP-1. Taken together, these novel data suggest that AMPK employs both intra- and extra-cellular inhibitory signals to effectively increase VSMC spatial stability while also inhibiting cell cycle progression in an effort to promote cell senescence.

It is important to note that over the 2-week timeframe of our studies there were no observable side effects of AICAR (following either local or systemic dosing) or local A-769662, particularly with body weight, fluid and food intake, or activity. We have previously shown that approximately 60% of the initial localized dose following injury is released over 24 hours (112). This is a reasonable estimate for the duration of AICAR and A-769662 bioactivity following localized dosing. Based on previous studies by our lab using localized dosing of agonists following balloon injury (47, 113, 114), we utilized 1 mg AICAR and 1 mg A-769662 in this study. For systemic dosing of AICAR, previous reports (67) were used to determine an optimal dosing strategy that is devoid of potential side effects.

In conclusion, convincing data presented here provide strong evidence that AMPK is a desirable anti-growth target in VSM. Using the AMPK mimetic AICAR or the AMPK-activating small molecule A-769662, we present *in vivo* and *in vitro* data supporting our claims that AMPK abrogates neointimal formation and reduces VSMC proliferation and migration. Mechanistically, ample evidence suggests that AMPK acts to promote S-phase cytostasis and to inhibit cell migration via stabilizing FA contacts and reducing extracellular matrix turnover, thereby minimizing cytoskeleton reorganization necessary for migration and reducing pro-migratory signals between the membrane and the nucleus. These data paint a comprehensive picture of discrete AMPK-mediated cytostatic signaling networks that have significant clinical relevance in efforts to reduce vasculoproliferative pathologies.

Grants

This project was supported by Award Number R01HL081720 from the National Heart, Lung, and Blood Institute, National Institutes of Health (DAT) and by a Pre-doctoral Fellowship from the American Heart Association (JDS). The content is solely the responsibility of the authors and does not necessarily represent the official views of the National Heart, Lung, and Blood Institute, the National Institutes of Health or the American Heart Association.

Disclosers

None

Author Contributions

Participated in research design: Stone, Tulis

Conducted experiments: Stone, Narine, Shaver, Fox, Vuncannon

Data analysis: Stone

Manuscript preparation: Stone, Tulis

Acknowledgements

We would like to acknowledge the academic and support staff of the Department of Physiology for their assistance. We would particularly like to thank Robert Lust, Ph.D., for his support and tutelage as Department Chair.

Chapter 4: Inhibition of Vascular Smooth Muscle Growth via Signaling Crosstalk between AMP-Activated Protein Kinase and cAMP-Dependent Protein Kinase

Joshua D. Stone; Avinash Narine; M6

.D., David A. Tulis, Ph.D., F.A.H.A.

Published

Front Physiol. 2012;3:409. doi: 10.3389

Abstract

Abnormal vascular smooth muscle (VSM) growth is central in the pathophysiology of vascular disease yet fully effective therapies to curb this growth are lacking. Recent findings from our lab and others support growth control of VSM by adenosine monophosphate (AMP)-based approaches including the metabolic sensor AMP-activated protein kinase (AMPK) and cAMP-dependent protein kinase (PKA). Molecular crosstalk between AMPK and PKA has been previously suggested, yet the extent to which this occurs and its biological significance in VSM remains unclear. Considering their common structural AMP backbone and similar biochemical signaling characteristics, we hypothesized that crosstalk exists between AMPK and PKA in the regulation of VSM growth. Using rat primary VSM cells, the AMPK agonist AICAR significantly increased AMPK activity and phosphorylation of the catalytic Thr172 site on AMPK. Interestingly, AICAR also phosphorylated a suspected PKA-inhibitory Ser485 site on AMPK, and these cumulative events were reversed by the PKA inhibitor PKI suggesting possible PKA-mediated regulation of AMPK. AICAR also increased PKA activity in reversible fashion. The cAMP stimulator forskolin increased PKA activity and completely ameliorated Ser/Thr protein phosphatase-2C activity, suggesting a potential mechanism of AMPK modulation by PKA since inhibition of PKA by PKI reduced AMPK activity. Functionally, AMPK inhibited serum-stimulated cell cycle progression and cellular proliferation; however, PKA failed to do so. Moreover, AMPK and PKA independently reduced PDGF-β-stimulated VSM cell migration. Collectively, these results show that AMPK is capable of reducing VSM growth in both anti-proliferative and anti-migratory fashions. Furthermore, these data suggest that AMPK may be

modulated by PKA and that positive feedback may exist between these two systems. These findings reveal a discrete nexus between AMPK and PKA in VSM and provide basis for metabolically-directed targets in reducing pathologic VSM growth.

Introduction

Cyclic adenosine monophosphate (cAMP) and its canonical downstream kinase PKA are critical signaling factors that exert a variety of functional effects in cardiac and vascular tissues. It is reported that Thr197 of the catalytic subunit of PKA is phosphorylated in proportion to PKA activity (94, 98) and is a more precise indicator of activity than the previously reported Ser338 moiety (96); however, the exact phospho-specific mechanisms of activation of PKA and their impact on kinase efficacy in VSM remain unclear.

It has been previously suggested that a biochemical relationship may exist between AMPK and PKA (19, 42, 52), although the exact nature of this relationship and the extent to which they relate in VSM is uncertain. The cyclic AMP/PKA system, like AMPK, has ability to enhance vasodilation (117, 127) and inhibit vessel growth (18, 39). Additionally, PKA and AMPK exhibit capacity either discretely or collectively to regulate cellular metabolism, and coordination between their pathways has been reported to exist either synergistically (16, 21, 80) or antagonistically (19, 119), depending the contextual metabolic demands and the tissue type. Cellular proliferation is normally under tight metabolic control, and although little work has been done to elucidate the relationship between these two signaling systems in the control of cellular growth, crosstalk has been implicated in the inhibition of cancer cell hyperplasia (32, 60). Therefore, it is intriguing to speculate that crosstalk may exist between PKA and AMPK in VSM and that this crosstalk may be of biological significance in its ability to modulate VSM growth.

The purpose of this study was to further characterize the AMPK and PKA signaling pathways and to determine what role(s) they play in the collaborative inhibition of VSM growth. Our hypothesis was that AMPK and PKA possess biochemical crosstalk and, in turn, may act cooperatively to inhibit VSMC proliferation and migration. Novel results show that AMPK controls VSMC proliferation and migration and that these events are regulated at least in part by PKA. These findings offer insight to a potential metabolic signaling network that may provide new therapeutic targets for control and potential reduction of vascular growth disorders.

Results

AMPK enhances PKA activity

Initial experiments focused on activation of AMPK in rat primary VSMCs. Treatment of cells with 1 mM of the AMPK agonist AICAR **(**60 min), a concentration previously documented to effectively induce AMPK activity in vascular cells without observable side-effects (14, 29), significantly enhanced catalytic phosphorylation (121) of AMPK Thr172 (Fig. 4.1A) as well as acetyl Co-A carboxylase (ACC) at Ser80 (Fig. 4.1B), a traditional marker of AMPK activity (120)**.** Both basal and AICAR-stimulated pAMPK-Thr172 and pACCSer80 were inhibited by 30 min pre-treatment with Compound C (CC; 10 uM), a selective AMPK inhibitor established for use in VSM (14, 97, 103)**.** Intriguingly, inhibition of PKA with PKI (10 uM) also reversed AICAR-induced increases in AMPK-Thr172 and ACC-Ser80 phosphorylation (Figs. 4.1A, 4.B). In agreement, using an AMPK-specific activity assay AICAR induced a significant increase in AMPK activity that was reversed by CC and PKI under stimulated conditions and by CC under basal conditions (Fig. 4.1C).

Figure 4.1

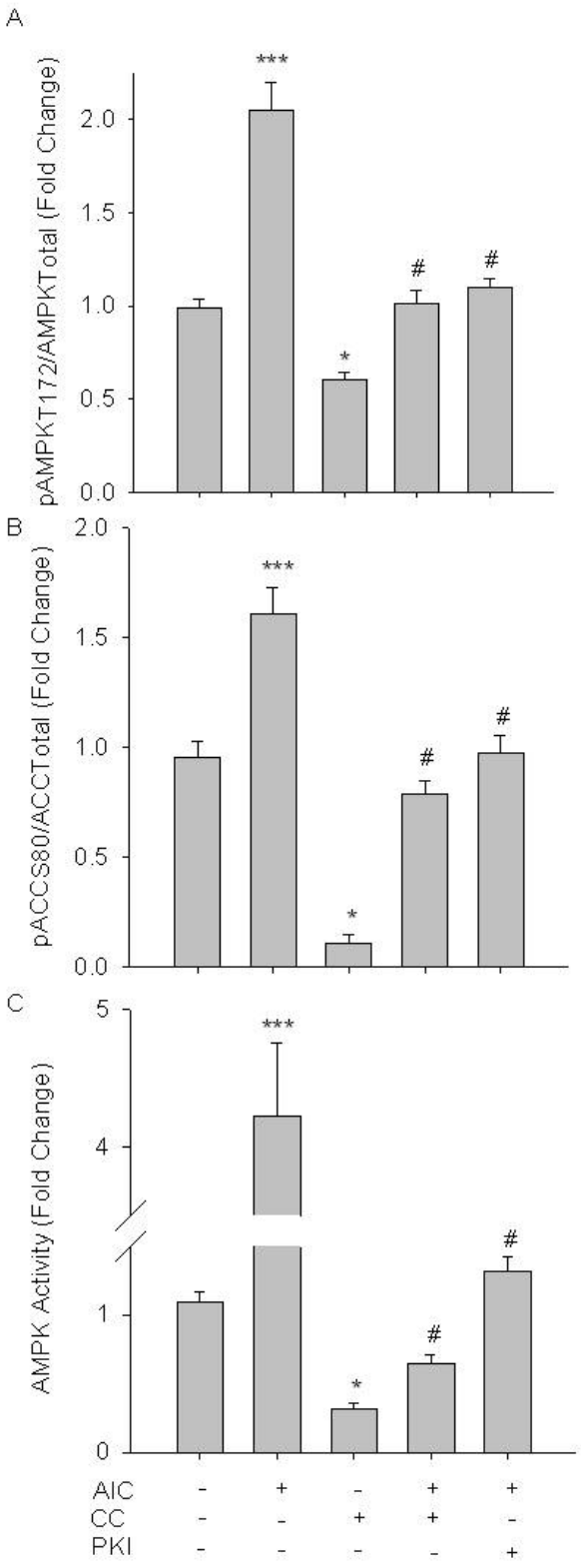

Figure 4.1. AICAR increases AMPK signaling in rat primary VSMCs as measured via InCell Western blotting. Cells were treated with AICAR (1 mM), Compound C (CC; 10 uM) or their

combination for 60 min and AMPK Thr172 phosphorylation (A), ACC Ser80 phosphorylation (B), and AMPK activity (C) were measured. AICAR significantly increased phosphorylation of both AMPK Thr172 (A) and ACC Ser80 (B) as well as AMPK activity (C), all in CC-reversible fashion. CC also significantly reduced basal levels of phosphorylated AMPK Thr172, ACC Ser80 and AMPK activity. In all cases addition of the PKA-inhibitor PKI significantly decreased AMPK signaling and activity. Expression data were normalized to DNA content (Draq 5/Sapphire 700) and presented as phosphorylated AMPK/total AMPK (A) or phosphorylated ACC/total ACC (B). Activity was measured via absorbance at 450 nm. P values less than 0.05 were considered statistically significant for n=5-7 per group. * $p<0.05$ compared to control; *** $p<0.001$ compared to control; # $p<0.05$ compared to respective activator treatment.

Considering relative novelty of the In-Cell Western approach, traditional ECL-based Western blotting was used in primary cell lysates to support In-Cell Western results for these initial experiments. VSMC lysates were probed for pAMPK Thr172 and pACC Ser80 as indicators of AMPK activity. As shown in Figure 4.2, AICAR (1 mM, 60 min) increased AMPK catalytic phosphorylation and downstream ACC signaling as documented through ECL-based Western blotting (Figs. 4.2A and 4.2B). AICAR-mediated increases in pAMPK and pACC were then reduced to control levels in the presence of CC (data not shown). These findings confirm our In-Cell Western results and establish utility of the In-Cell Western approach in primary VSM preparations.

Figure 4.2

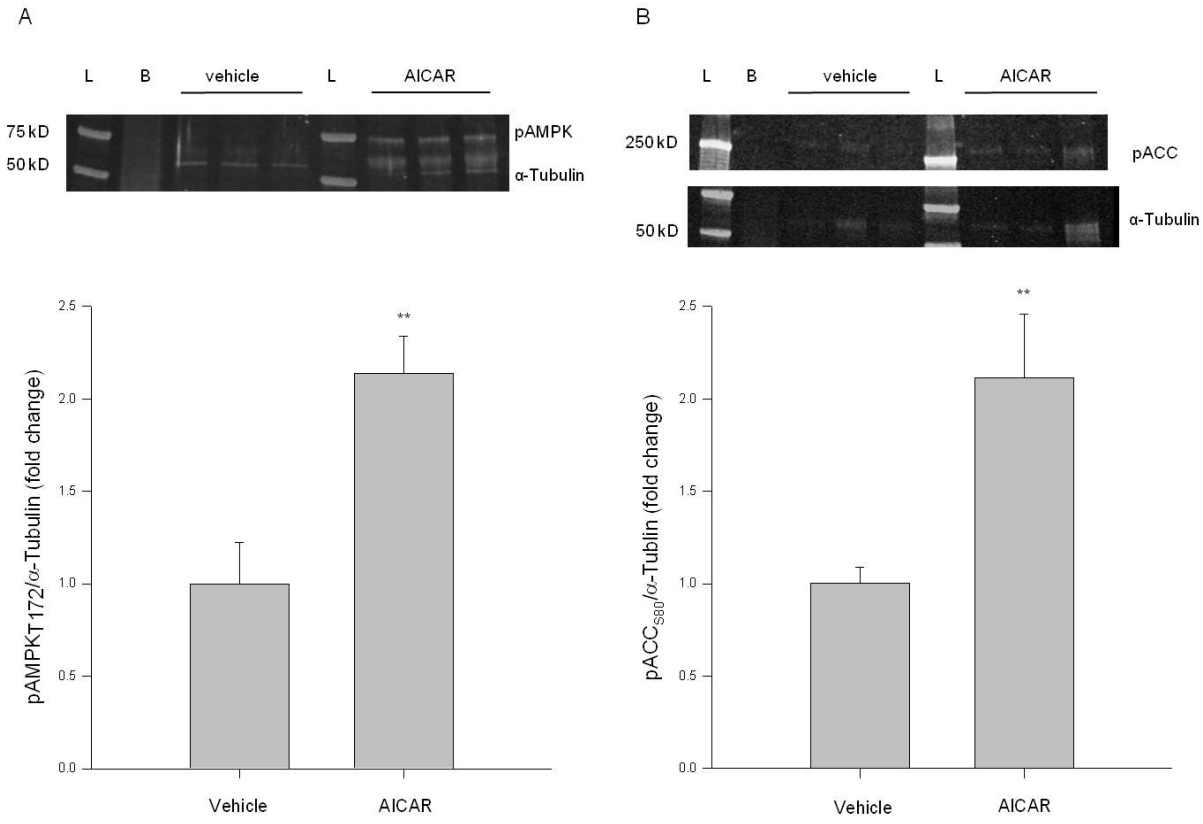

Figure 4.2. AICAR increases AMPK signaling in rat primary VSMC lysates as measured via ECL-based Western blotting. Cells were treated with AICAR **(**1 mM) for 60 min and AMPK Thr172 phosphorylation (A) and ACC Ser80 phosphorylation (B) were measured by traditional ECL-based Western blotting using IR-linked antibodies. AICAR significantly increased phosphorylation of both AMPK Thr172 (A) and ACC Ser80 (B). Phosphorylated protein levels were normalized to α-tubulin and data presented as fold change over control values. P values less than 0.05 were considered statistically significant for n=3 per group. ** $p<0.01$ compared to control.

Studies were then performed to evaluate the influence of AMPK on PKA signaling. AICAR induced a significant increase in vasodilator-stimulated phosphoprotein (VASP) Ser157 phosphorylation, a reported marker of active PKA (22, 47), and this was completely reversed by CC (Fig. 4.3A). Additionally, co-treatment of AICAR with a PKA

inhibitor PKI (10 uM; 60 min) also reversed AICAR-induced phosphorylation of VASP Ser157 (Fig. 4.3A). Furthermore, using an activity assay AICAR induced a significant increase in PKA activity which was also fully reversed by CC and PKI (Fig. 4.3B). Neither basal levels of pVASP Ser157 nor PKA activity were affected by CC.

Figure 4.3

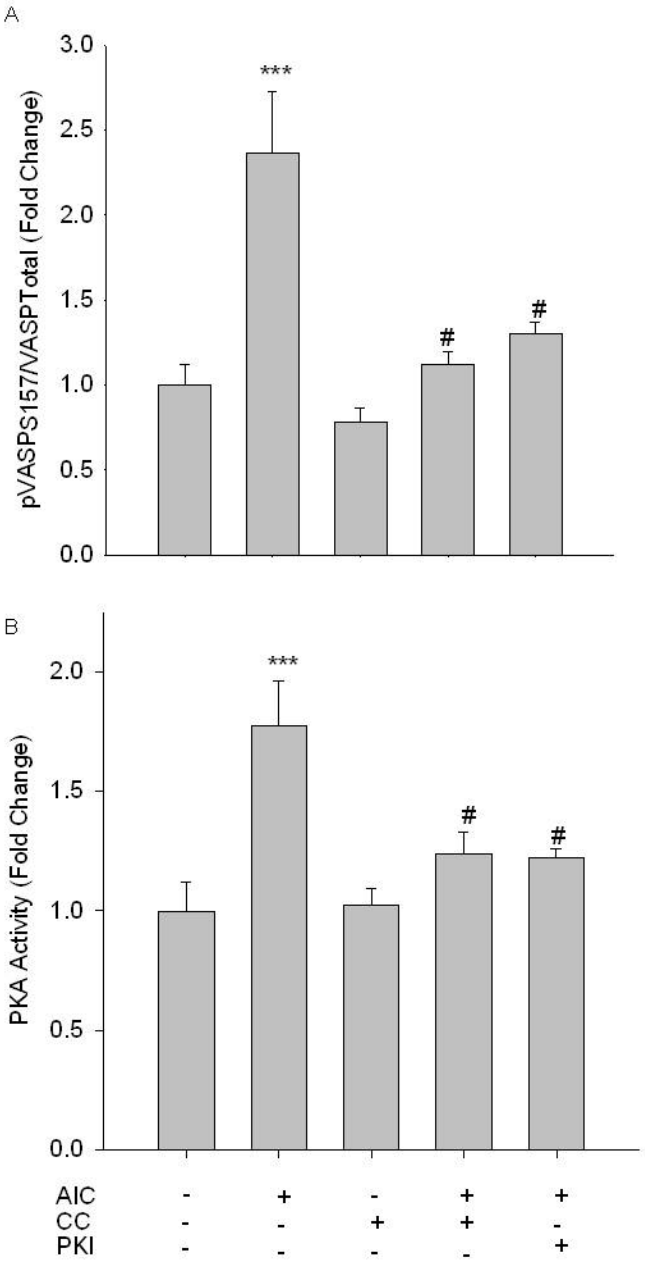

Figure 4.3. AMPK enhances PKA activity. Cells were treated with AICAR (1 mM), Compound C (CC; 10 uM) or a combination of both, and/or PKI (10 uM) for 60 min, and phosphorylation of VASP at Ser157 (A) and PKA activity (B) were measured. In-Cell Western analysis revealed that AICAR significantly increased VASP Ser157 phosphorylation (A). A PKA activity assay shows that AICAR increased PKA activity (B). Both analyses revealed full reversal with concomitant CC and/or PKI. Data are presented as phosphorylated VASP/total VASP and normalized to DNA content (Draq 5/Sapphire 700) or absorbance at 450 nm for activity. P values less than 0.05 were considered statistically significant for n=5-7 per group. *** $p<0.001$ compared to control; # $p<0.05$ compared to respective activator treatment.

PKA preserves AMPK activity

While phosphorylation of PKA at Thr197 is suggested to be indicative of catalytic activity (98), neither the adenylyl cyclase agonist Forskolin (FSK, 10 uM; 60 min) nor AICAR induced changes in phosphorylation of this site (data not shown). However, treatment of VSMCs with FSK with or without the broad phosphodiesterase (PDE) inhibitor IBMX (10uM; 60 min) induced significant increases in pVASP Ser157, which were reversed by the PKA inhibitor PKI (10 uM; Fig. 4.4A). In addition, using an activity assay, while FSK alone induced a non-significant increase in PKA activity, addition of IBMX induced a significant increase in PKA activity that was reversed by PKI (Fig. 4.4B). Additionally, concomitant treatments of FSK and AICAR significantly increased PKA activity (Fig. 4.4B).

Figure 4.4

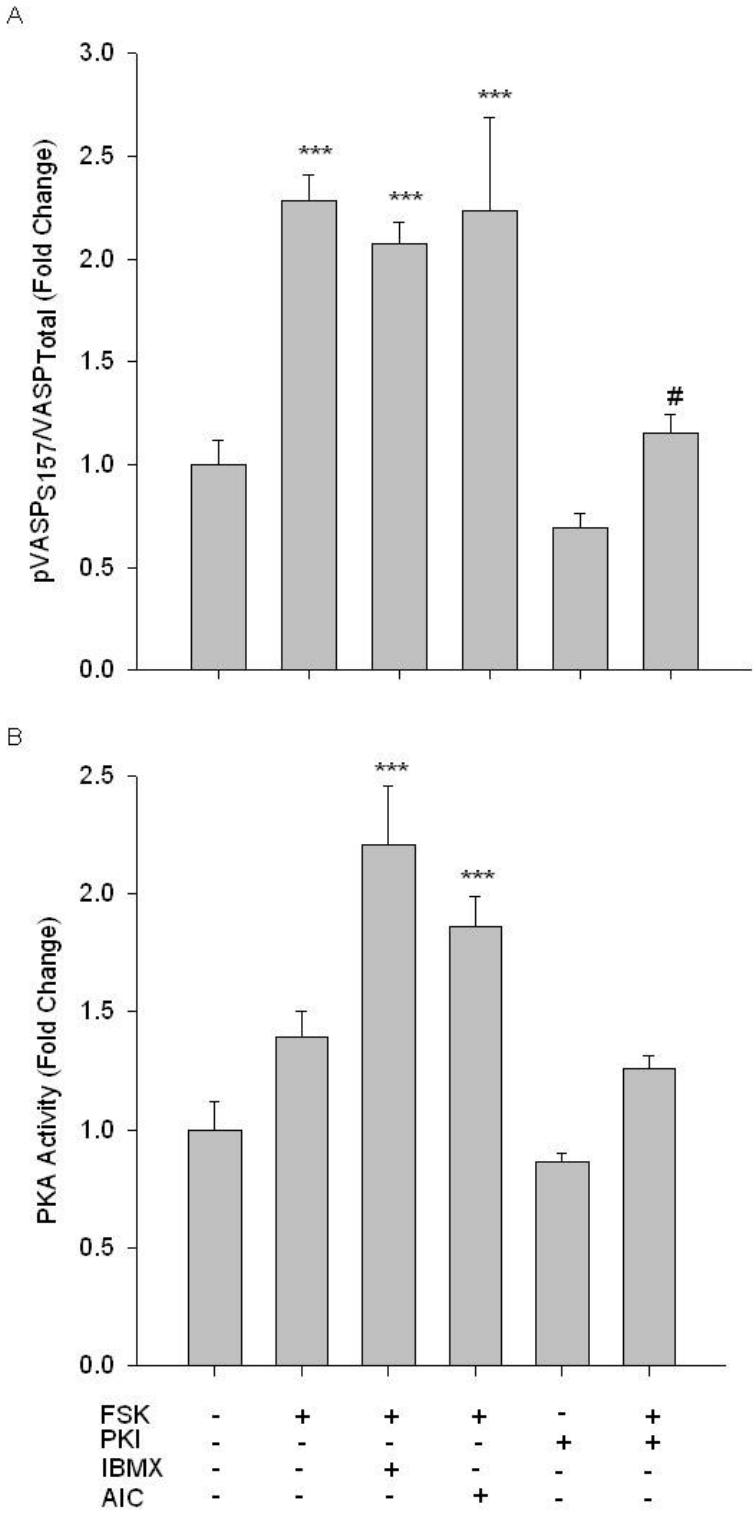
A
3.0
2.5
2.0
1.5
1.0
0.5
0.0
pVASPS157/VASPTotal (Fold Change)
***
***
***
#
B
2.5
2.0
1.5
1.0
0.5
0.0
PKA Activity (Fold Change)
***
***
FSK - + + + - +
PKI - - - - + +
IBMX - - + - - -
AIC - - - + - -

Figure 4.4. FSK increases PKA signaling in rat primary VSMCs. Cells were treated with combinations of FSK (10uM), PKI (10 uM), IBMX (10 uM), and/or AIC (1 mM) for 60 min and pVASP Ser157 phosphorylation and PKA activity were determined. In-Cell Westerns revealed that FSK significantly increased pVASP Ser157 alone or in the presence of IBMX and/or AICAR, and these were largely reversed with the PKA inhibitor PKI (A). A PKA activity assay revealed that FSK with IBMX or AIC synergistically increased PKA activity (B). Data are presented as phosphorylated VASP/total VASP and normalized to DNA content (Draq 5/Sapphire 700) or absorbance at 450 nm for activity. P values less than 0.05 were considered statistically significant for n=3-5 per group. *** $p<0.001$ compared to control; # $p<0.05$ compared to respective activator treatment.

Next, studies were performed to evaluate if PKA mediates changes in AMPK signaling. FSK alone failed to alter pAMPK Thr172; however, when PDE activity was inhibited by IBMX, a significant increase in pAMPK Thr172 was observed (Fig. 4.5A). Intriguingly, synergistic responses in pAMPK Thr172, pACC Ser80, and specific AMPK activity were observed with co-treatments of FSK and AICAR (Fig. 4.5). Also of note, PKI alone induced a significant inhibitory effect on basal AMPK activity, which returned to control levels with FSK co-treatment (Figs. 4.5A, 4.5C).

Figure 4.5

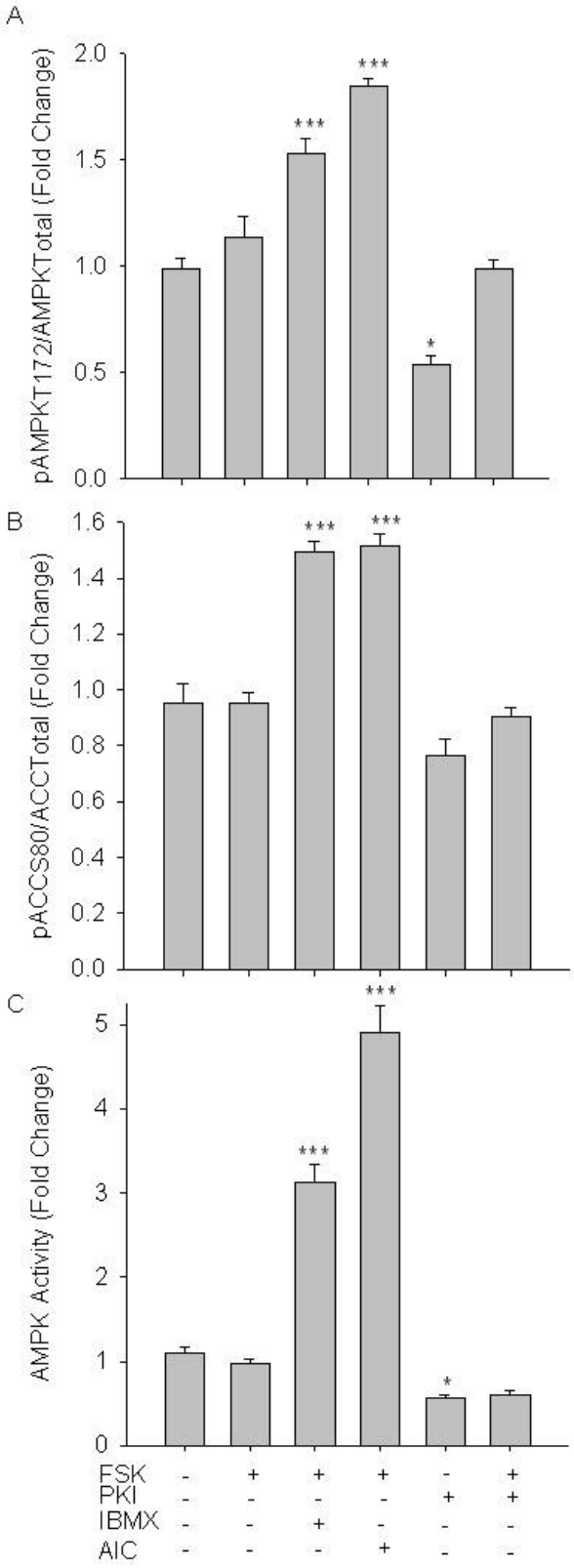
A
pAMPKT172/AMPKTotal (Fold Change)
2.0
1.5
1.0
0.5
0.0
***
***
***
*
B
pACCS80/ACCTotal (Fold Change)
1.6
1.4
1.2
1.0
0.8
0.6
0.4
0.2
0.0
***
***
C
AMPK Activity (Fold Change)
5
4
3
2
1
0
***
***
*
FSK - + + + - +
PKI - - - - + +
IBMX - - + - - -
AIC - - - + - -

Figure 4.5. PKA increases AMPK activity in VSMCs. Cells were treated with FSK **(**10 uM), PKI (10 uM) or a combination of FSK and PKI or IBMX (10 uM) or AIC (1 mM) for 60 min. Phosphorylation of AMPK Thr172 and ACC Ser80 were measured by In-Cell Western (A) and (B) and AMPK activity was measured by pAMPK-specific activity assay (C). FSK alone failed to significantly increase AMPK Thr172 or ACC Ser80 phosphorylation or AMPK activity; however, in the presence of IBMX or AICAR all were significantly elevated. PKI alone significantly reduced both pAMPK Thr172 and activity. Data are presented as phosphorylated AMPK/total AMPK and normalized to DNA content (Draq 5/Sapphire 700) or absorbance at 540 nm for activity. P values less than 0.05 were considered statistically significant for n=5-7 per group. * $p<0.05$ compared to control; *** $p<0.001$ compared to control.

Considering that phosphorylation at Ser485 has been associated with an inhibition of AMPK activity (69, 102), we investigated pAMPK Ser485 expression under both AMPK- and PKA-stimulated and -inhibited conditions. In primary VSMCs, AICAR induced a significant increase in pAMPK Ser485, which was fully reversed by CC (Fig. 4.6A). CC alone failed to significantly alter basal pAMPK Ser485 levels. While FSK with or without IBMX failed to significantly alter Ser485 phosphorylation, treatment with PKI alone significantly reduced basal pAMPK Ser485, which returned to control levels with concomitant FSK treatment (Fig. 4.6B).

Figure 4.6

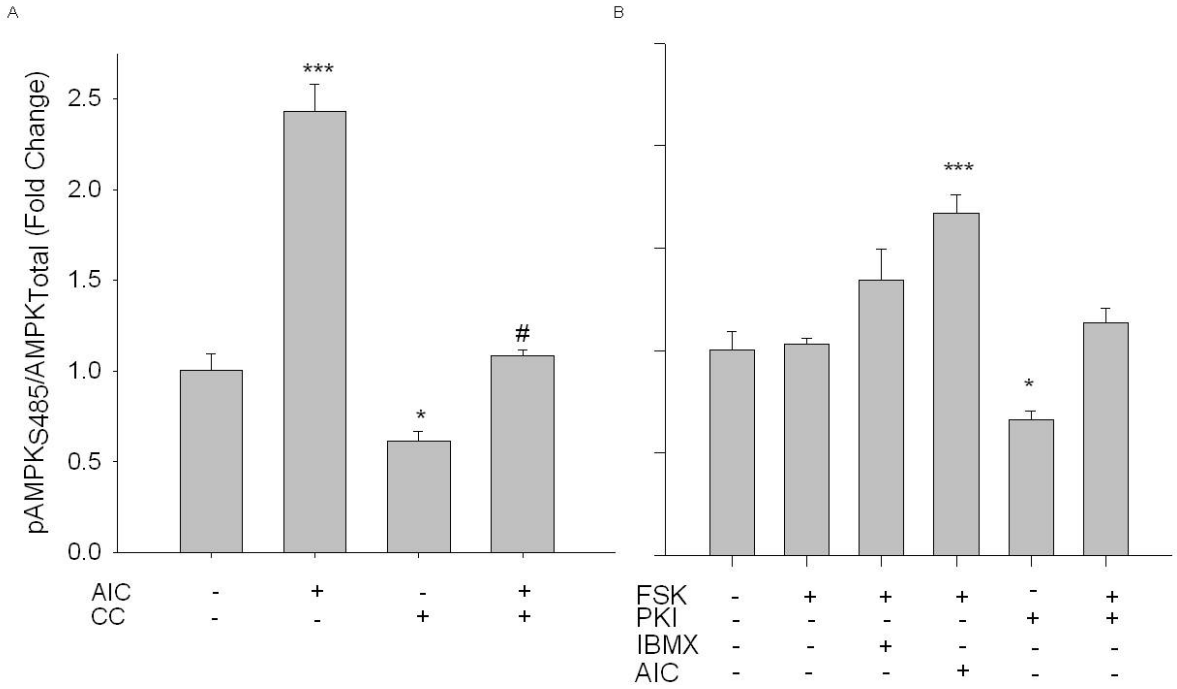

Figure 4.6. AICAR increases phosphorylation of AMPK at Ser485 in PKA-independent fashion. (A) Cells were treated with AICAR **(**1 mM), Compound C (CC; 10 uM) or a combination of both for 60 min, or (B) with FSK **(**10 uM), PKI (10 uM) or a combination of both, or IBMX (10 uM), or AICAR (1 mM) for 60 min. In-Cell Western analyses revealed that (A) pAMPK Ser485 was elevated with AICAR in a CC-reversible fashion. While FSK with/without IBMX had no effect on pAMPK Ser485, FSK + AICAR did significantly increase pAMPK Ser485. Intriguingly, PKI alone significantly decreased Ser485 phosphorylation. Data are presented as phosphorylated AMPK/total AMPK and normalized to DNA content (Draq 5/Sapphire 700). P values less than 0.05 were considered statistically significant for n=5-7 per group. * $p<0.05$ compared to control; *** $p<0.001$ compared to control; # $p<0.05$ compared to respective activator treatment.

PKA Inhibits Protein Phosphatases

Serine/Threonine protein phosphatases (PPs), in particular PP-2A and PP-2C (51), have been reported to negatively modulate AMPK activity via kinase dephosphorylation. Therefore, we assessed the ability of PKA to inhibit Ser/Thr PP activity as a possible mechanism of PKA-mediated modulation of AMPK activity. Surprisingly, treatment of VSMCs with AICAR steadily increased global PP activity in significant fashion compared to vehicle-treated control lysates (Fig. 4.7A). Intriguingly, FSK treatment completely inhibited global PP activity in VSMC lysates compared to controls (Fig. 4.7A). With addition of $NiCl_2$ (1 mM) to the reaction buffer to specifically monitor PP-2A activity (72), we found that AMPK specifically activated PP-2A in AICAR-treated lysates compared to controls while no differences were detected in FSK-treated cells (Fig. 4.7B). Likewise, when $MgCl_2$ (20 mM) was added to the reaction buffer to selectively monitor PP-2C (72), we found that FSK specifically and completely inhibited PP-2C levels compared to controls with no differences detected in AICAR-treated lysates (Fig. 4.7C). Importantly, cumulative reductions in PP activity observed in these experiments (global, PP-2A, PP-2C) were reversible with simultaneous CC- or PKI-inhibition of AMPK or PKA, respectively (data not shown for clarity).

Figure 4.7

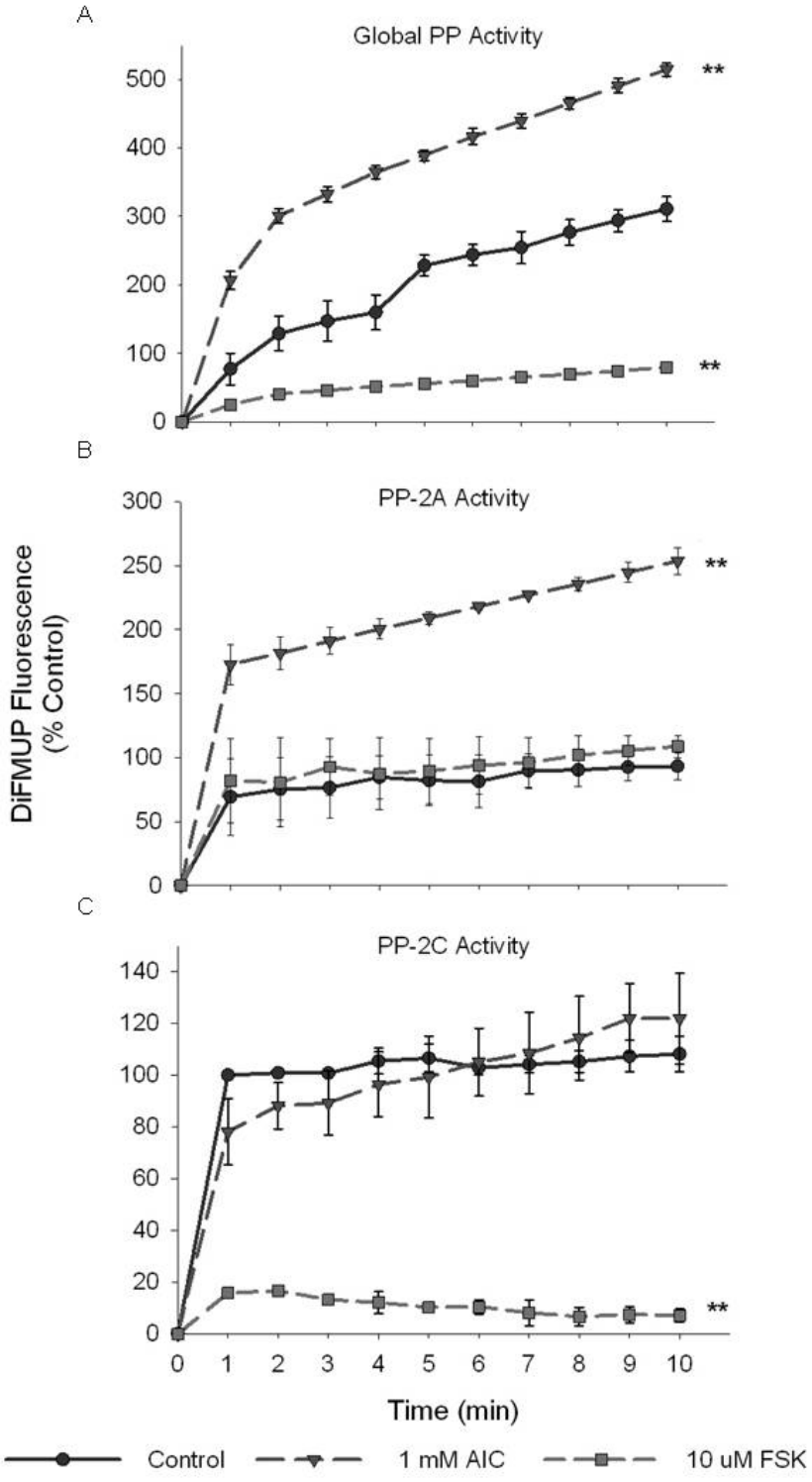
A
Global PP Activity
500
400
300
200
100
0
**
**
B
PP-2A Activity
DiFMUP Fluorescence (% Control)
300
250
200
150
100
50
0
**
C
PP-2C Activity
140
120
100
80
60
40
20
0
**
0 1 2 3 4 5 6 7 8 9 10
Time (min)
Control
1 mM AIC
10 uM FSK

Figure 4.7. PKA inhibits global and isoform-specific Ser/Thr phosphatase activity. Cell lysates were prepared from cells treated with AICAR **(**1 mM), or a combination of both AICAR and Compound C (CC; 10 uM) for 60 min, or with FSK **(**10 uM), or a combination of FSK and PKI (10 uM) for 60 min. Phosphatase activity of diluted (1:10) lysate samples was measured by DiFMUP fluorescence at 452 nm after 10 minutes of incubation in the dark. Activity analysis revealed that AICAR induced while FSK inhibited global Ser/Thr phosphatase activity compared to control values (A). With addition of $NiCl_2$ (1 mM) to the reaction buffer, PP-2A-specific activity was tested and revealed that AICAR significantly elevated PP-2A activity (B). Similarly, with addition of $MgCl_2$ (20 mM), DTT (2 mM), and EGTA (1 mM) to the assay buffer, PP-2C-specific activity was assessed and revealed that FSK significantly inhibited its activity (C). Two-way ANOVA with Tukey's post-hoc testing was used for multiple comparisons across time points as well as within each treatment group. P values less than 0.05 across time within each group were considered statistically significant for n=3 per group. ** $p<0.01$ compared to control.

Cooperative signaling inhibits VSMC proliferation and migration

The functional impact of these signaling events was assessed in VSMCs by examination of chemotactic cell migration and cellular proliferation. The influence of AMPK signaling on PDGFβ-stimulated cell migration was assessed using a modified Boyden transwell chemotactic assay over 18 hours. AICAR (1 mM) significantly reduced the number of migratory cells which was fully reversed with CC (Fig. 4.8). Interestingly, while only a trend ($p=0.102$) towards anti-migration was observed with FSK (10 uM) across the entire 18 hour experiment, two-way ANOVA revealed that the net migration at 18 hours was statistically significant compared to controls and was reversed with PKI (Fig. 4.8). Of note, both CC and PKI alone showed no significance across time or at 18 hours compared to vehicle controls (data not shown for clarity).

Figure 4.8

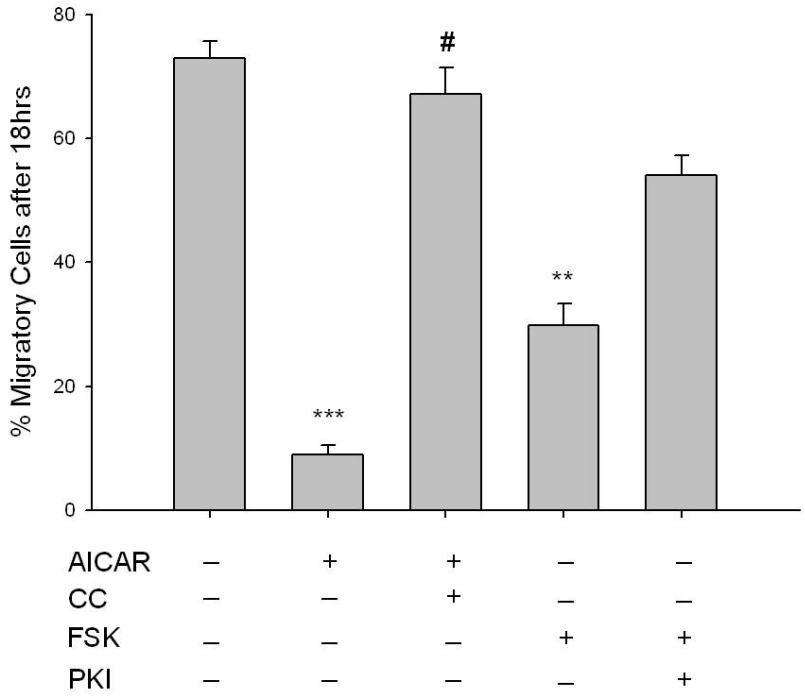

Figure 4.8. AMPK inhibits VSMC migration. Cells were labeled with CellTracker Green and treated throughout the assay with AICAR **(**1 mM), Compound C (CC; 10 uM) or a combination of both for 60 min, or with FSK **(**10 uM), PKI (10 uM), or a combination of both for 60 min, and cell migration was determined using a modified Boyden chamber apparatus and bottom-read fluorescence at 525 nm through 18 hours. AICAR significantly reduced cell migration across the entirety of the experiment and was reversed by CC. When looking across all time points, FSK had no significant effect on cell migration ($p = 0.102$); however, net migration at time=18 hours was significantly reduced with FSK. The mean score of the best curve fit at 18 hours is portrayed by histogram. Significance was determined by two-way ANOVA (with Tukey's post-hoc testing for multiple comparisons) across the entirety of the 18 hour timeframe and at 18 hours with all time points compared to vehicle. P values less than 0.05 across time within each group were considered statistically significant for n=5-8 per group. **= $p<0.01$ compared to control; *** $p<0.001$ compared to control; # $p<0.05$ compared to respective activator treatment.

Cell cycle progression and cell proliferation and viability were examined by flow cytometry and automated cell counting with trypan blue exclusion staining, respectively. Cell cycle analysis following 24 hour serum stimulation revealed AICAR significantly inhibited progression of cells from the S- to G_2/M-phase, manifested as reduced cell numbers in G_2/M and elevated cell numbers in S (Figs. 4.9A, 4.9B), and these were fully reversed by CC (Fig. 4.9A). FSK did not significantly reduce G_2/M cell populations or increase G_0/G_1-phase cells (Figs. 4.9A, 4.9B). Automated cell counts after 48 hour serum stimulation revealed that AICAR significantly reduced cell numbers (Fig. 4.9C); however, CC failed to reverse this effect (data not shown). As with the cell cycle data, while a trend was observed FSK alone did not significantly alter cell numbers compared to vehicle controls (Fig. 4.9C).

Figure 4.9

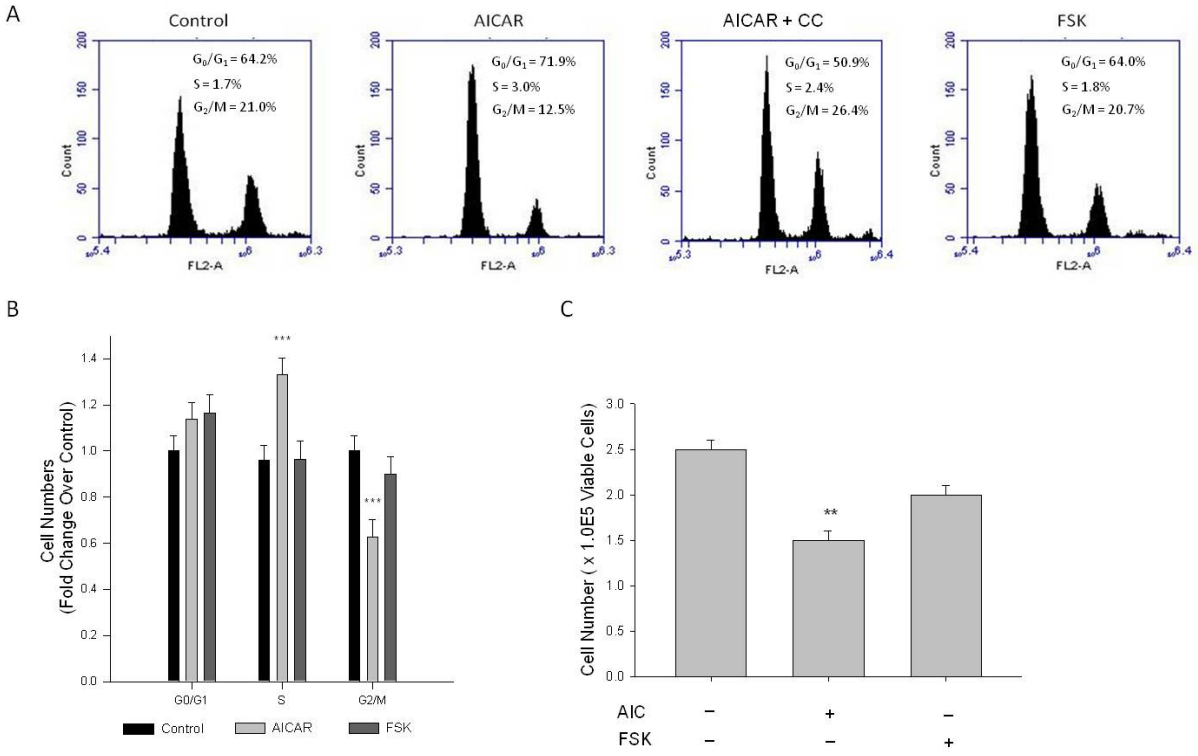

Figure 4.9. AMPK induces cell cycle arrest and inhibits VSMC proliferation. Cells were treated with AICAR **(**1 mM), with/without Compound C (CC; 10 uM), or with FSK **(**10 uM) with/without PKI (10 uM) following overnight quiescence. Cell cycle progression was analyzed by flow cytometry using the DNA stain propidium iodide after 24 hours (A) and cell numbers were quantified after 48 hours by automated cell counting and trypan blue exclusion (B). Representative peaks from flow cytometry and histograms of these data illustrate that AICAR significantly inhibits cell cycle progression from S to the G_2/M phase, revealed by increased numbers in S and reduced numbers in G_2/M (A) and (B), and these were fully reversed by CC (A). Cell cycle analysis revealed that FSK had no effect on cell cycle progression in primary VSMCs (A) and (B). Cell count analysis also revealed that AICAR significantly reduced cell numbers after 48 hours, and while a trend was observed, two-way ANOVA reveals that FSK had no significant effect on cell numbers after 48 hours **(C)**. P values less than 0.05 were considered statistically significant after multiple comparisons and two-way ANOVA for n=3-5 per group. ** p<0.01 compared to control; *** p<0.001 compared to control (control comparison was made within each stage of the cell cycle for cell cycle analysis).

Discussion

Findings in this study support our hypothesis that AMPK, in conjunction with PKA, has capacity to inhibit growth of VSM. We show that AMPK inhibits proliferation and migration of rat primary VSMCs and mechanistic data suggest that these growth-mitigating effects of AMPK are at least partly regulated by PKA. Novel findings also reveal that AMPK can reciprocally modulate PKA activity, suggesting that crosstalk exists between these two pivotal signaling factors. It has been reported in adipocytes and endothelial cells that a biochemical relationship exists between AMPK and PKA (19, 42, 52); however, this relationship has not been established in VSM. Since both cAMP/PKA and AMPK act to regulate cellular metabolism in response to intra- and extra-cellular signals (16, 19, 21, 80, 119), it is reasonable to speculate that a signaling relationship exists between the two signaling cascades in response to energy-consuming cellular processes as proliferation and migration. A synergistic relationship between AMPK and PKA has been suggested in the regulation of cancer growth (32, 60), and each factor has been implicated individually in VSM growth inhibition (43, 47, 67); therefore, based on the current study we propose a cooperative relationship exists between AMPK and PKA in the control of VSM growth. Data presented here support our theory that AMPK acts to inhibit VSM growth and that PKA acts as an adjuvant to maintain and/or possibly enhance this capacity.

Using rat primary VSMCs, AMPK expression and activity were successfully and specifically induced with AICAR, and this positively influenced the PKA pathway (Figs. 4.1 – 4.3). Conversely, the PKA system was successfully induced using FSK, and this

led to increased AMPK activity. Following establishment of treatments to specifically modulate AMPK and PKA activities (Figs. 4.1, 4.4), potential crosstalk between the two systems was investigated. AICAR increased PKA activity in AMPK-specific fashion (Fig. 4.3), suggesting that AMPK has the ability to increase PKA activity in VSMCs. Paradoxically, as shown in Figure 4.5 PKA also has the ability to modulate AMPK activity. Although we were unable to detect increases in AMPK Thr172 phosphorylation or AMPK activity from FSK alone, as has been reported in other tissues (19, 42, 63, 102), under conditions of PDE blockade with IBMX FSK did increase both AMPK Thr172 phosphorylation and AMPK activity. This may reflect robust basal PDE activity under cell culture conditions as described recently (2). Additionally, a synergistic effect was observed with concomitant AICAR and FSK treatments, suggesting these two may indeed act cooperatively as biochemical signaling molecules. Moreover, inhibition of PKA by PKI showed a significant reduction in both AMPK phosphorylation and activity, and these were partially restored with concomitant FSK treatment. These findings suggest that PKA may not directly modulate AMPK activity by phosphorylation, but may do so indirectly in a non-Ser172-dependent mechanism, and thus may serve to maintain a basal level of AMPK activity under stimulated conditions.

A suggested mechanism by which PKA may modulate AMPK activity *in vitro* is by inhibitory phosphorylation of AMPK at Ser485 (42, 69). We tested AMPK Ser485 phosphorylation under stimulated (10% FBS) and growth-arrested (0.5% FBS) conditions with or without AMPK or PKA induction. Our findings reveal that AICAR not only increased catalytic T172 phosphorylation of AMPK but also significantly increased Ser485 phosphorylation which was completely reversed by CC (Fig. 4.6). Furthermore,

PKA inhibition significantly reduced Ser485 phosphorylation, further suggesting a possible regulatory role of PKA on AMPK. Serum-starved cells showed a similar but much lower Ser485 phospho-reduction in response to PKI, but failed to exhibit altered phosphorylation in response to AICAR, CC, and/or FSK treatments (data not shown). Our data suggest that AMPK Ser485 phosphorylation may act to modulate AMPK activity and that PKA may play an important role in regulating this site. In agreement, Hurley and colleagues showed significant auto-phosphorylation of AMPK Ser485 in a cell-free system after just 10 min of incubation with ATP (42). Therefore, expanding on these data we suggest that Ser485 may be a site for auto-phosphorylation and "self-inhibition" of AMPK to fine-tune the dynamic metabolic conditions of stimulated cells on a minute-by-minute basis.

For kinases, the balance between "on" and "off" is highly regulated and is largely mediated by dephosphorylation by specific protein phosphatases. Phosphatase activity, in particularly PP-2A and PP-2C, are major contributors to the reduction of AMPK activity (51). In this light, we examined the ability of PKA to inhibit global and isoform-specific Ser/Thr phosphatase activity. We show that PKA stimulation completely inhibits global PP activity and more specifically PP-2C activity in primary VSMC lysates (Fig. 4.7). Taken together with our earlier data showing that PKA inhibition by PKI significantly reduced pAMPK Thr172 and pAMPK Ser485, a non-kinase mechanism of PKA-mediated regulation of AMPK is suspected. Therefore, we suggest that in VSMCs PKA may indirectly mediate AMPK activity via reduced PP-2C activity thus inhibiting kinase de-phosphorylation and de-activation. Conversely, specific PP-2A activity was significantly increased in AICAR-treated cells (Fig. 4.7B). While seemingly

counterintuitive, we and others (45) suggest that PP-2A may play an inhibitory role on cell cycle progression via inactivation of cyclin/CDK complexes providing a possible mechanism by which AMPK acts to inhibit cell cycle progression as our data show (Fig. 4.9). Taken together, these biochemical findings suggest for the first time in primary VSMCs that AMPK and PKA exhibit the capacity for synergistic crosstalk, a finding that may play significant roles in the proposed AMPK-mediated inhibition of VSM growth.

Complementing these biochemical data, functional roles for the cooperative signaling between AMPK and PKA were examined. Vascular smooth muscle proliferation and migration are functional mechanisms underlying aberrant vessel growth. Data using a transwell chemotactic assay (Fig. 4.8) clearly show that AICAR significantly inhibits PDGFβ-stimulated VSMC migration. This is the first report demonstrating ability of AMPK to inhibit migration of VSMCs. Additionally, data show that AICAR increases the down-regulatory phosphorylation of VASP at Thr157 (Fig. 4.3A), a protein responsible for actin polymerization, which provides an intriguing hypothetical mechanism for how AMPK disrupts actin dynamics required for migration. Interestingly, after two-way ANOVA evaluating time-dependent migration over 18 hours FSK had no significant effect on VSMC migration compared to controls; however, overall migration after 18 hours showed a significant FSK-mediated anti-migratory effect. Importantly, the degree to which FSK induced these anti-migratory effects remained significantly higher (29.8 +/- 3.6) than the AICAR-mediated effects (8.9 +/- 1.5) on VSMC migration. These functional data support our biochemical data and together give further credence to our hypothesis that PKA may act to enhance AMPK activity in an indirect manner. In light of these new findings, it is reasonable to postulate

that the heretofore PKA-mediated actions within VSMCs that act to modulate proliferation and migration (47) may indeed be AMPK-mediated.

Upon activation, normally contractile VSMCs undergo a phenotypic change and become synthetic and proliferative. With this in mind, cell cycle analysis after 24 hours and automated cell counting after 48 hours revealed that AICAR significantly decreased cell cycle progression resulting in a significant reduction in cell numbers (Fig. 4.9). Of note, while AICAR-induced cell cycle inhibition was reversed with CC after 24 h, cell proliferation after 48 h was not affected. A recent study by collaborating investigators revealed that CC alone has capacity to inhibit VSMC proliferation (63, 74), perhaps due to the irreversible inhibitory actions of CC on AMPK (33), and in the current study we observed powerful cytostatic effects of CC and AICAR that kept cell numbers at reduced levels. Moreover, in our study while FSK failed to significantly alter cell cycle progression and cell proliferation, a trend toward cytostasis in PKI-reversible fashion was observed (Fig. 4.9). AMPK has been suggested to promote cell senescence; however, these intriguing findings together with our biochemical data suggest that while PKA stimulation alone may not promote cytostasis, PKA may act to enhance AMPK activity thus supporting and/or promoting AMPK-mediated cytostasis. These data provide further evidence for the importance of AMPK in the inhibition of serum-stimulated VSMC growth and shed new light on a signaling network that may provide robust growth reduction in a more specific and targetable manner.

In conclusion, novel data presented here provide ample evidence that AMPK and PKA communicate biochemically and act in concert as a signaling network capable of controlling growth of VSMCs. This signaling crosstalk may be important in the control of

cellular metabolism as has been proposed by others (16, 19, 21, 80, 119), and our data highlight its potential importance in the control of VSM growth. The schematic in Figure 4.10 highlights the proposed cooperative relationship by which AMPK and PKA are believed to inhibit VSMC proliferation and migration. We suggest that AMPK increases PKA activity and that PKA may independently or in turn inhibit Ser/Thr PP-2C activity, thus indirectly modulating AMPK activity. Additionally, these data suggest that PKA may modulate AMPK activity by regulating phosphorylation of a proposed inhibitory AMPK Ser485 site. These findings suggest a reciprocal and feed-forward mechanism by which PKA modulates AMPK activity in serum-stimulated VSMCs to further potentiate the anti-growth properties associated with AMPK.

Figure 4.10

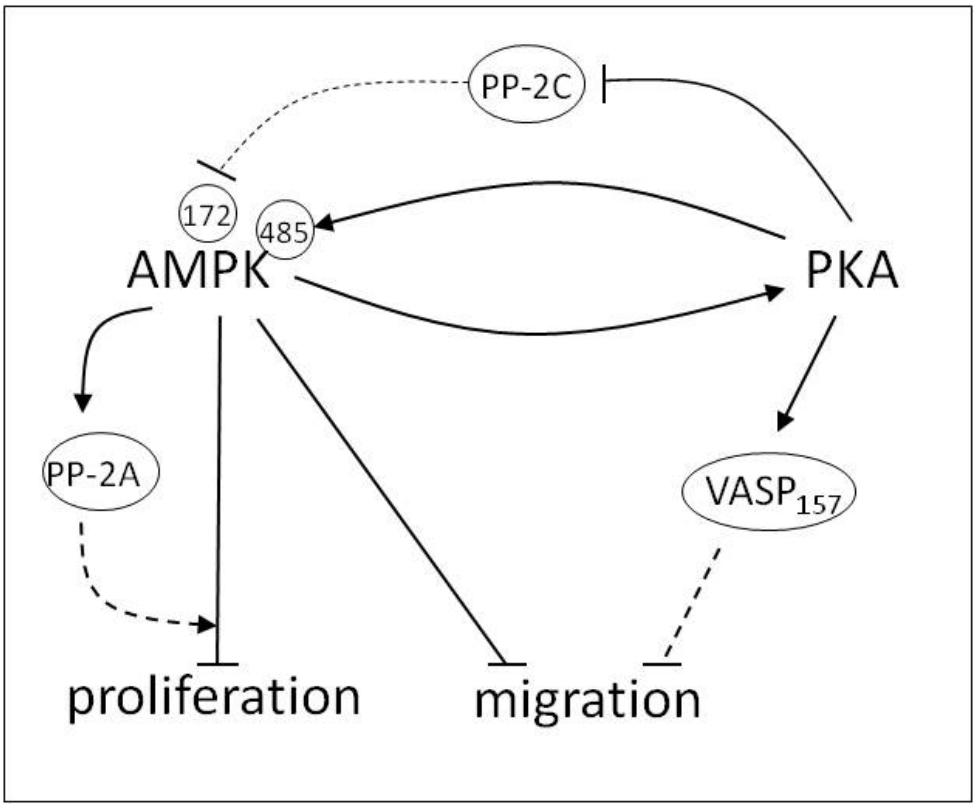

Figure 4.10. Schematic depicting the proposed cooperative relationship between AMPK and PKA in the control of VSM growth. In this diagram blunt lines represent proposed inhibitory while arrows represent proposed stimulatory mechanisms. Those pathways that were not directly tested and remain part of the overall hypothesis of this report are presented as dashed lines. Biochemical data described herein reveal that AMPK increases PKA activity and reciprocally, that PKA may modulate AMPK activity by regulation of proposed AMPK-inhibitory Ser485 phosphorylation. Furthermore, data show that PKA abrogates Ser/Thr phosphatase-2C activity, which may play a crucial role in regulating AMPK activity. Functional data confirm that AMPK reduces VSMC growth by inhibiting cell proliferation and migration. Intriguingly, these data show an increase in reported PKA-specific VASP Ser157 phosphorylation, suggesting AMPK may act indirectly through increased PKA activation to inhibit VASP-directed actin polymerization necessary for cell movement. Additionally, novel findings from this study suggest that AMPK increases PP-2A activity in VSMCs, which provides a possible mechanism for AMPK-mediated cell cycle inhibition, a reported function of PP-2A. Altogether these findings illustrate important cooperative signaling between AMPK and PKA in serum-stimulated VSMCs that may further potentiate the anti-growth properties associated with AMPK.

In addition to its static effects on proliferation, we show for the first time that AMPK has capacity to inhibit VSMC migration, providing a functional mechanism for the prevention of VSMC-mediated vessel remodeling following disease or injury. Intriguingly, our data show an increase in proposed PKA-specific VASP Ser157 phosphorylation, suggesting AMPK may indirectly through increased PKA activation to inhibit VASP-directed actin polymerization necessary for cell movement. Additionally, novel findings from this study suggest that AMPK increases PP-2A activity in VSMCs, providing a possible mechanism for AMPK-mediated cell cycle inhibition, a reported function of PP-2A. Altogether, these data elucidate a signaling network that has

potential clinical importance as a foundation for current therapeutics targeting VSM growth disorders.

Grants: This project was supported by Award Number R01HL081720 from the National Heart, Lung, and Blood Institute, National Institutes of Health (DAT) and by an American Heart Association Pre-doctoral Fellowship (JDS). The content is solely the responsibility of the authors and does not necessarily represent the official views of the National Heart, Lung, and Blood Institute, the National Institutes of Health, or the American Heart Association.

Disclosers: None

Acknowledgements: We would like to acknowledge the academic and support staff of the Department of Physiology and in particular Robert M. Lust, Ph.D., for guidance and assistance. In addition, we would like to thank Jonathan Clay Fox and Patti R. Shaver for their technical assistance.

Chapter 5: AMP-Activated Protein Kinase Inhibits Transforming Growth Factor-β-Mediated Vascular Smooth Muscle Cell Growth

Joshua D. Stone; Jackson R. Vuncannon; Andrew W. Holt; David A. Tulis, Ph.D., F.A.H.A.

Unpublished

Abstract

Vascular growth disorders are a major contributing factor to cardiovascular disease, the leading cause of morbidity and mortality in the United States. In this pathophysiologic process, growth factor activation of normally quiescent vascular smooth muscle cells (VSMCs) results in an aberrant proliferative and synthetic phenotype that can lead to vascular occlusion. Transforming growth factor-beta (TGF-β) is a multifunctional signaling protein capable of potent growth stimulation via its canonical Smad signaling cascade. Although Smad signaling is well characterized in many tissues, its exact role in vascular smooth muscle (VSM)-dependent proliferative disorders remains uncertain. Recent data from our lab and others implicate the metabolic regulator AMP-activated protein kinase (AMPK) in the inhibition of VSMC proliferation. Therefore, this study explored the hypothesis that AMPK inhibits VSMC proliferation by reducing TGFβ-mediated VSMC growth. Treatment of rat VSMCs with the AMPK agonist AICAR significantly decreased TGFβ-mediated activation of pro-synthetic Smad2 and Smad3 and increased expression of inhibitory Smad7 after 24 hours. Flow cytometry and automated cell counting revealed that AMPK activation specifically reversed TGFβ-mediated cell cycle progression at 24 hours and viable cell numbers at 48 hours. Mechanistically, induced TGFβ/Smad signaling increased both the G_0/G_1 cell cycle regulators cyclins D1 and E as well as their dependent kinases CDK4 and CDK2, respectively, while AMPK activation significantly reduced cyclins D1 and E and CDKs 2 and 4 and was associated with an increase in the cytostatic CDK-inhibitor p21. Taken together, these findings provide ample evidence of a novel AMPK target in TGFβ/Smad signaling for the control of VSM growth and support continued

investigation of AMPK as a valuable therapeutic target aimed at reducing the progression of vascular growth disorders.

Introduction

Transforming growth factor-beta1 (TGFβ1) is a multifunctional cytokine acting canonically through Smad signaling to exert its effects in a wide range of cell types. In VSMCs, TGFβ has historically been considered to have anti-proliferative effects (3, 70, 75, 78); however, recent findings suggest that TGFβ signaling stimulates growth in primary VSMCs (40, 56, 57, 85, 86, 104, 105, 108). TGFβ elicits its effects by binding to cell-surface receptors, whereupon it stimulates the phosphorylation of cytoplasmic receptor-activated Smads (R-Smads) Smad2 and Smad3. The activated R-Smads combine with the common Smad4 and the complex is transported to the nucleus to act on targeted, growth-regulatory genes (85, 88, 105, 125). Moreover, the capacity of TGFβ to control cellular growth has been shown to be mediated, at least in part, by the cyclin-dependent-kinase (CDK) inhibitor p27 (75). Additionally, it has been recently demonstrated that the pro-growth effects of TGFβ in VSMCs involve Smad3-mediated phosphorylation and nuclear export of p27 (108). A further component of this signal transduction pathway is inhibitory Smad7 which suppresses TGFβ signaling by interfering with the activation of the R-Smads (85, 88, 125). In light of these recent findings, the controversial nature of TGFβ/Smad signaling particularly in VSM justifies continued study and presents an attractive target for future therapeutic interests.

To date, no studies have examined the potential role of AMPK in modulating TGFβ-induced VSMC growth. The purpose of this study then was to characterize the capacity of AMPK to modulate growth in response to TGFβ stimulation in rat VSMCs. Our hypothesis was that AMPK reduces TGFβ-stimulated VSMC growth via reduction in Smad signaling and via inhibitory modulation of cell cycle regulators. Novel results

provide evidence for a new target in AMPK for the control of vascular growth and shed light on the role of TGFβ signaling in VSM. Altogether, our findings provide further support for the continued investigation of AMPK as a valuable target for therapies aimed at reducing the progression of vascular growth disorders.

Results

TGFβ promotes VSMC growth

Growth control of VSM has been previously suggested to be dependent at least in part on mechanisms involving cyclic AMP (47, 101) or TGFβ (3, 75, 78). We recently observed that cyclic AMP in communication with the metabolic gauge AMPK also has capacity to exert growth control of VSM (101). Considering that the canonical growth-regulating TGFβ pathway operates primarily through Smad signaling (85, 88, 105, 125), in the current study we explored whether AMPK controls growth of VSM through mechanisms involving TGFβ and Smads.

The pleiotropic and often discordant nature of TGFβ signaling to control tissue growth demands attention. Historically considered anti-proliferative in a variety of cell types (3, 8, 70, 75, 78), new findings suggest that TGFβ1 through Smad stimulates growth in primary VSMCs (85, 86, 104, 105, 108). Adding to this uncertainty, in cultured cells TGFβ1 is suggested to switch between growth stimulation and growth suppression depending on concentration (5, 85) and cell density (40). Thus, our initial experiments aimed to verify the capacity of TGFβ1 to induce Smad signaling and to determine its ability to regulate growth in rat VSMCs. Using flow cytometry and automatic cell counting, cells treated with recombinant TGFβ1 (10 ng/ml) for 24 hours show significantly elevated levels of phosphorylated (at Thr8) Smad2 and phosphorylated (at Ser423/425) Smad3 (each normalized to total Smad2 or Smad3, respectively) and moderately (20%) decreased expression of inhibitory Smad7 compared to cells treated with vehicle controls (Figs. 5.1A, 5.1B, 5.1C). Next, recombinant TGFβ1 (10 ng/ml) significantly increased cell numbers in the G_2/M phase of the cell cycle after 24 hours

(Fig. 5.2), significantly elevated viable cell numbers after 48 hours (Fig. 5.3), and significantly increased growth-promoting cell cycle regulatory cyclins D1 and E (Fig. 5.4) and the cyclin-dependent kinase (CDK) 2 and CDK4 (Fig. 5.5) compared to vehicle controls. Interestingly, TGFβ1 (10 ng/ml) only marginally reduced expression of the CDK inhibitors p21 and p27 compared to vehicle controls (Fig. 5.6). Nonetheless, these initial findings verify that TFGβ1 operates through Smad signaling and serves to stimulate growth in cultured VSMCs.

AMPK inhibits TGFβ1-mediated Smad signaling

We recently demonstrated that activation of AMPK via the AMP mimetic AICAR (1 mM) effectively reduces serum-stimulated proliferation and migration of rat primary VSMCs (100, 101). In the current study in an effort to examine the influence of AMPK on TGFβ1 signaling and TGFβ1/Smad-dependent VSMC growth, we treated cells with AICAR (1 mM) for 24 hours in the presence or absence of recombinant TGFβ1 (10 ng/ml) and then evaluated Smad signaling and indices of vascular growth. As shown in Figure 5.1, AICAR alone had modest effects on phosphorylated Smad2 or phosphorylated Smad3 yet significantly increased Smad7 compared to vehicle controls. Interestingly, AICAR in the presence of TGFβ1 significantly reversed the increases in phosphorylated Smad2 and phosphorylated Smad3 observed with TGFβ1 alone. Moreover, concomitant AICAR and TGFβ1 significantly increased Smad7 compared to both vehicle and sole TGFβ1 treatments (Fig. 5.1C).

Figure 5.1

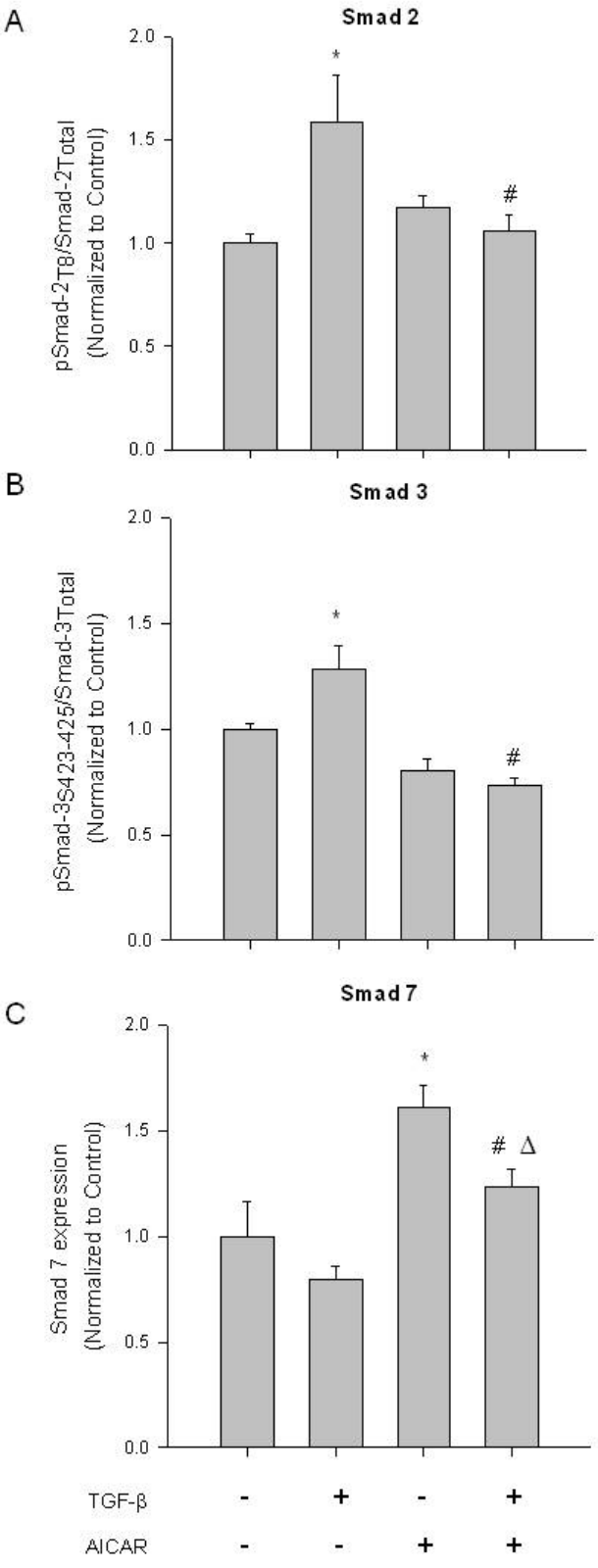
A
Smad 2
pSmad-2T8/Smad-2Total
(Normalized to Control)
2.0
1.5
1.0
0.5
0.0
*
#
B
Smad 3
pSmad-3S423-425/Smad-3Total
(Normalized to Control)
2.0
1.5
1.0
0.5
0.0
*
#
C
Smad 7
Smad 7 expression
(Normalized to Control)
2.0
1.5
1.0
0.5
0.0
*
Δ
TGF-β - + - +
AICAR - - + +

Figure 5.1. AMPK inhibits TGFβ1 signaling. Rat VSMCs were treated with recombinant TGFβ1 (10 ng, 60 min) and/or AICAR **(**1 mM, 60 min) and Smad proteins were analyzed by immunofluorescence and flow cytometry. TGFβ1 alone significantly induced expression of phosphorylated Smad2 and phosphorylated Smad3 (each normalized to total Smad2 or Smad3 protein, respectively) which were fully reversed with AICAR dosing. TGFβ1 alone moderately reduced expression of inhibitory Smad7, but AICAR alone or in the presence of TGFβ1 significantly increased Smad7. Data are presented as pSmad/total Smad and normalized to total protein, n = 3-5 per group. P values less than 0.05 were considered statistically significant. *= $p<0.05$ compared to control; # = $p<0.05$ compared to TGFβ1 alone; Δ = $p<0.05$ compared to AICAR alone.

AMPK inhibits TGFβ1-induced VSMC proliferation

To determine the extent to which AMP kinase mediates TGFβ1-induced VSM growth, we analyzed cell cycle progression via flow cytometry under non-stimulated and TGFβ1-stimulated conditions in the absence or presence of AICAR. First, supporting our previous observations (100, 101) AICAR alone induced significant increases in S-phase cell numbers and significantly reduced G_2/M-phase cell numbers compared to vehicle controls (Fig. 5.2). TGFβ1 alone (10 ng/ml) induced significant increases in cell numbers in G_2/M which were completely reversed with concomitant AICAR (1mM) after 24 hours (Fig. 5.2). No significant changes were observed in G_0/G_1 following TGFβ1 and/or AICAR dosing at this time point. In complement, automated cell counting after 48 hours revealed that TGFβ1 alone induced significant increases in cell numbers that were completely abrogated by concomitant AICAR (Fig. 5.3). As expected, AICAR alone significantly reduced cell numbers compared to vehicle controls at this time point. Notably, no significant differences in cell viability were detected for any individual or combined TGFβ1/AICAR treatment groups (data not shown).

Figure 5.2

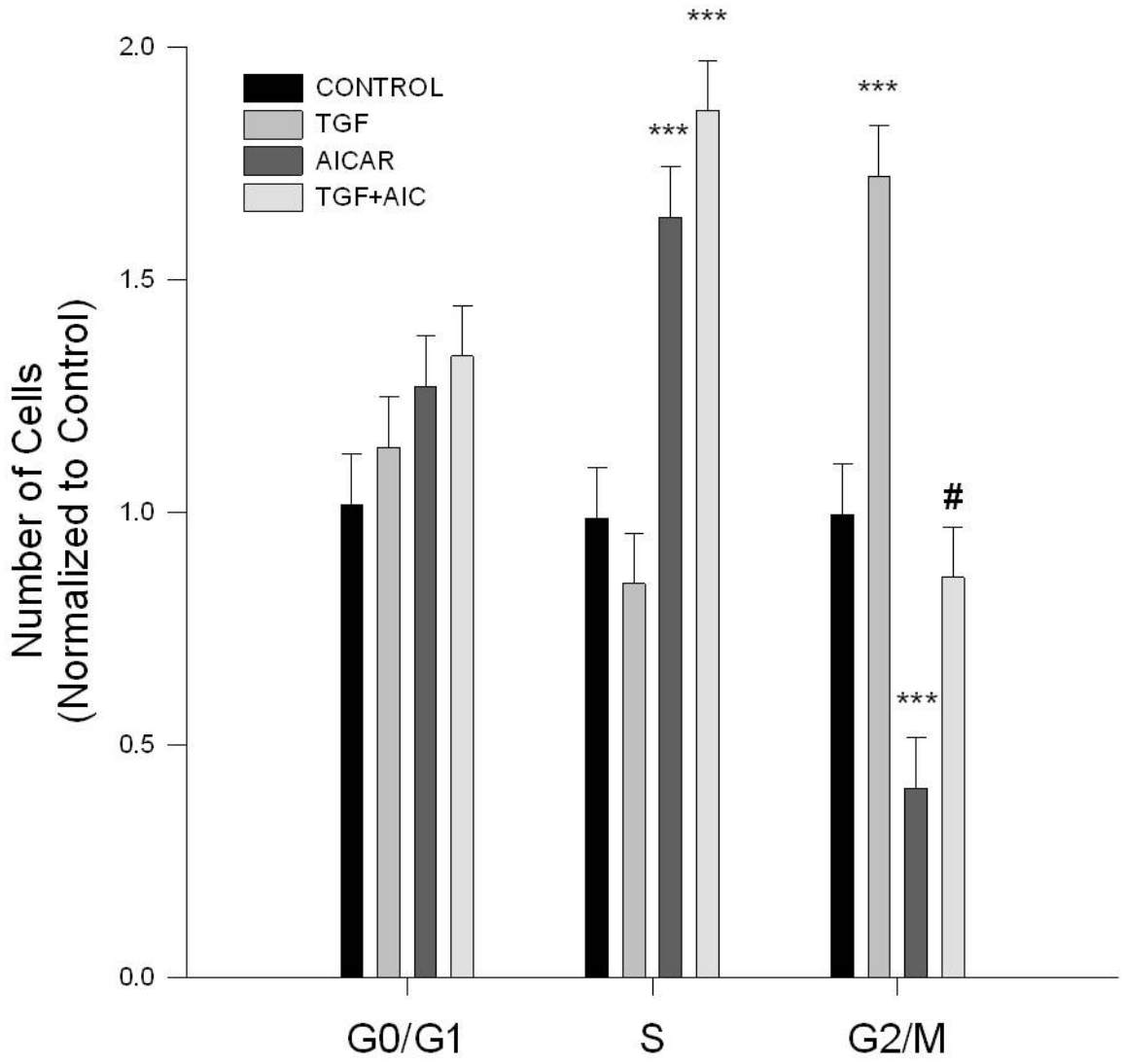

Figure 5.2. AMPK reverses TGFβ1-induced cell cycle progression. Rat VSMCs were treated with TGFβ1 (10 ng) and/or AICAR **(**1 mM) for 24 hours following overnight quiescence. Cell cycle progression was analyzed by flow cytometry using Draq5. TGFβ1 induced cell cycle progression as indicated by increased G_2/M cell populations. AICAR significantly inhibited cell cycle progression revealed by insignificant increases in G_0/G_1, significant increases in S-phase, and significant reduction of G_2/M cell numbers. P values less than 0.05 were considered statistically significant after multiple comparisons and two-way ANOVA for n=3-5 experiments. *** = $p<0.001$ compared to control; # = $p<0.05$ compared to TGFβ1 alone.

Figure 5.3

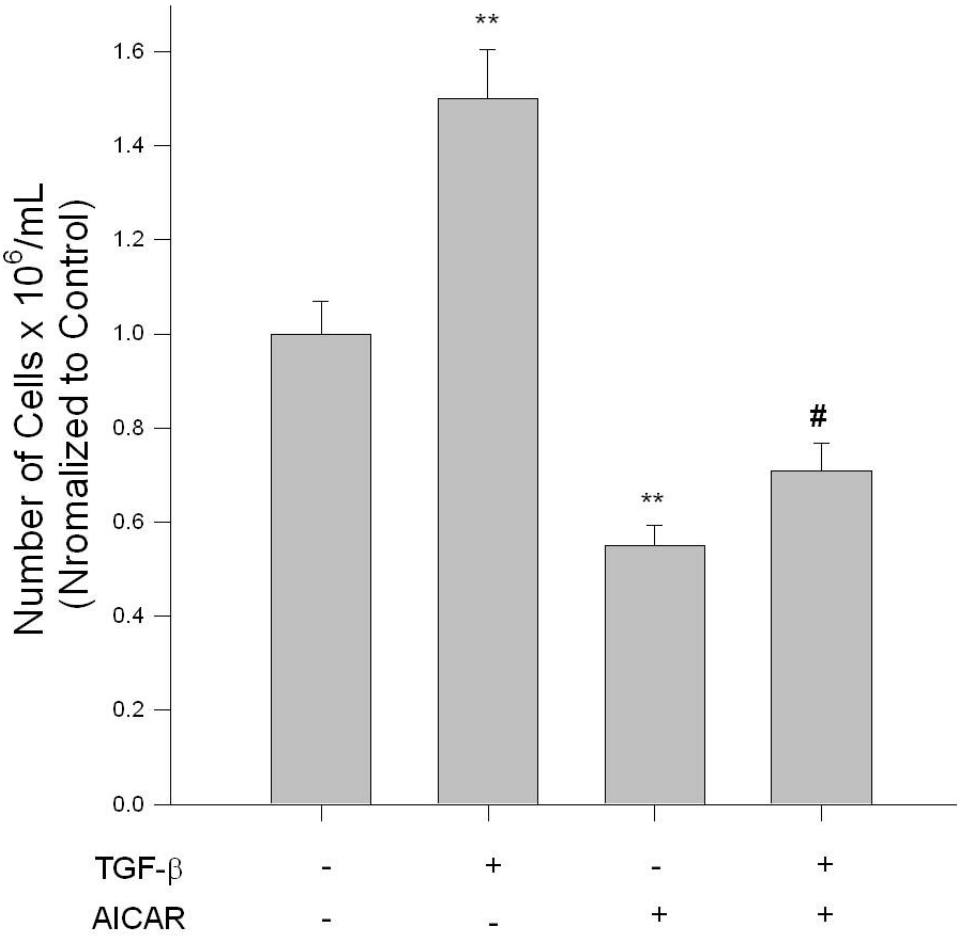

Figure 5.3. AMPK reverses TGFβ1-induced cell proliferation. Cells were treated with TGFβ1 (10 ng) and/or AICAR **(**1 mM) for 48 hours following overnight quiescence. Cell numbers were quantified by automated cell counting and trypan blue exclusion staining. TGFβ1 alone significantly increased cell numbers while AICAR alone significantly reduced cells numbers compared to vehicle controls. Concomitant TGFβ1 and AICAR revealed significant reduction in cell numbers compared to sole TGFβ1 treatment. Trypan blue exclusion failed to detect any differences in cell viability in any treatment group (data not shown). P values less than 0.05 were considered statistically significant after multiple comparisons and two-way ANOVA for n=3-5 experiments. ** = $p<0.01$ compared to control; # = $p<0.05$ compared to TGF-β1 alone.

AMPK reverses TGFβ1-induced cell cycle proteins

In order to determine the mechanisms by which AMPK inhibits TGFβ1-induced cell cycle progression and cell proliferation, we investigated the expression profile of key cell cycle regulators in the presence or absence of TGFβ1 with/without AICAR. TGFβ1 alone induced significant increases in the cell cycle promoters cyclin D1 and cyclin E (Figs. 5.4A, 5.4B) as well as in catalytic CDK2 and CDK4 (Fig. 5A, 5B) compared to vehicle controls after 24 hours. While AICAR had no effect on non-stimulated cyclin expression, a nonsignificant reduction in CDK2 ($p=0.07$) and a significant reduction in CDK4 were observed following sole AICAR dosing (Figs. 5.5A, 5.5B). Notably, in co-treated cells AICAR reversed TGFβ1-induced increases in cyclins D and E and CDK2 and CDK4 (Figs. 5.4A, 5.4B, 5.5A, 5.5B, respectively). Interestingly, no changes were observed in CDK6 expression following TGFβ1 or AICAR stimulation (Fig. 5.5C). Additionally, we investigated the CDK inhibitors p21 and p27 after 24 hours and found that AICAR increased p21 expression under both TGFβ1-stimulated and non-stimulated conditions (Fig. 5.6A). AICAR also significantly increased p27 content, which was reversed with concomitant TGFβ1 (Fig. 5.6B). TGFβ1 alone failed to significantly alter p21 or p27 expression compared to vehicle controls.

Figure 5.4

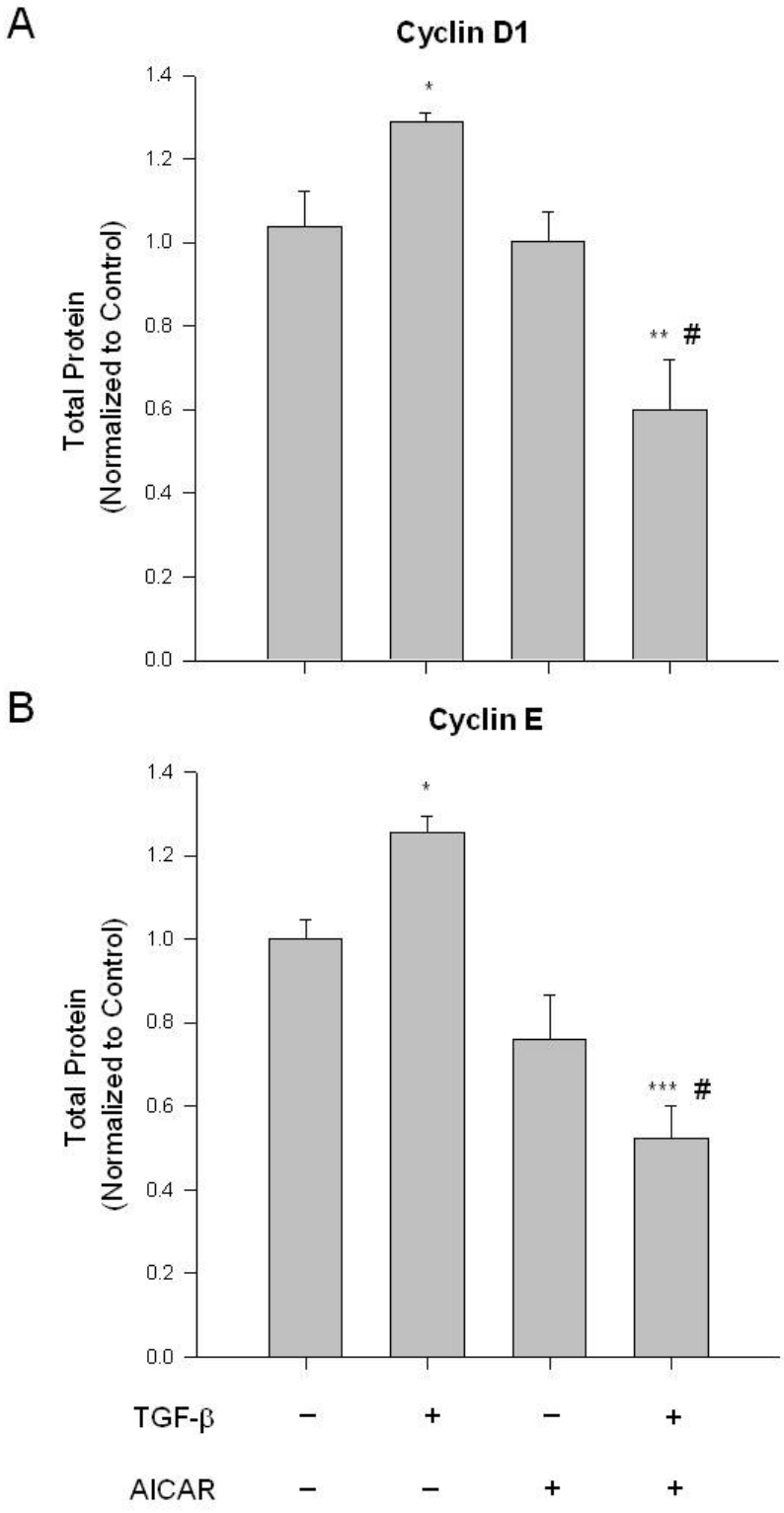
A
Cyclin D1
Total Protein
(Normalized to Control)
1.4
1.2
1.0
0.8
0.6
0.4
0.2
0.0
*
** #
B
Cyclin E
Total Protein
(Normalized to Control)
1.4
1.2
1.0
0.8
0.6
0.4
0.2
0.0
*
*** #
TGF-β – + – +
AICAR – – + +

Figure 5.4. AMPK inhibits TGFβ1-induced cyclin expression. Cells were treated with recombinant TGFβ1 (10 ng) and/or AICAR **(**1 mM) for 24 hours following overnight quiescence. Cell cycle regulatory cyclins D1 and E were analyzed by immuno-fluorescence with flow cytometry. TGFβ1 alone induced expression of cyclins D1 and E, which were significantly reversed in the presence of AICAR. Data are presented as total cyclin content normalized to total protein, n = 3-5. P values less than 0.05 were considered statistically significant. *= $p<0.05$ compared to control; ** = $p<0.005$ compared to control; *** = $p<0.001$ compared to control; # = $p<0.05$ compared to TGF-β1 alone.

Figure 5.5

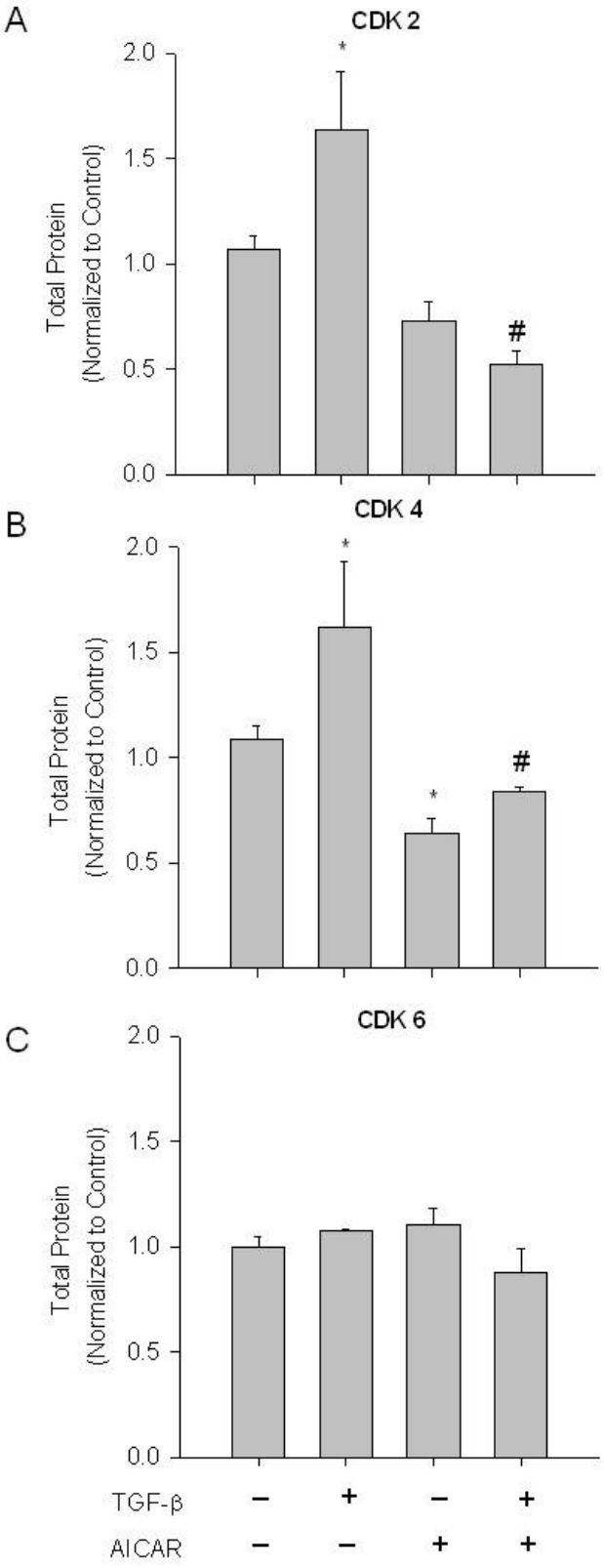
A
CDK 2
Total Protein
(Normalized to Control)
2.0
1.5
1.0
0.5
0.0
*
#
B
CDK 4
Total Protein
(Normalized to Control)
2.0
1.5
1.0
0.5
0.0
*
*
#
C
CDK 6
Total Protein
(Normalized to Control)
2.0
1.5
1.0
0.5
0.0
TGF-β – + – +
AICAR – – + +

Figure 5.5. AMPK inhibits TGFβ1-induced CDK expression. Cells were treated with recombinant TGFβ1 (10 ng) and/or AICAR **(**1 mM) for 24 hours following overnight quiescence. Catalytic cell cycle regulatory cyclin dependent kinase (CDK)2, CDK4 and CDK6 were analyzed by immunofluorescence with flow cytometry. TGFβ1 alone induced expression of the cyclin E agonist CDK2 and the cyclin D agonist CDK4, which were both significantly reversed in the presence of AICAR. No changes were observed in CDK6 expression with any treatment. Data are presented as total CDK normalized to total protein, n = 3-5. P values less than 0.05 were considered statistically significant. *= $p<0.05$ compared to control; # = $p<0.05$ compared to TGFβ1 alone.

Figure 5.6

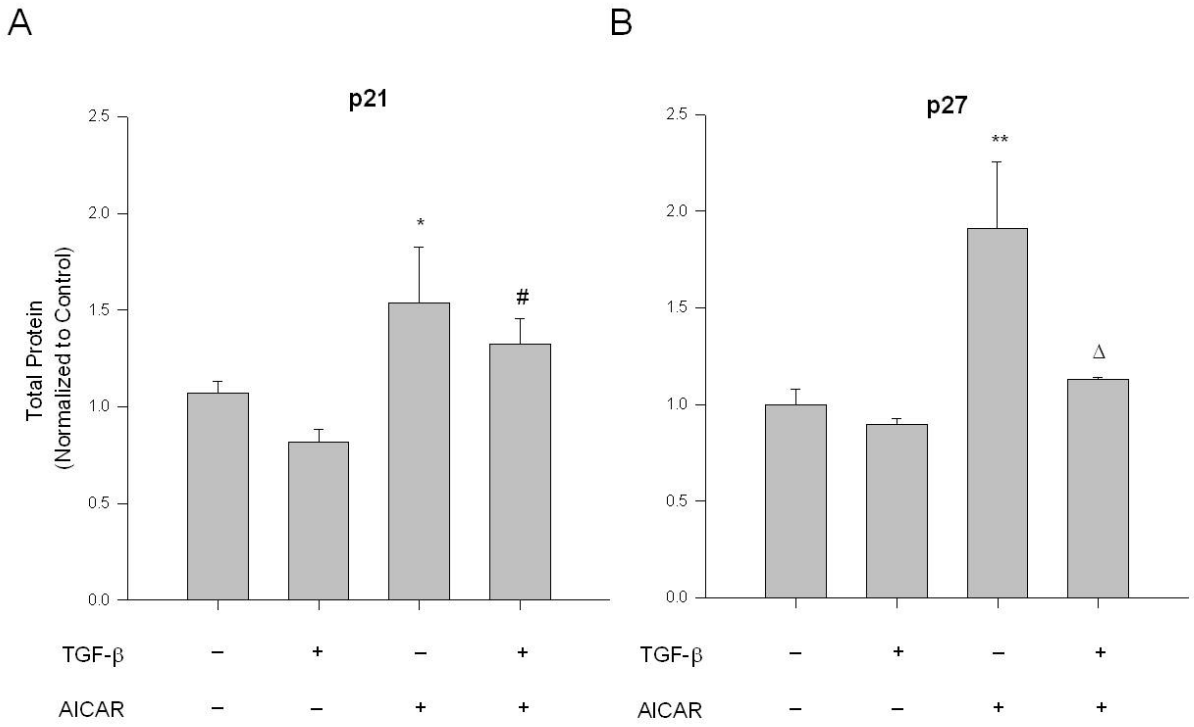

Figure 5.6. AMPK induces CDK inhibitor expression. Cells were treated with recombinant TGFβ1 (10 ng) and/or AICAR **(**1 mM) for 24 hours following overnight quiescence. Cyclin dependent kinase inhibitors p21 and p27 were analyzed by immunofluorescence with flow cytometry. AICAR alone induced significant elevation of p21 and p27; however, only p21 remained significantly elevated following TGFβ1 treatment. Data are presented as total p21 or p27 normalized to total protein, n = 3-5. P values less than 0.05 were considered statistically significant. *= $p<0.05$ compared to control; **= $p<0.005$; # = $p<0.05$ compared to TGFβ1 alone; Δ= $p<0.05$ compared to AICAR alone.

Discussion

Data presented in this study support our hypothesis that AMPK significantly inhibits VSMC growth through a mechanism at least partly dependent upon the TGFβ/Smad signaling pathway. Novel findings show that AMPK, stimulated to biologically active levels by AICAR as established recently (100, 101), serves to markedly reduce TGFβ/Smad signaling and its growth-stimulating effects in VSMCs. We found AMPK to reverse TGFβ-mediated increases in Smad2 and Smad3 and its negative effects on Smad7, to reverse exaggerated cell numbers in G_2/M as well as total viable cell numbers, to reduce expression of growth-promoting cyclins D and E and CDK2 and CDK4, and to stimulate expression of cytostatic p21. These findings are among the first to suggest that AMPK inhibits VSMC growth associated with the proliferative and synthetic TGFβ signaling network. This research provides novel insights into AMPK signaling as a biologically capable system to offer significant remediation of TGFβ-induced vascular growth. Smooth muscle-mediated vascular remodeling is integral in the onset and complication of vasculoproliferative diseases (44, 62, 77); therefore, growth-targeting therapeutic strategies are highly relevant and important clinically. Data presented here in conjunction with our recently published findings (100, 101) strongly support AMPK as a biologically active signaling molecule within VSM that is capable of inhibiting pathologic TGFβ-induced cell cycle progression and proliferation.

TGFβ is suggested to promote VSMC growth via activation of its canonical Smad signaling cascade (85, 88, 104, 105, 125). In this process, TGFβ (following binding to the TGFβ1 Receptor I) phosphorylates receptor-activated Smad3 and Smad2, which then bind to the common Smad4 to form an activated complex which translocates to the

nucleus to activate or repress transcription of growth-regulatory genes. At the same time, Smad3 activates inhibitory Smad7 in negative feedback to antagonize TGFβ signaling. Data presented here demonstrate the ability of TGFβ to increase VSMC proliferation determined through cell cycle progression (Fig. 5.2) and cell proliferation (Fig. 5.3). TGFβ alone significantly increased both cell cycle progression as indicated by a doubling of cells entering the G_2/M phase of the cell cycle as well as a ~50% increase in cell numbers after 48 hours. Together these data support recent reports that TGFβ promotes proliferation in VSMCs (41, 85, 86, 104, 105, 108). In both cases, and as we have previously reported (100, 101), AICAR alone significantly reduced cell proliferation, and here we show that AICAR is sufficient to prevent TGFβ-induced VSMC proliferation. AMPK has previously been reported to possess anti-proliferative properties (23, 35, 61, 64, 100, 101); however, this report provides novel mechanistic understanding of AMPK and its ability to specifically prevent growth of VSMCs induced by TGFβ. These findings offer new insight into a possible therapeutic target for the prevention of aberrant vascular growth as well as specific inhibition of TGFβ signal transduction which is traditionally suggested to promotes collagen synthesis and secretion, but also is suggested to have various off-target effects such as stimulating MAPKinases (56, 78, 104, 105, 126), RhoGTPases (86), and cdc42/Rac (41) which play critical roles in cell proliferation, growth and adhesion. Vascular SMC growth and migration have been the focus of much research in our lab and others for their key role in the progression of vascular growth disorders; therefore, implication of AMPK as heretofore uncharacterized inhibitor of TGFβ signaling has great biological and clinical impact.

To determine possible mechanisms by which AMPK inhibits TGFβ signaling and cell growth we utilized immunofluorescence with flow cytometry to investigate the influence of AICAR treatment on the TGFβ/Smad network. Figure 5.1 demonstrates that while AMPK alone has no effect on expression of Smad2 or Smad3, when AICAR was used in conjunction with TGFβ a complete reversal of TGFβ-induced increases of both Smad2 and Smad3 was observed. Intriguingly, when VSMCs were treated with AICAR +/- TGFβ a significant increase in the expression of inhibitory Smad7 was apparent. These data suggest that while under basal conditions AMPK may play little or no role in regulating TGFβ receptor signaling; however, under cytokine-induced growth-provoking conditions AMPK plays a significant inhibitory role on TGFβ signaling by promoting the inhibitory actions of Smad7. This increase in Smad7 inhibits oligomerization of pSmad2/pSmad3 with the cytoplasmic signal transducer Smad4. Reducing the TGFβ signal transduction in this manner inhibits the translocation of the Smad oligomer into the nucleus thus inhibiting activation of growth-promoting gene transcription (85, 88). Together with our anti-proliferative data, we suggest that AMPK-mediated inhibition of TGFβ signal transduction by increasing Smad7 contributes to the reduction of cell cycle progression and cell proliferation.

In order to determine mechanisms for the observed functional inhibition of AMPK on TGFβ signaling, we next investigated the role of TGFβ and AMPK on the G_0/G_1 cell cycle regulatory proteins cyclin D/CDK4/6, cyclin E/CDK2, and p21 and p27. Early G_0/G_1-dependent cyclin D and late G_0/G_1-dependent cyclin E were both significantly elevated by TGFβ; however, concomitant treatment with AICAR significantly reduced both cyclin D1 and cyclin E compared to control and cytokine-induced conditions (Fig.

5.4). Both cyclin D1-associated CDK4 as well as cyclin E-associated CDK2 were significantly elevated by TGFβ but were completely reversed to below basal levels with concomitant AICAR (Fig. 5.5). Intriguingly, no change was observed in cyclin D-associated CDK6, possibly suggesting that TGFβ promotes cell cycle progression in a cyclin D/CDK4- then cyclin E/CDK2-specific fashion. Furthermore, AICAR elevated both CDK inhibitors p21 and p27; however, only p21 remained elevated following co-treatment with TGFβ (Fig. 5.6). Taken together, these data suggest that AMPK has ability to inhibit TGFβ-induced cell cycle progression via reduction in G_0/G_1 cyclin D/CDK4 and cyclin E/CDK2 complexes possibly through CDK inhibition via p21.

While there may be some concern with the use of commercial rat VSMCs as used in this this study, we found that the endpoints analyzed in this study had no differences than what we've previously observed in rat primary VSMCs (100, 101). Neither baseline nor AICAR-stimulated activation of AMPK nor phosphorylation of the downstream targets acetyl CoA carboxylase and vasodilator stimulated phosphoprotein was different in A7R5 VSMCs compared to primary cells as reported (100, 101). Therefore, we feel that the data presented in this study is fully representative of what would be expected in primary preparations and should be considered highly translatable and biologically relevant.

Taken together, findings in this study suggest a discrete signaling network exists by which AMPK inhibits the proliferative signaling cascade elicited by TGFβ/Smad which is presented as a theoretical schematic in Figure 5.7. Here we show that AMPK inhibits pSmad2/3 presumably by promoting Smad7. This inhibition of TGFβ signaling results in reversal of TGFβ-induced G_0/G_1 cell cycle progression via inhibition of cyclins/CDKs D/4

and E/2 which we suggest is mediated by cytostatic, growth-inhibitory p21. Cumulatively, these data paint the picture of a novel and biologically important signaling cascade by which a metabolically activated protein such as AMPK has capability of inhibiting cytokine-induced pro-growth/pro-synthetic signaling events. This has clear biological importance as a therapeutically desirable approach to reversing cell growth associated with various disease processes.

Figure 5.7

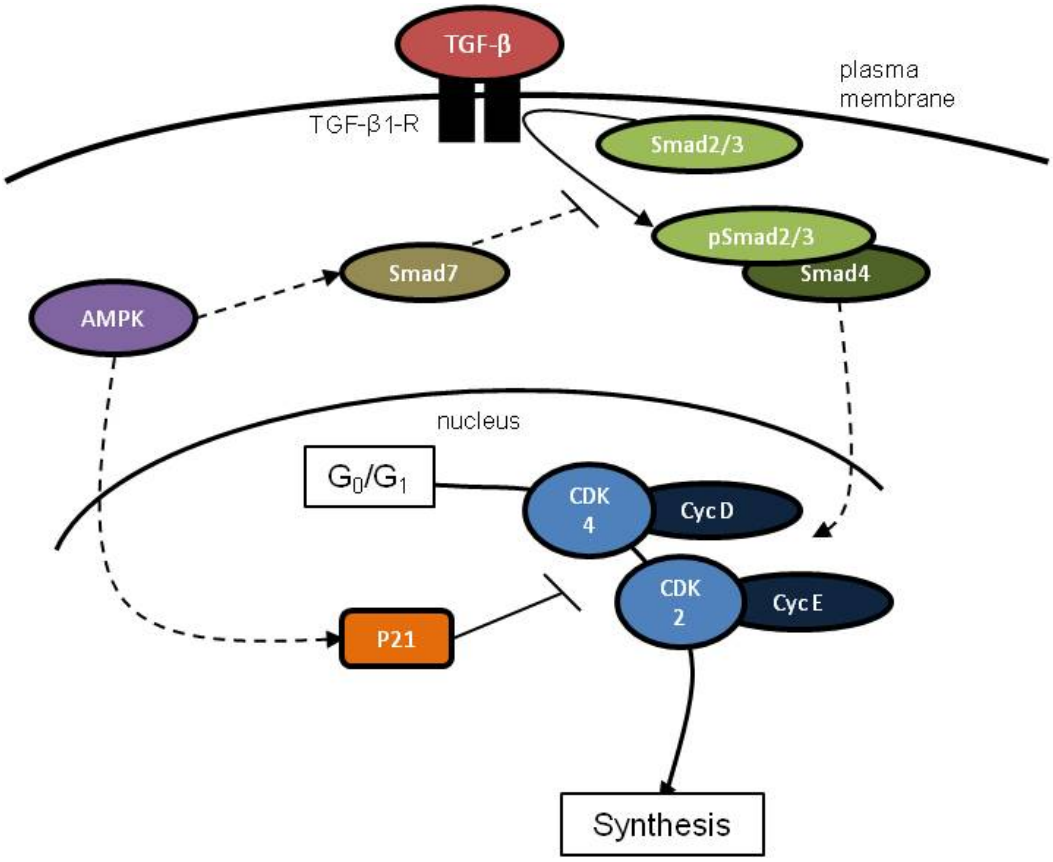

Figure 5.7. Schematic depicting the proposed inhibitory actions of AMPK on TGFβ1-induced VSMC growth. Data presented in this study suggest that AMPK has ability to inhibit TGFβ1-mediated

Smad signaling via promoting inhibitory Smad7 and by preventing growth-promoting Smad2/Smad3. Prevention of Smad2/3 phosphorylation and oligomerization with accessory Smad4 prevents their nuclear translocation and transcriptome activation of growth regulatory genes. We propose a possible pro-synthetic mechanism of TGFβ1/Smad signaling in VSMC in the promotion of cell cycle progression and cell proliferation through cyclinD/CDK4 and cyclinE/CDK2. Additionally, AMPK possesses ability to enhance the CDK inhibitor p21 which acts to further inhibit TGFβ1-mediated G_0/G_1 cell cycle progression. Solid lines represent well supported signaling events previously characterized in the literature while dashed lines represent signaling events supported by novel findings from this study.

Grants

This project was supported by was supported by Award Number 12PRE12060400 from the American Heart Association (JDS) and Award Number R01HL81720 from the National Heart, Lung, and Blood Institute, National Institutes of Health (DAT). The content is solely the responsibility of the authors and does not necessarily represent the official views of the American Heart Association, the National Heart, Lung, and Blood Institute or the National Institutes of Health.

Disclosers

None

Acknowledgements

We would like to acknowledge the academic and support staff of the East Carolina University Department of Physiology for their assistance. We would like to thank Robert M. Lust, Ph.D., for his support and guidance as Department Chair.

Chapter 6: AMP-Activated Protein Kinase Inhibits Vascular Smooth Muscle Cell Growth in a Vasodilator-Activated Serum Phosphoprotein-Dependent Manner

Joshua D. Stone; Jackson R. Vuncannon; Patti R. Shaver; Andrew W. Holt; David A. Tulis, Ph.D., F.A.H.A.

Unpublished Data

Abstract

Abnormal vascular smooth muscle cell (VSMC) growth is a major contributor to vascular disease etiology. We have previously reported that the metabolic switch AMP-activated protein kinase (AMPK) has ability to inhibit vascular growth *in vivo* and *in vitro*. The microfilament-associated vasodilator-stimulated phosphoprotein (VASP) has been implicated in cell growth via its dynamic interaction with actin cytoskeleton and focal adhesion (FA) complexes, via increased Rho-A GTPase activity, and through Rho-A-mediated serum response element (Sre)-dependent transcriptional activity. Published data by our lab and others reveals direct signaling between AMPK and VASP; therefore, the hypothesis of this study is that AMPK reduces VSMC growth through a mechanism dependent upon inhibition of VASP. Our data reveal that activation of AMPK by the AMP-mimetic AICAR in rat A7R5 VSMCs increases inhibitory Ser157 and Thr278 phosphorylation of VASP with concomitant increased G- to F-actin ratio compared to vehicle control conditions. Additionally, reduced catalytic Tyr397 phosphorylation of focal adhesion kinase (FAK) and increased cytostatic-associated paxillin were observed in AICAR treated VSMCs compared to controls. Functionally, AICAR inhibited VSMC PDGF-stimulated transwell migration and serum-stimulated cell cycle progression after 24 hours. To determine if these events were VASP-dependent, we cultured lentiviral-mediated VASP-deficient VSMCs and found that VASP deficiency reversed the AMPK-mediated cell cycle inhibition and anti-migration observed in wild type cells. Taken together, these findings suggest that AMPK has ability to reduce serum-stimulated VSMC growth by inhibiting VASP-directed actin cytoskeletal dynamics that play key roles in cell migration as well as transcriptional activity implicated in cell growth. This

discrete signaling network provides further insight into the anti-growth properties of AMPK and provides rationale for further exploration of AMPK as a target for the inhibition of vascular growth disorders.

Introduction

The actin cytoskeleton is a highly dynamic structure that plays a vital role in directing cellular signaling events as well as mechanically regulating cell migration and proliferation. Many of the pathologies associated with vasculoproliferative disorders such as, vessel hypertrophy, and restenosis following clinical intervention are attributed to phenotypic switching of vascular smooth muscle cells (VSMC) from a contractile to a synthetic state (44, 62, 77). In this synthetic state VSMCs become proliferative and migratory and promote the synthesis and turnover of extracellular matrix. This destabilization of the vessel wall leads to deleterious lesion formation and vessel stenosis associated with vascular growth disorders (11, 24, 34, 44, 62, 76, 77, 82).

The actin-associated accessory protein vasodilator-activated serum phosphoprotein (VASP) is a key regulator of the actin cytoskeleton, serving to promote polymerization as an anti-capping protein. As actin fibers grow, VASP delivers monomeric actin to the barbed end of the growing filament and acts to inhibit filament capping by capping proteins (4, 6, 10). VASP has been implicated in the control of intra- and extra-cellular signaling events associated with cell migration and proliferation and transcriptional activity (4, 6, 7, 10, 15, 31, 91, 123, 129). Due to its role as a signal transducer, differential VASP phosphorylation at Ser157, Ser239, and Thr278, which act to inhibit its activity, has been traditionally used as readout of protein kinase signaling (2, 7, 9, 47). Given its ability to be quickly turned on or off by phosphorylation, it is logical to think that investigating VASP as a downstream target of protein kinases capable of inhibiting VSMC growth could elucidate previously unclear signaling and growth control mechanisms within VSMCs and thus is the focus of this project. In addition, we and

others have recently reported the ability of AMPK to specifically phosphorylate VASP (9, 100, 101), suggesting this may offer insight into the mechanisms by which AMPK regulates vascular growth.

Altogether, these reports strongly implicate the ability of AMPK to significantly regulate VASP activity and to inhibit VSMC growth. Therefore, the purpose of this study was to investigate the hypothesis that AMPK acts to inhibit VSMC proliferation and migration and that it does so in VASP-dependent manner. Data presented here support this notion and provide further evidence that AMPK has capacity to significantly regulate VSMC growth and has potential as a therapeutic target for the prevention and treatment of vasculoproliferative disorders.

Results

AMPK specifically phosphorylates VASP

Actin cytoskeleton-associated vasodilator-activated serum phosphoprotein (VASP) is implicated in the directionality of extra- to intra-cellular signaling events and in the regulation of focal adhesions and, via nucleotide exchange factor regulation, in the control of transcriptional activation (10, 31, 123, 129). Site-specific VASP phosphorylation has also been used as readout of differential protein kinase signaling as we have recently reported (2, 47, 100, 101). Moreover, we recently showed that AMPK has capacity to control differential VASP phosphorylation in the inhibition of growth in rat primary VSM cells (100, 101). In the current study utilizing commercially-available rat A7R5 VSMCs we verified these signaling events using the AMP mimetic AICAR (1mM, 1 hr) and found significant doubling of phosphorylation of both the PKA-specific VASP Ser157 and the AMPK-specific VASP Thr278 (Fig. 6.1A). As expected, there was no change in VASP Ser239 phosphorylation which has been previously reported to be PKG-dependant (2, 7, 9, 47). Considering these data implicating VASP in the mechanisms of action of AMPK, in order to determine the extent to which VASP phosphorylation by AMPK plays a role in regulating cell growth we generated VASP-deficient VSMCs using Lv-mediated shRNA directed against full-length VASP. Figure 6.1B is a representative Western blot performed on VSMC homogenates that illustrates efficient protein knockdown of VASP 24 hours post-transduction. In this photo A, B, and C are replicates of Lv-shRNA-treated [(-)VASP] cells, NTC represents a non-targeting (scrambled) control, and Veh is the vehicle control (DMEM, 15% FBS, penicillin/streptomycin). InCell Western blotting on adherent VSMCs was also

performed 48 hours post-transduction, and Figure 6.1C shows densitometric results for VASP protein expression. In both ECL-based Western blotting (Fig. 6.1B) and ICW blotting (Fig. 6.1C) significant reduction in total VASP expression is clearly evident in the Lv-shRNA treated VSMCs compared to NTC and Veh controls. Next, we examined VASP Ser157 and VASP Thr278 phosphorylation in normal and VASP-deficient cells in order to confirm site-specific VASP knockdown. Significant loss of phosphorylation of both residues in the (-)VASP cells was observed (Figs. 6.1D and 6.1E). Finally, when treated with AICAR the (-)VASP cells exhibited no change in phosphorylation status at either Ser157 or Thr278 compared to controls and, notably, significantly less phosphorylation compared to AICAR treatments alone (Figs. 6.1D and 6.1E).

Figure 6.1

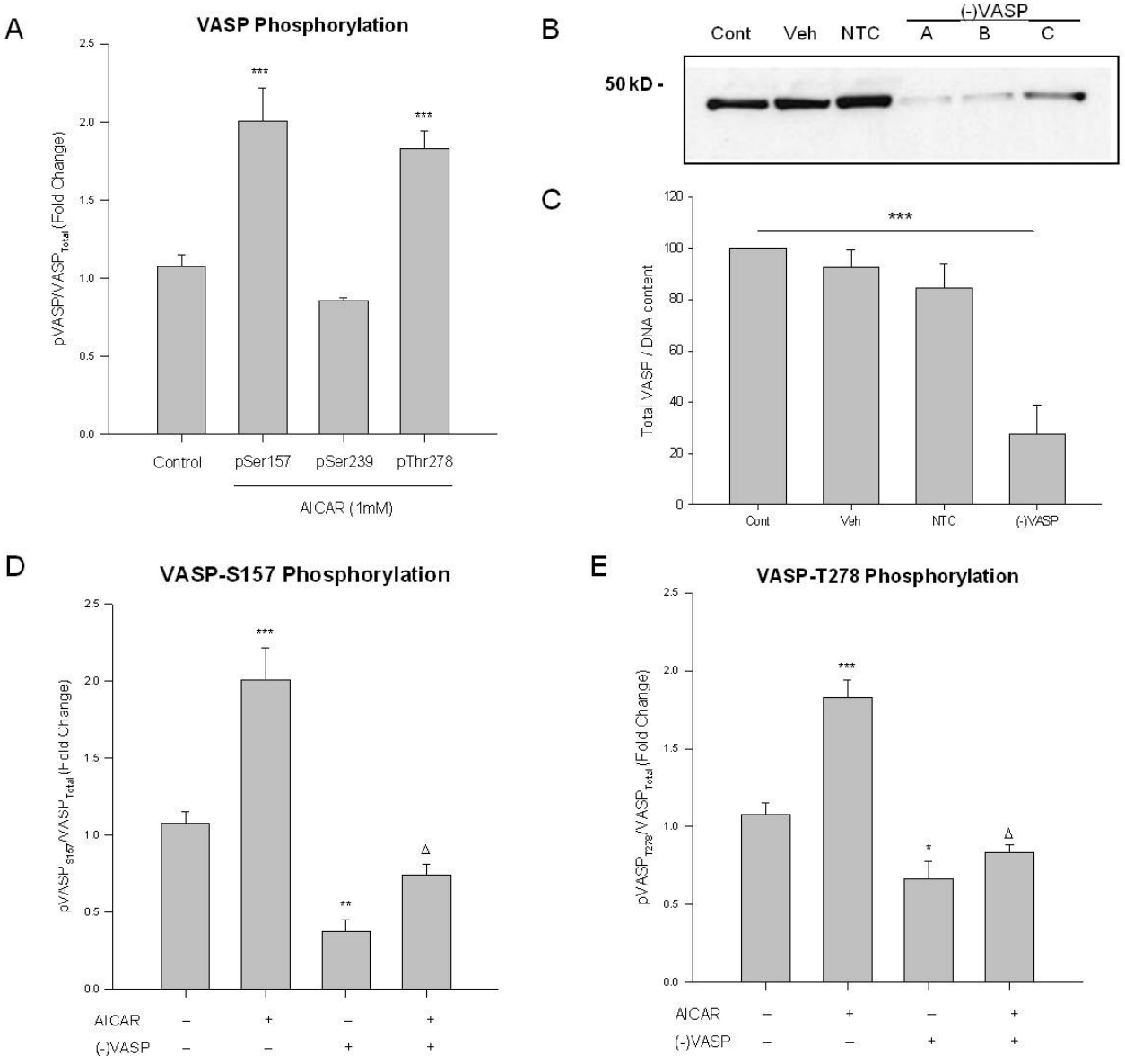
A
VASP Phosphorylation
pVASP/VASP Total (Fold Change)
Control
pSer157
pSer239
pThr278
AICAR (1mM)
B
Cont
Veh
NTC
(-)VASP
A
B
C
50 kD -
C
Total VASP / DNA content
Cont
Veh
NTC
(-)VASP
D
VASP-S157 Phosphorylation
pVASP S157/VASP Total (Fold Change)
AICAR
(-)VASP
E
VASP-T278 Phosphorylation
pVASP T278/VASP Total (Fold Change)
AICAR
(-)VASP

Figure 6.1. AMPK specifically phosphorylates VASP. Cells were treated with AICAR **(**1 mM, 60 min) and VASP phosphorylation was analyzed by immunofluorescence with flow cytometry. (A) AICAR significantly increases phosphorylation of VASP at Ser157 and Thr 278. (B) Representative photograph of an ECL-based Western blot performed on A7R5 VSMC homogenates that reveals successful transduction of Lv-shRNA directed against full length VASP after incubation for 24 hours. Lanes correspond to untreated control, vehicle control (Veh), non-targeting (scrambled) Lv-shRNA control (NTC), and three replicates of anti-VASP-Lv-shRNA-treated cells ((-)VASP). (C) Graphical representation of results obtained from InCell Western blotting on intact adherent A7R5 VSMCs after 48 hours incubation with vehicle (Veh), NTC, or anti-VASP-Lv-shRNA ((-)VASP). No changes were observed with Veh or NTC compared to controls (Cont); however, three replicates of VASP-deficient cells reveal significant and consistent knockout of VASP protein. (D) and (E) Specificity of AICAR-induced phosphorylation of VASP Ser157 and VASP Thr278, respectively, in non-transduced and VASP-deficient A7R5 VSMCs. VASP knockdown in cells reveal significantly less site-specific phosphorylation compared to controls and no differences were found following treatment with AICAR suggesting specificity of AMPK-induced phosphorylation of these residues. Data are presented as pVASP/total VASP, n=3-5 per group. P values less than 0.05 were considered statistically significant. *= $p<0.05$ compared to control; **= $p<0.005$ compared to control; ***= $p<0.001$ compared to control; Δ = $p<0.05$ compared to AICAR alone.

VASP inhibition increases G:F-actin

VASP acts as an anti-capping protein associated with polymerizing actin filaments; therefore, it is logical that increased inhibitory phosphorylation of VASP by AMPK would increase the cytoplasmic G-actin pool. We have previously shown that AICAR-induced AMPK increases cytoplasmic G-actin in primary VSMCs (100), and data presented here show that AICAR stimulation significantly increases G:F-actin in commercial A7R5 VSMCs (Fig. 6.2). Additionally, as expected, VASP-deficient cells displayed even greater G:F-actin ratios and no significant differences were observed when VASP-

deficient cells were treated with AICAR (Fig. 6.2), suggesting AMPK-specific inhibition of VASP leading to increased G:F-actin.

Figure 6.2

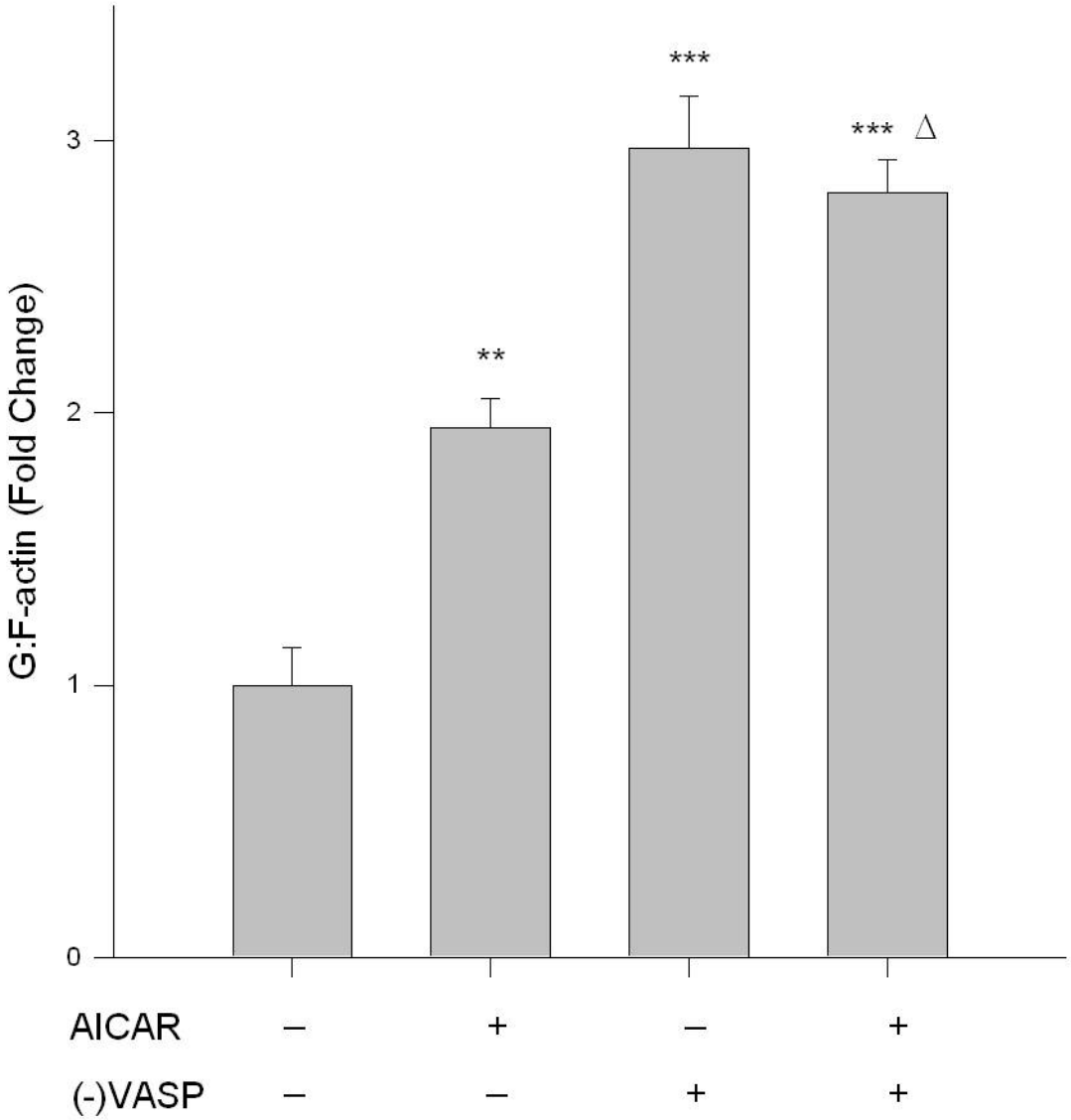

Figure 6.2. AMPK/VASP promotes actin de-polymerization. Non-transduced and VASP-deficient VSMCs were treated with or without AICAR (1 mM, 60 min), fixed and stained for F-actin (fluorescently-tagged phalloidin) or G-actin (fluorescently-tagged deoxyribonuclease I), and fluorescence was read by flow cytometry. Immunofluorescence reveals that AICAR promotes F-actin disassembly as shown by increased G:F actin ratios. VASP deficiency further increased G:F-actin, yet no differences were detected when VASP-deficient cells were treated with AICAR. Data are presented as fold change of the total G-actin to F-actin fluorescence detected by flow cytometry for n=3-5 per group. P values less than 0.05 were considered statistically significant. ** = $p<0.005$ compared to control; ***= $p<0.001$ compared to control; Δ = $p<0.05$ compared to AICAR alone.

VASP inhibition reduces actin strain on focal adhesions

A proposed mechanism of focal adhesion kinase (FAK) autophosphorylation of Tyr397, an event necessary for kinase activation and focal adhesion turnover, is F-actin strain on the focal adhesion complex (26, 93, 107, 128). It has been suggested that VASP may play a role in adhesion-directed actin polymerization (26, 129); therefore, the interaction of AMPK with VASP may subsequently reduce FAK auto-activation and warrants investigation. We have previously reported AMPK-mediated inhibition of pFAK Tyr397; therefore, in light of the aforementioned data suggesting AMPK inhibition of VASP-mediated actin polymerization, we treated VASP-deficient cells with and without AICAR (1mM) and found that AICAR and VASP ablation each individually significantly reduced pFAK Tyr397 compared to control cells (Fig. 6.3). Intriguingly, VASP-deficient cells treated with AICAR also showed significant reduction in pFAK Tyr397 (Fig. 6.3), yet to levels not significantly different than AICAR-treated or VASP-deficient cells alone suggesting these effects were indeed AMPK mediated.

Figure 6.3

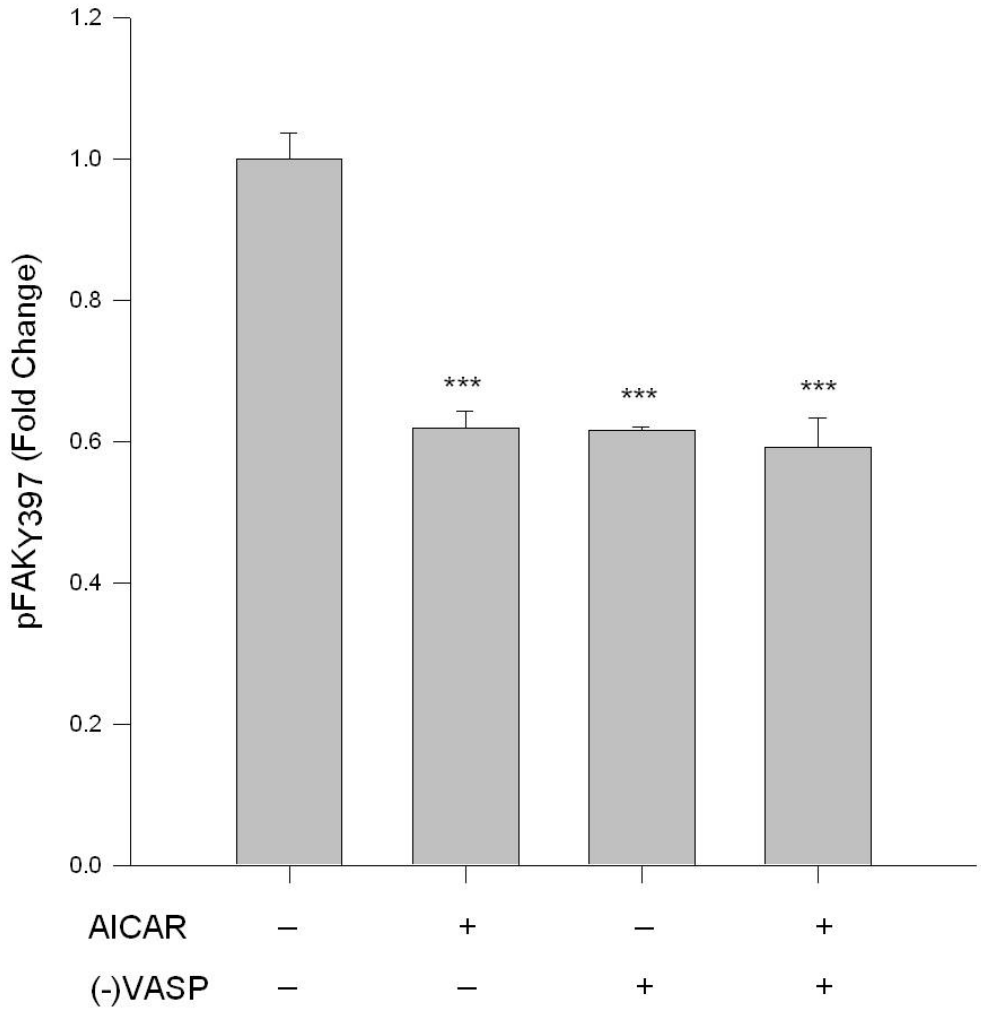

Figure 6.3. AMPK/VASP inhibits FAK activation. Non-transduced and VASP-deficient VSMCs were treated with or without AICAR **(**1 mM, 60 min) and FAK Tyr397 phosphorylation was measured by flow cytometry as an indication of kinase activity. AICAR treated cells revealed significant reduction in FAK activation. Notably, VASP-deficient cells also revealed reduced FAK activity and no differences were observed when cells were simultaneously treated with AICAR. Data are presented at pFAK Tyr397/total FAK detected by flow cytometry for 3-5 separate experiments. P values less than 0.05 were considered statistically significant. *** = $p<0.001$ compared to control.

The focal adhesion accessory protein paxillin is a marker of stable focal adhesions. Thus, in this study we treated non-transduced and VASP-deficient cells with AICAR and found significant increases in paxillin expression under both conditions (Fig. 6.4). Once again, VASP-deficient cells treated with AICAR showed similar results yet were not significantly different than the other treatment group (Fig. 6.4) suggesting these results were AMPK specific.

Figure 6.4

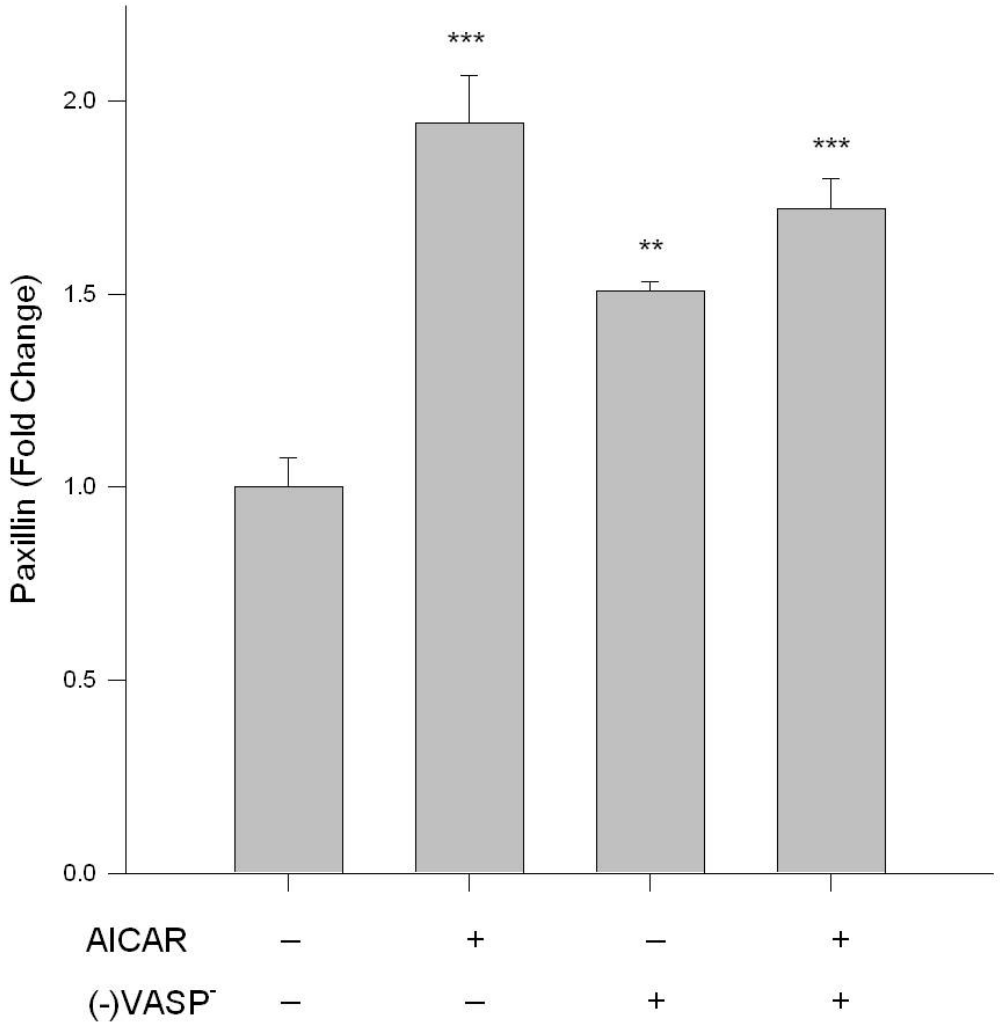

Figure 6.4. AMPK/VASP promotes focal adhesion stability. Non-transduced and VASP-deficient VSMCs were treated with or without AICAR **(**1 mM, 60 min) and paxillin expression was analyzed by immunolabeling and flow cytometry. Protein analysis reveals that AMPK increases paxillin content, indicative of focal adhesion stability and anti-migratory signaling. VASP-deficient VSMCs also showed significant elevation of paxillin expression. Addition of AICAR to VASP-deficient cells revealed no significant differences from non-transduced cells suggesting VASP-dependence of AMPK on focal adhesion stability. P values less than 0.05 were considered statistically significant for n=3-5 per group. ** = $p<0.005$ compared to control; *** = $p<0.001$ compared to control.

VASP knockdown inhibits VSMC migration

If VASP inhibition reduces actin polymerization and subsequent actin strain on focal adhesions, then it would make sense that VASP inhibition, either by phosphorylation or genetic knockdown, should result in functional inhibition of VSMC migration. We have previously shown AMPK-mediated inhibition of rat primary VSMCs (100, 101), and in the current study we demonstrate that AICAR significantly inhibits migration of rat A7R5 VSMCs after 18 hours (Fig. 6.5). As expected, migration was also inhibited with VASP deficiency which was not significantly different than AICAR alone or when VASP-/- cells were treated with AICAR (Fig. 6.5), providing further evidence for a functional relationship between AMPK and VASP.

Figure 6.5

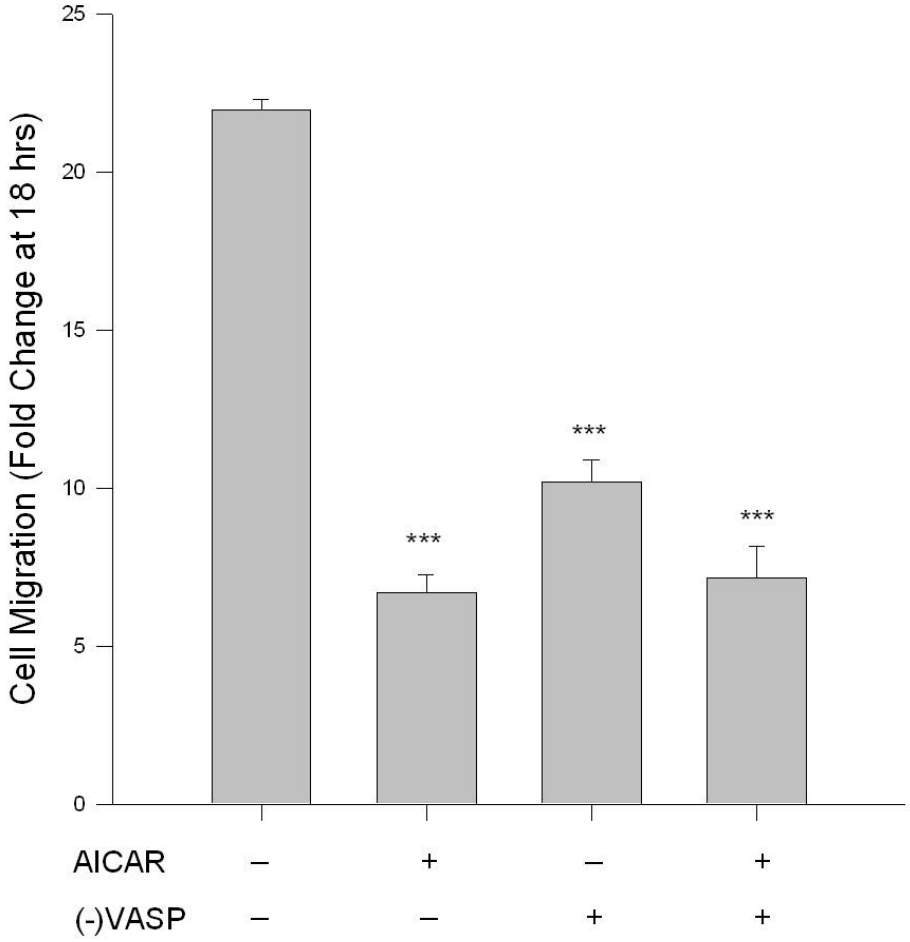

Figure 6.5. AMPK/VASP inhibits VSMC migration. Non-transduced and VASP-deficient VSMCs were labeled with CellTracker Green and treated with AICAR **(**1 mM), and PDGF-stimulated (10ng/mL) chemotaxis was evaluated using a modified Boyden chamber apparatus and bottom-read fluorescence at 525 nm between 0 and 18 hours. AICAR significantly reduced cell migration in non-transduced cells at 18 hours. VASP-deficient VSMCs also showed a significant reduction in migration; however, there were no significant differences between VASP-deficient with or without AICAR. Two-way ANOVA with Tukey's post-hoc testing was used for multiple comparisons across time and within each treatment group. P values less than 0.05 across time within each group were considered statistically significant for n=3. *** = $p<0.001$ compared to control.

VASP knockdown promotes VSMC cytostasis

It has been suggested that VASP serves as a necessary mediator of Rho-induced serum response element transcriptional activity (129); therefore, we tested the effects of VASP ablation on VSMC proliferation. In non-transduced A7R5 cells, AICAR reduced cells entering the G_2/M phase of the cell cycle which corresponds to significant increases in cells found in the G_0/G_1 and S phases (Fig. 6.6). Intriguingly, VASP deficiency completely reversed this AMPK-mediated cytostatic effect (Fig. 6.6) supporting the notion that VASP is necessary for entry into the cell cycle and provide novel insight to the functional role of AMPK-mediated VASP inhibition.

Figure 6.6

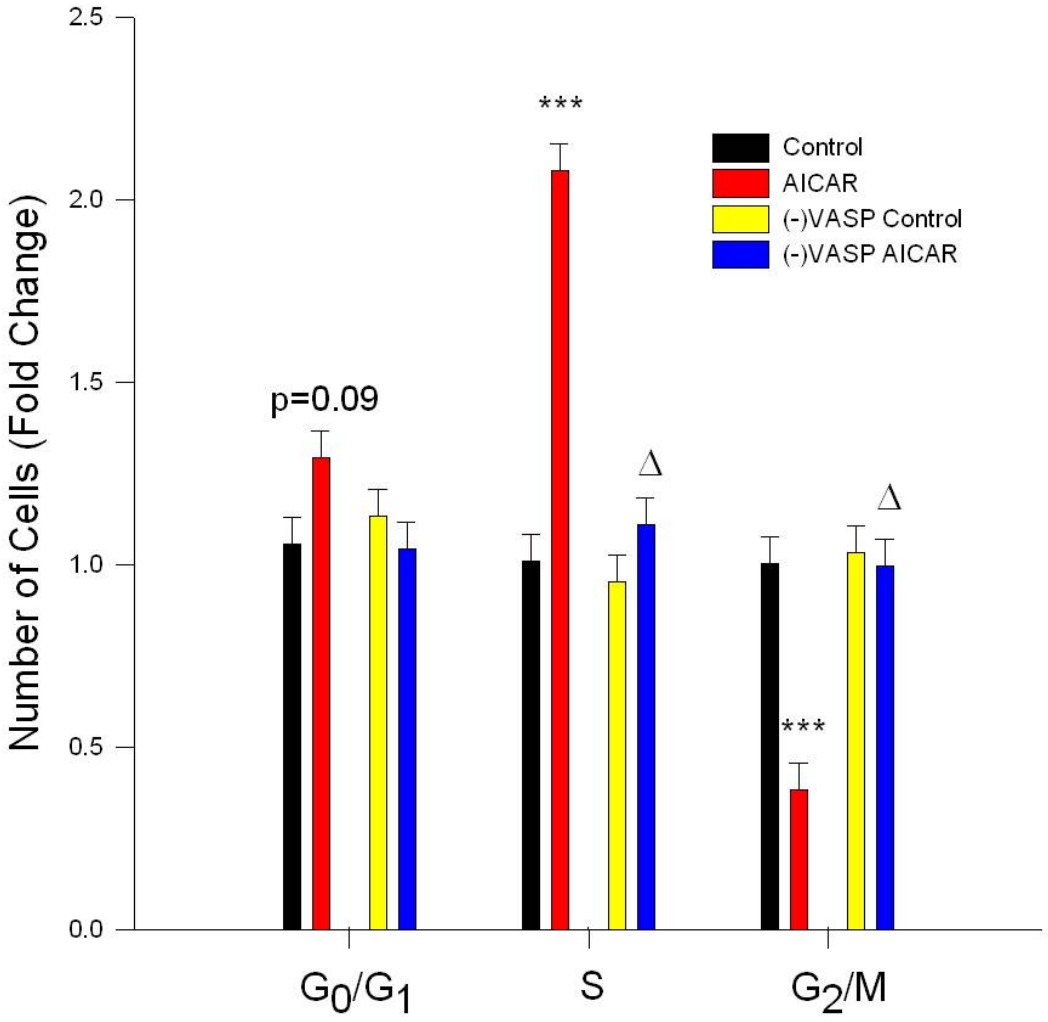

Figure 6.6. AMPK inhibits cell cycle progression in a VASP-dependent manner. Non-transduced and VASP-deficient VSMCs were treated with or without AICAR **(**1 mM) for 24 hours following overnight quiescence. Cell cycle progression was analyzed by flow cytometry using Draq5. AICAR significantly inhibited cell cycle progression revealed by insignificant increases in G_0/G_1 phase cells, significant increases in S-phase cells, and significant reduction in G_2/M cells. VASP deficiency inhibited the cytostatic effect of AMPK revealed by complete reversal of the observed increase in S-phase cells and reduction in G_2/M phase cells. P values less than 0.05 were considered statistically significant after multiple comparisons and two-way ANOVA for n=3 experiments. *** = $p<0.001$ compared to control; Δ = $p<0.05$ compared to AICAR alone.

Discussion

Findings presented in this study support our hypothesis that AMPK inhibits VSMC growth in VASP-dependent manner. We have previously shown in rat primary VSMCs (101), and herein confirm in rat A7R5 VSMCs that AMPK has th ability to increase phosphorylation of VASP at both Ser157 and Thr278. AMPK also possess anti-migratory and anti-proliferative properties in VSMCs which we and others have previously documented (43, 67, 98, 100). Given the role VASP as a conductor of cell signaling and regulator of cytoskeletal arrangement (4, 6, 7, 10, 15, 31, 91, 123, 129), in this study we investigated the dependence of AMPK on VASP to inhibit migration and proliferation of A7R5 VSMCs with an emphasis on focal adhesion biology. Utilizing Lv-shRNA targeted against full-length VASP, we successfully knocked down VASP as documented by Western blotting on cell homogenates and ICW blotting on intact adherent cells. In turn, VASP deficiency resulted in reduction in f-actin polymerization, focal adhesion kinase activation and focal adhesion turnover as well as in cell migration and cell cycle progression. Moreover, after treatment with AICAR to activate AMPK, the cytostatic functions of AMPK observed in control non-transduced cells was completely reversed with VASP knockdown. Data presented here provide evidence for a novel signaling network in VASP through which AMPK inhibits VSMC growth and further support its role as a biologically active signaling protein within VSM capable of modulating deleterious VSM growth.

The actin cytoskeleton acts as an anchoring point for focal adhesion and cell attachment; therefore, with decreased actin polymerization less force will be exerted on focal adhesions and in turn, directed filament elongation required for lamellipodia and

filopodia formation will be minimized. Additionally, turnover of focal adhesions requires catalytic phosphorylation of FAK at Tyr397. One suggested mechanism of FAK activation is by auto-phosphorylation following actin strain (26, 107, 128). Therefore, in this study we sought to investigate the functional role of the AMPK/VASP relationship on actin dynamics and focal adhesion stability in light of VSM growth. We have previously reported in rat primary VSMCs that AMPK has ability to increase phosphorylation of VASP at Ser157 and Thr278 either directly or via crosstalk with protein kinase A (101). In similar fashion, in this study AICAR significantly increased pVASP Ser157 and Thr278 in A7R5 VSMCs (Fig. 6.1). As VASP acts in a pro-polymerization manner, when VASP gets phosphorylated by AMPK the G-actin pool should increase. Figure 6.2 reveals that with AICAR treatment to stimulate AMPK, G-actin is significantly increased compared to controls suggesting an inhibitory action of AMPK on VASP. Catalytic phosphorylation of FAK was also significantly reduced after treatment with AICAR (Fig. 6.3) suggesting a functional link between inhibition of VASP-mediated filament elongation and focal adhesion turnover. Furthermore, Figure 6.4 reveals that AMPK increased expression of the focal adhesion protein paxillin, which indicates a more stable focal adhesion complex. Altogether, these data reveal a discrete signaling network between AMPK and VASP that leads to an inhibition of actin filament elongation and focal adhesion turnover. Finally, as a functional readout of this biochemical relationship, VSMCs were exposed to PDGF-mediated chemotaxis in a transwell migration assay and results show that with AMPK stimulation, migration was reduced nearly fourfold after 18 hours compared to vehicle controls (Fig. 6.5).

To investigate the dependence of AMPK on VASP in its inhibition of VSMC growth we utilized Lv-shRNA against full length VASP and successfully knocked the protein down nearly ~80 percent as documented through ECL-based Western blotting on cellular homogenates and ICW blotting on intact cells (Figs. 6.1 B and 6.1C). Again, testing the specificity of AMPK-mediated phosphorylation of VASP Ser157 and VASP Thr278, we analyzed VASP-deficient cells treated with and without AICAR and found no differences among the groups, thus suggesting AMPK dependence (Figs. 6.1 D and 6.1E). As expected, G-actin was even further increased with under conditions of VASP knockdown yet no difference was detected when VASP-deficient cells were treated with AICAR. Additionally, pFAK Tyr397 was reduced significantly and paxillin was increased significantly in in VASP-deficient cells, yet with both pFAK and paxillin no differences were found between VASP-deficient cells treated with or without AICAR. Finally, when VASP-deficient cells were exposed to PDGF stimulation and transwell chemotaxis, significant reduction in VSMC migration was observed in VASP mutants with no significant difference observed with or without AICAR. Together these data suggest that the observed AMPK-mediated reduction in VSMC migration is indeed VASP-dependent and operates through inhibitory phosphorylation of VASP leading to reduced microfilament elongation and strain on focal complexes.

In this study we also tested the dependence of AMPK on VASP in its ability to inhibit VSM cell cycle progression. We have previously reported that AMPK has capacity to inhibit VSM cell cycle progression and cell proliferation in primary VSMCs (100, 101) and herein we report similar findings. In A7R5 VSMCs, AICAR was sufficient to significantly reduce cell cycle progression as illustrated by ~60% reduction in cells in the

G_2/M phase of the cell cycle and significant increase in cells in the S phase with moderate increase in cells found in the G_0/G_1 phase. Intriguingly, when we treated VASP-deficient cells with AICAR we found a complete reversal of the cytostatic effects of AMPK seen in non-transduced cells (Fig. 6.6). While it remains unclear the exact mechanism of this VASP-dependent inhibition of cell cycle progression, it has been suggested that VASP is necessary for Rho-dependent serum response element (Sre) transcriptional activity (31, 129). Additionally, it has been suggested that AMPK exhibits inhibitory crosstalk with RhoA in VSMCs (27). Given this insight and the new evidence presented here that AMPK plays a regulatory role on VASP, we can confidently speculate that AMPK inhibits VSMC proliferation via inhibitory regulation of VASP and VASP-dependent Sre transcriptional activity; however, further investigation into this exact mechanism is needed. Altogether, these data suggest that AMPK-mediated VSMC cytostasis is dependent upon VASP inhibition.

Figure 6.7 depicts the suggested central role of VASP on AMPK-mediated control of VSMC proliferation and migration in A7R5 VSMCs based on these findings. Through phosphorylation, AMPK exerts inhibitory control on VASP which reduces directed microfilament elongation and relieves focal adhesion strain. This reduction in focal adhesion strain results in a more stable focal adhesion complex by reducing autophosphorylation of FAK and subsequent phosphorylation of accessory focal adhesion proteins. VASP knockdown-mediated reduction in microfilament elongation reduces lamellipodia and filopodia formation required for cell chemotaxis, and with a more stable focal adhesion complex, membrane detachment from the extracellular matrix required for cell movement is ameliorated. Additionally, VASP ablation appears

to reverse the observed AMPK-mediated cytostatic effect on VSMCs. While the exact mechanism of this novel interaction remain unclear, it is certain that AMPK operates via VASP regulation to inhibit cell cycle progression and cell proliferation. Altogether, this discrete AMPK/VASP nexus provides an attractive target for the regulation of VSMC growth in an effort to curb the deleterious growth associated with VSM-dependent proliferative disorders.

Figure 6.7

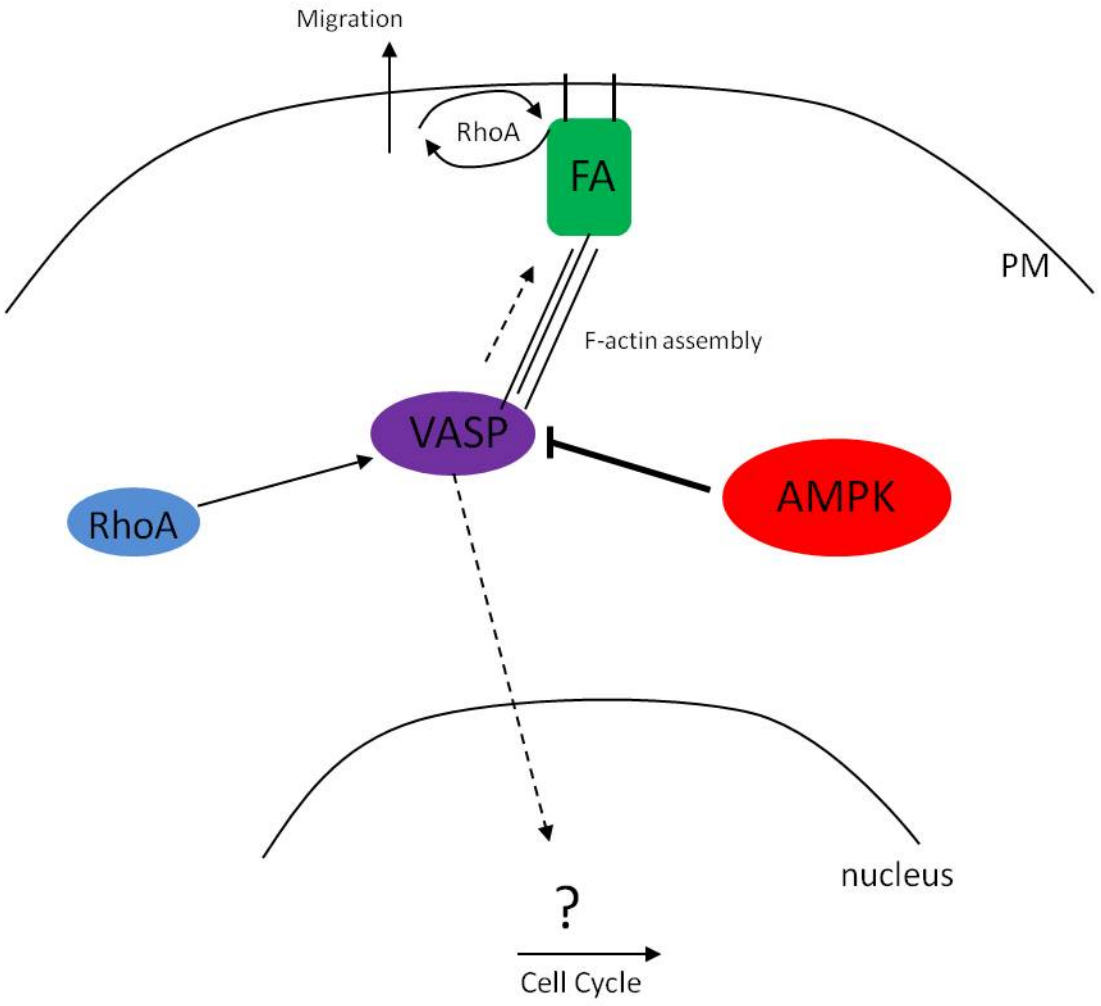

Figure 6.7. Schematic depicting the proposed functional relationship of AMPK and VASP in the inhibition of VSMC growth. AMPK exhibits inhibitory control of VASP through phosphorylation which reduces directed microfilament elongation and relieves focal adhesion strain. A reduction in focal adhesion strain results in reduced autophosphorylation of focal adhesion kinase (FAK) and subsequent activation of accessory focal adhesion proteins including the GTP-ase RhoA. Increased stability of focal adhesions ultimately reduces membrane detachment from the extracellular matrix which is required for cell movement. Additionally, VASP inhibition reduces microfilament elongation necessary for lamellipodia and filopodia formation also required for cell movement. Finally, VASP inhibition appears to reverse the observed AMPK-mediated cytostatic effect on VSMCs. While the exact mechanism remains unclear, it is certain that AMPK operates to inhibit cell cycle progression and cell proliferation via regulation of VASP.

Chapter 7: Unified Discussion

Key findings from this research project support our global hypothesis that AMPK has capacity to reduce arterial remodeling via inhibition of VSMC proliferation and migration. Ample data provide convincing evidence that AMPK operates by provoking cell cycle arrest and preventing cytoskeletal/focal adhesion restructuring necessary for VSMC migration. These findings offer unique insight into AMPK signaling as a novel system with significant therapeutic potential in the remediation of vascular growth disorders. Smooth muscle-mediated vascular remodeling plays a pivotal role in the onset and complication of vasculoproliferative diseases (44, 62, 77); therefore, targeted therapies are of great clinical importance. Data presented here lend strong support for AMPK as a biologically active signaling molecule within VSM capable of curbing cell migration and proliferation, key players in pathologic vessel remodeling.

Using the well-established balloon injury model to induce VSMC-mediated vessel remodeling (109, 114, 116), we have illustrated that both systemic and local activation of AMPK is sufficient to markedly reducing neointimal formation (Figs. 3.1, 3.2). In an effort to confirm the results observed by treatment with AICAR, we also utilized a specific and non-metabolic agonist of AMPK, the small molecule A-769662. This agent has been documented to directly activate AMPK in cell-free systems, in intact cells, and *in vivo* without the side effects associated with the more traditional AMPK-activating biguanides (30). Importantly, A-769662 has been recently characterized for use in activating AMPK in vascular cells (73). In this study the results obtained from localized treatment of injured vessels with A-769662 paralleled the results obtained with use of

AICAR, thus confirming that the *in vivo* results as well as those obtained *in vitro* are attributed to AMPK and not off-target drug-specific effects. Results using localized, perivascular delivery of AICAR or A-769662 are noteworthy and represent the first report demonstrating that local delivery of AMPK agonists immediately following intervention are biologically effective. Often, an *a priori* treatment to reduce vessel remodeling is not possible and systemic therapies can suffer from undesired side effects; however, localized delivery of an agent at the time of vascular intervention capable of reducing iatrogenic complications offers high clinical translation.

In order to examine underlying mechanisms of growth suppression by AMPK, in rat primary VSMCs following verification of the biologic activity of AICAR (Fig. 3.3) we show its ability to significantly reduce cell numbers through inhibition of cell cycle progression (Fig. 3.4, 4.9, 5.2, 6.6). Flow cytometry revealed that AICAR exerts cytostasis in the G_0/G_1 and S phases with concomitant reduction in progression through to the G_2/M phase. Of note, no changes in cell viability were observed in any treatment group; therefore, the observed changes in cell number are likely due directly to alterations in cell cycle progression and not from overt cytotoxicity. Additionally, these cytostatic effects were further supported by significant reductions in cell numbers analyzed by automated cell counting after 48 hours AICAR treatment (Figs. 3.4, 4.9, 5.3).

It was previously suggested that AMPK has ability to promote cytostasis by cyclin-dependent kinase inhibition via a p53/p21 pathway in a commercialized human VSM cell line (43); however, in addition to these findings, alternate mechanisms by which AMPK inhibits cell cycle progression are plausible. Here we demonstrate that AMPK may operate through the G_0/G_1 cell cycle regulatory proteins cyclin D/CDK4/6, cyclin

E/CDK2, and p21 and p27 to promote VSMC cytostasis. Early G_0/G_1-dependent cyclin D and late G_0/G_1-dependent cyclin E were both significantly elevated by TGFβ; however, concomitant treatment with AICAR significantly reduced both cyclin D and cyclin E compared to control and cytokine-induced conditions (Fig. 5.4). Both cyclin D-associated CDK4 as well as cyclin E-associated CDK2 were significantly elevated by TGFβ but were completely reversed to below basal levels with concomitant AICAR (Fig. 5.5). Intriguingly, no change was observed in cyclin D-associated CDK6, possibly suggesting that TGFβ promotes cell cycle progression in a cyclin D/CDK4- then cyclin E/CDK2-specific fashion. Furthermore, AICAR elevated both CDK inhibitors p21 and p27; however, only p21 remained elevated following co-treatment with TGFβ (Fig. 5.6). Taken together, these data suggest that AMPK has ability to inhibit TGFβ-induced cell cycle progression via reduction in G_0/G_1 cyclin D/CDK4 and cyclin E/CDK2 complexes through p21-mediated CDK inhibition.

It has been reported that PP-2A has the ability to disrupt the cdc/cyclin B complex and inhibit G_2/M progression. Although traditional cell cycle inhibition occurs primarily in the G_0/G_1 phase, our cell cycle analysis revealed a large increase in S-phase cells; therefore, we investigated the hypothesis that PP-2A contributes to the mechanism for AMPK inhibition of VSMC proliferation. Our data reveal that AMPK specifically induces PP-2A activity (Fig. 4.5A) and concomitantly reduces cdc2/cyclinB expression after 24 hours (Fig. 4.5B) in nuclear fractions. It is possible that in a pathologic state, as with our stimulated VSMCs, cell cycle regulation may occur at various points outside of G_0/G_1 as we observed. Therefore, we suggest that AMPK has ability to induce S-phase cytostasis through increased PP-2A activity.

Finally, using rat A7R5 VSMCs, AICAR was sufficient to significantly reduce cell cycle progression as illustrated by ~60% reduction in cells in the G_2/M phase of the cell cycle, a significant increase in cells in the S phase, and moderate increases in cells in the G_0/G_1 phase. Intriguingly, when we treated Lv-shRNA-mediated VASP-deficient cells with AICAR we found a complete reversal of the cytostatic effects of AMPK seen in non-transduced cells (Fig. 6.6). While the exact mechanism remains uncertain, it has been suggested that VASP is necessary for Rho-dependent serum response element (Sre) transcriptional activity and subsequent cell cylce progression (31, 129). Additionally, it has been suggested that AMPK exhibits inhibitory crosstalk with RhoA in VSMCs (27). Given this new insight and the evidence presented here that AMPK plays a regulatory role on VASP, we can speculate that AMPK inhibits VSMC proliferation via inhibitory regulation of VASP and VASP-dependent transcriptional activity; however, further investigation is needed to confirm these early results.

In addition to proliferation, VSMC migration is important in the pathophysiology of vessel remodeling. The physical movement of cells across a substrate is a complex process highly dependent upon the actin cytoskeleton and its interface with focal contacts and the extracellular matrix. In this study we demonstrate that AMPK plays a key role in the inhibition of VSMC migration after 18 hours revealed by significant reduction in chemotaxis analyzed by PDGF-stimulated transwell migration (Figs. 3.6, 4.8, 6.5). We present here one of the first reports demonstrating that AMPK acts to inhibit VSMC migration, which could offer significant therapeutic insight for the curbing of multiple disease processes that arise from an induction of cell migration.

Next we sought to explore specific mechanism employed by AMPK to inhibit VSMC migration and found discrete mechanisms suggesting AMPK regulates cytoskeletal and focal adhesion dynamics necessary to promote VSMC migration. Actin polymerization and leading edge formation are critical for directional cellular movement; however, AMPK impairs actin polymerization, presumably by inhibiting the anti-capping potential of VASP through direct, site-specific phosphorylation (9). The actin cytoskeleton-associated protein VASP is implicated in the directionality of extra- to intra-cellular signaling events and regulation of focal adhesions, and, via nucleotide exchange factor regulation, helps control transcriptional activation (10, 31, 123, 129). Site-specific VASP phosphorylation has also been used as readout of protein kinase signaling as we have recently reported (2, 47, 100, 101). Here we observed significant enhancement of pVASP at T157 and the AMPK-specific T278 site by AICAR (Figs. 3.7, 4.3, 6.1). The resulting impairment of actin polymerization is evidenced by concomitant accumulation of G-actin in the cytosol and increased stress fiber formation in cultured VSMCs (Figs. 3.8, 6.2). This reduction in F-actin was completely reversed with VASP deletion and no difference was detected with concomitant AICAR treatment (Fig. 6.2). Together, these data argue that AMPK mechanistically hinders actin cytoskeletal rearrangement providing migration and growth retardation in a VASP-dependent manner.

Unique findings presented here also reveal that AMPK has potential to inhibit focal adhesion turnover necessary for the movement of cells across or through substrata. We show that AICAR treatment impairs FAK activation by inhibiting Tyr397 phosphorylation (Fig. 3.9 and 6.3), a necessary event for kinase activity (107). Upon activation, FAK induces paxillin phosphorylation and targets GTPase activity at the focal

adhesion allowing for focal contact release (107). Therefore, inhibition of FAK activity offers another possible mechanism by which AMPK mediates inhibition of migration. Additionally, it has been suggested that paxillin acts as a bi-directional membrane-to-nucleus signaling molecule and that differential accumulation of paxillin in each cellular compartment is indicative of either a pro- or anti-synthetic/migratory event (38, 122). Our data reveal that AICAR prevents cytosolic accumulation of paxillin while promoting membrane stability (Fig. 3.10 and 6.4). Additionally, pFAK Tyr397 was reduced and paxillin was significantly increased in VASP-deficient cells, yet with both pFAK and paxillin no differences were found in VASP-deficient cells treated with AICAR. Taken together, these data reveal a potential anti-migratory signaling network via AMPK-mediated inhibition of FAK and focal adhesion dissociation, potentially in a VASP-dependent manner, thereby reducing pro-migratory signals and promoting focal adhesion stability and growth suppression.

To more comprehensively address the biophysics of migrating and synthetic VSMCs, we assessed activity of the extracellular matrix (ECM)-degrading gelatinolytic MMPs. Upon activation, VSMCs produce and secrete MMP-2 and MMP-9 that act to degrade the ECM and that allow for VSMC expansion/migration and collagen deposition (11, 46, 68). Here we show that AICAR selectively impairs MMP-9 activity (Fig. 3.11), which we suggest promotes a more stable focal adhesion via reduced extracellular matrix degradation thus increasing focal adhesion/substratum connectivity. Combined, these data suggest a novel role for AMPK in the reduction of MMP-9 activity that may play a key role in the inhibition of cellular migration via enhanced focal adhesion

contacts as well as matrix-based morphological changes in the vessel wall following injury.

The scope of this project was quite extensive; however, there are potential limitations to this work, which include the absence of a transgenic model in our *in vivo* studies and knockdown of specific focal adhesion proteins downstream of our proposed AMPK/VASP nexus. Additionally, further insight into the exact mechanism employed by VASP to promote cell proliferation is needed since our data clearly indicates a reversal of AMPK-mediated cell senescence with VASP knockdown. With these limitations in mind, we have established collaboration with Dr. Nair Sreejayan at The University of Wyoming who has agreed to provide AMPKα2 kinase dead (AMPKα2-KD) mice for our *in vivo* studies and to provide primary cells from the knockouts for our *in vitro* studies. We plan to use these animals to provide further evidence of isoform specific growth inhibition by AMPK in VSMCs. Additionally, since viral-mediated knockdown of proteins *in vitro* has been established in our lab, we plan to make further use of this technique to knockdown proteins integral to the AMPK/VASP growth inhibition nexus. Similar work has already begun as we have established collaboration with Dr. Jeff Brault at East Carolina University to provide Smad3 viral constructs in an effort to establish this as the primary TGFβ-induced growth-promoting pathway inhibited by AMPK in cultured VSMCs. With these methods established, we hope to have the data from chapters 4 and 5 of this dissertation completed in the near future which will provide two additional manuscripts as well as a more complete picture of mechanisms employed by AMPK within VSMCs for growth inhibition.

In conclusion, convincing data presented here provide strong evidence that AMPK is a desirable anti-growth target in VSM. Using the AMPK mimetic AICAR or the AMPK-activating small molecule A-769662, we present *in vivo* and *in vitro* data supporting our claims that AMPK abrogates neointimal formation and reduces VSMC proliferation and migration. Mechanistically, ample evidence suggests that AMPK acts to promote VSMC cytostasis via G_0/G_1 and S-phase inhibition and subsequent VSMC proliferation and through cell migration inhibition. Specific mechanisms of AMPK-mediated cytostasis include the inhibition of growth-promoting signals and cell cycle regulatory cyclin/cdk proteins as well as VASP inhibition and microfilament/focal adhesion stability and reduced extracellular matrix turnover. Intriguing early data from Chapter 6 suggest that the anti-migratory signals employed by AMPK, namely VASP and focal adhesions, may also play a central role in AMPK-mediated anti-proliferation. All cytoskeletal rearrangements tested that are necessary for cell migration were ablated by AMPK, yet were reversed when VASP was knocked down. Additionally, the functional inhibition of cell migration and proliferation by AMPK were also reversed with VASP deficiency. Together these early findings suggest that AMPK has capacity to inhibit VSMC growth through attenuation of migration and proliferation and that these events are at least in part dependent on it's interaction with the microfilament and focal adhesion proteins. Thus, these data paint a comprehensive picture of discrete AMPK-mediated cytostatic signaling networks (Fig. 7.1) that have significant clinical relevance and could potentially be manipulated in efforts to reduce vasculoproliferative pathologies.

Figure 7.1

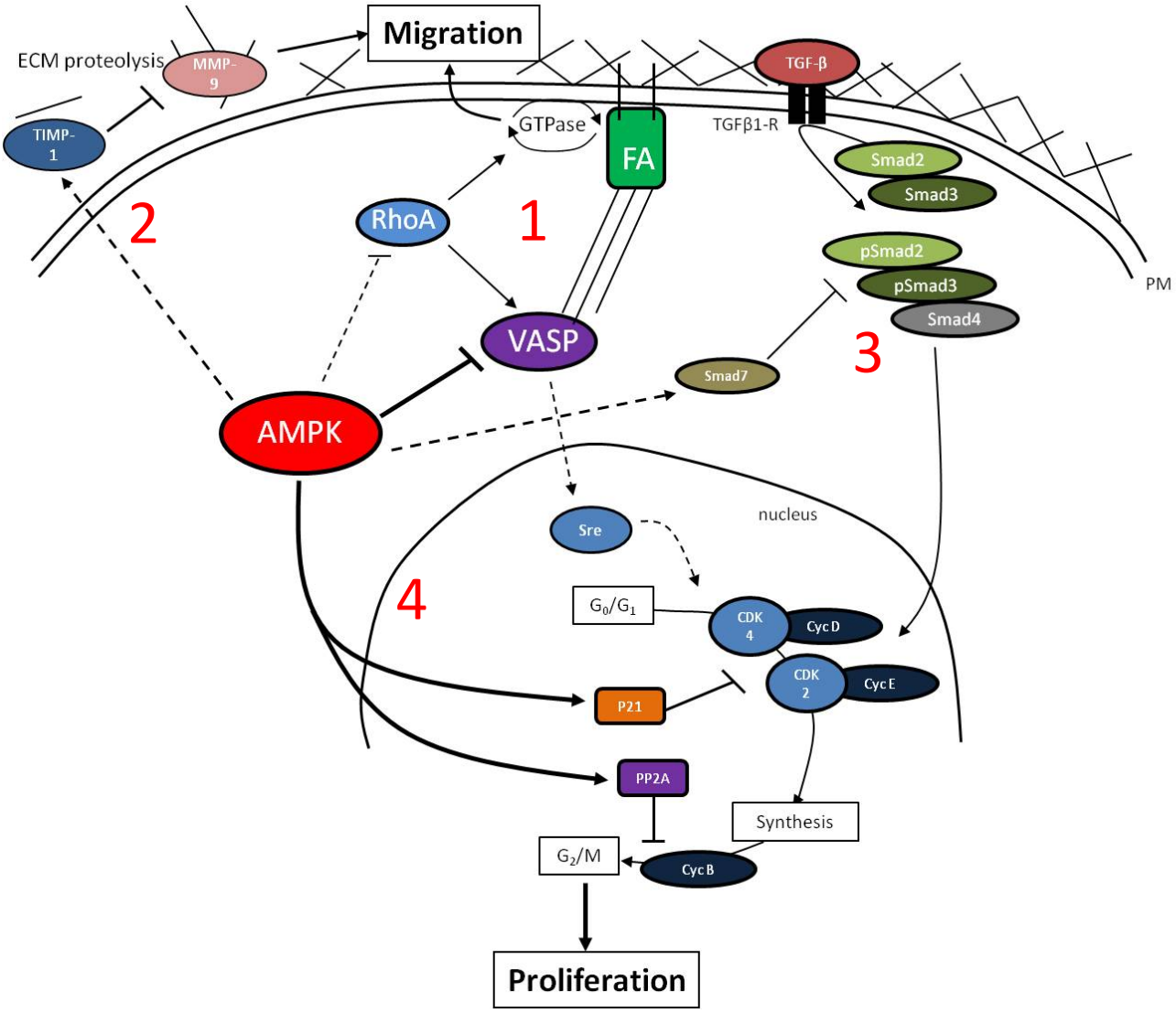
Migration
ECM proteolysis
MMP-9
TIMP-1
GTPase
FA
TGF-β
TGFβ1-R
Smad2
Smad3
pSmad2
pSmad3
Smad4
PM
RhoA
1
2
3
4
VASP
Smad7
AMPK
nucleus
Sre
G0/G1
CDK 4
Cyc D
CDK 2
Cyc E
P21
PP2A
Synthesis
G2/M
Cyc B
Proliferation

Figure 7.1. Schematic of proposed signaling network for AMPK-mediated cytostasis in VSMCs. Collectively, our data suggest AMPK plays a key role in regulating both intra- and extra-cellular events involved in VSMC proliferation and migration. Vasodilator-stimulated phosphoprotein (VASP) is an actin polymerization protein which leads to directed microfilament elongation. Given its connection with focal adhesions (FA), increased actin strain by microfilament elongation provides the physical stress necessary for focal adhesion kinase (FAK) activation via autophosphorylation at Tyr397. Upon activation, FAK phosphorylates other FA proteins and recruits RhoA GTPases necessary for FA disassembly. This FA turnover and simulatenous microfilament push on the cell membrane allows for directed cell migration. Here we illustrate that AMPK has ability to inhibit FAK activation and RhoA recruitment to FA complexes. Additionally, we show increased FA stability as indicated by increased membranous paxillin expression, a marker of stable FAs. We suggest that the observed reduction in FAK activation with AICAR is due to reduced actin strain via inhibition of VASP. These data illustrate that VASP inhibition results in reduced F-actin assembly. Together, these data suggest that VASP inhibition reduces FA actin strain and subsequent FA turnover necessary to produce cell migration and are illustrated by sequence 1.

Treatment of VSMCs with AICAR revealed significant reduction of matrix metalloproteinase-9 (MMP9) activity in conditioned media as well as a significant increase in tissue inhibitor of metalloproteinase-1 (TIMP-1), an inhibitor of MMP-2 and MMP-9. During vessel remodeling or cell migration, extracellular matrix proteins are continually broken down by MMPs and then re-synthesized in the extracellular space. Sequence 2 illustrates our proposed mechanism of AMPK activation of TIMP-1 and subsequent TIMP-1 inhibition of MMP-9. This mechanism of AMPK-mediated extracellular matrix stability could be utilized *in vivo* following injury to inhibit vessel remodeling and fibrosis, and *in vitro* by inhibiting VSMC migration.

The exact role of transforming growth factor-β (TGFβ) signaling in VSMCs remains elusive. Some reports suggest TGFβ signaling promotes cytostasis, while more recent reports suggest it promotes cell cycle progression. We analyzed the effect of recombinant human TGFβ treatment on VSMCs by analyzing the expression profile of the TGFβ-mediated Smad signaling pathway and growth promoting cyclin/cdk complexes. Sequence 3 illustrates how activated TGFβ receptors promote the phosphorylation of Smad2 and Smad3, which can then oligomerize with cytosolic Smad4 for nuclear translocation. Upon activation of Smad 2 and 3 we found increased cyclin D/cdk 4 and cyclin E/cdk 2, both G_0/G_1 promoting

complexes. However, with AICAR, both Smad3 and the cyclin/cdk complexes were significantly reduced with concomitant increase in inhibitory Smad7 and cell cycle inhibitor p21 (Sequence 4). Together AICAR-mediated inhibition of TGFβ/Smad and cell cycle signaling as well as a significant reduction in TGFβ-mediated cell cycle progression and clonal cell expansion (data not shown), these data suggest that TGFβ increases VSMC growth and that AMPK has capacity to reduce these growth promoting signals.

Literature Cited

1. **Adderley SP JC, Martin DN and Tulis DA**. Phosphodiesterases regulate BAY 41-2272-induced VASP phosphorylation in vascular smooth muscle cells. *Front Pharmacol* 3: 2012.

2. **Adderley SP, Joshi CN, Martin DN, and Tulis DA**. Phosphodiesterases Regulate BAY 41-2272-Induced VASP Phosphorylation in Vascular Smooth Muscle Cells. *Front Pharmacol* 3: 10, 2012.

3. **Akhurst RJ, and Hata A**. Targeting the TGFbeta signalling pathway in disease. *Nat Rev Drug Discov* 11: 790-811, 2012.

4. **Barzik M, Kotova TI, Higgs HN, Hazelwood L, Hanein D, Gertler FB, and Schafer DA**. Ena/VASP proteins enhance actin polymerization in the presence of barbed end capping proteins. *The Journal of biological chemistry* 280: 28653-28662, 2005.

5. **Battegay EJ, Raines EW, Seifert RA, Bowen-Pope DF, and Ross R**. TGF-beta induces bimodal proliferation of connective tissue cells via complex control of an autocrine PDGF loop. *Cell* 63: 515-524, 1990.

6. **Bear JE, Svitkina TM, Krause M, Schafer DA, Loureiro JJ, Strasser GA, Maly IV, Chaga OY, Cooper JA, Borisy GG, and Gertler FB**. Antagonism between Ena/VASP proteins and actin filament capping regulates fibroblast motility. *Cell* 109: 509-521, 2002.

7. **Benz PM, Blume C, Seifert S, Wilhelm S, Waschke J, Schuh K, Gertler F, Munzel T, and Renne T**. Differential VASP phosphorylation controls remodeling of the actin cytoskeleton. *J Cell Sci* 122: 3954-3965, 2009.

8. **Berk BC**. Vascular smooth muscle growth: autocrine growth mechanisms. *Physiol Rev* 81: 999-1030, 2001.

9. **Blume C, Benz PM, Walter U, Ha J, Kemp BE, and Renne T**. AMP-activated protein kinase impairs endothelial actin cytoskeleton assembly by phosphorylating vasodilator-stimulated phosphoprotein. *The Journal of biological chemistry* 282: 4601-4612, 2007.

10. **Breitsprecher D, Kiesewetter AK, Linkner J, Urbanke C, Resch GP, Small JV, and Faix J**. Clustering of VASP actively drives processive, WH2 domain-mediated actin filament elongation. *The EMBO journal* 27: 2943-2954, 2008.

11. **Briones AM, Arribas SM, and Salaices M**. Role of extracellular matrix in vascular remodeling of hypertension. *Curr Opin Nephrol Hypertens* 19: 187-194, 2010.

12. **Browner NC, Dey NB, Bloch KD, and Lincoln TM**. Regulation of cGMP-dependent protein kinase expression by soluble guanylyl cyclase in vascular smooth muscle cells. *The Journal of biological chemistry* 279: 46631-46636, 2004.

13. **Cai Y, Teng X, Pan CS, Duan XH, Tang CS, and Qi YF**. Adrenomedullin up-regulates osteopontin and attenuates vascular calcification via the cAMP/PKA signaling pathway. *Acta Pharmacol Sin* 31: 1359-1366, 2010.

14. **Chang MY, Ho FM, Wang JS, Kang HC, Chang Y, Ye ZX, and Lin WW**. AICAR induces cyclooxygenase-2 expression through AMP-activated protein kinase-

transforming growth factor-beta-activated kinase 1-p38 mitogen-activated protein kinase signaling pathway. *Biochem Pharmacol* 80: 1210-1220, 2010.

15. **Chen L, Daum G, Chitaley K, Coats SA, Bowen-Pope DF, Eigenthaler M, Thumati NR, Walter U, and Clowes AW**. Vasodilator-stimulated phosphoprotein regulates proliferation and growth inhibition by nitric oxide in vascular smooth muscle cells. *Arterioscler Thromb Vasc Biol* 24: 1403-1408, 2004.

16. **Cohen P, and Hardie DG**. The actions of cyclic AMP on biosynthetic processes are mediated indirectly by cyclic AMP-dependent protein kinase. *Biochimica et biophysica acta* 1094: 292-299, 1991.

17. **Crute BE, Seefeld K, Gamble J, Kemp BE, and Witters LA**. Functional domains of the alpha1 catalytic subunit of the AMP-activated protein kinase. *The Journal of biological chemistry* 273: 35347-35354, 1998.

18. **D'Souza FM, Sparks RL, Chen H, Kadowitz PJ, and Jeter JR, Jr.** Mechanism of eNOS gene transfer inhibition of vascular smooth muscle cell proliferation. *American journal of physiology Cell physiology* 284: C191-199, 2003.

19. **Djouder N, Tuerk RD, Suter M, Salvioni P, Thali RF, Scholz R, Vaahtomeri K, Auchli Y, Rechsteiner H, Brunisholz RA, Viollet B, Makela TP, Wallimann T, Neumann D, and Krek W**. PKA phosphorylates and inactivates AMPKalpha to promote efficient lipolysis. *EMBO J* 29: 469-481, 2010.

20. **Durante W, Schini VB, Catovsky S, Kroll MH, Vanhoutte PM, and Schafer AI**. Plasmin potentiates induction of nitric oxide synthesis by interleukin-1 beta in vascular smooth muscle cells. *Am J Physiol* 264: H617-624, 1993.

21. **Dyck JR, Kudo N, Barr AJ, Davies SP, Hardie DG, and Lopaschuk GD**. Phosphorylation control of cardiac acetyl-CoA carboxylase by cAMP-dependent protein kinase and 5'-AMP activated protein kinase. *Eur J Biochem* 262: 184-190, 1999.

22. **Eckert RE, and Jones SL**. Regulation of VASP serine 157 phosphorylation in human neutrophils after stimulation by a chemoattractant. *J Leukoc Biol* 82: 1311-1321, 2007.

23. **Ewart MA, and Kennedy S**. AMPK and vasculoprotection. *Pharmacol Ther* 131: 242-253, 2011.

24. **Fluri F, Hatz F, Voss B, Lyrer PA, and Engelter ST**. Restenosis after carotid endarterectomy: significance of newly acquired risk factors. *Eur J Neurol* 17: 493-498, 2010.

25. **Ford RJ, Teschke SR, Reid EB, Durham KK, Kroetsch JT, and Rush JW**. AMP-activated protein kinase activator AICAR acutely lowers blood pressure and relaxes isolated resistance arteries of hypertensive rats. *J Hypertens* 30: 725-733, 2012.

26. **Friedland JC, Lee MH, and Boettiger D**. Mechanically activated integrin switch controls alpha5beta1 function. *Science* 323: 642-644, 2009.

27. **Gayard M, Guilluy C, Rousselle A, Viollet B, Henrion D, Pacaud P, Loirand G, and Rolli-Derkinderen M**. AMPK alpha 1-induced RhoA phosphorylation mediates vasoprotective effect of estradiol. *Arteriosclerosis, thrombosis, and vascular biology* 31: 2634-2642, 2011.

28. **Go AS, Mozaffarian D, Roger VL, Benjamin EJ, Berry JD, Borden WB, Bravata DM, Dai S, Ford ES, Fox CS, Franco S, Fullerton HJ, Gillespie C, Hailpern SM, Heit JA, Howard VJ, Huffman MD, Kissela BM, Kittner SJ, Lackland DT,**

Lichtman JH, Lisabeth LD, Magid D, Marcus GM, Marelli A, Matchar DB, McGuire DK, Mohler ER, Moy CS, Mussolino ME, Nichol G, Paynter NP, Schreiner PJ, Sorlie PD, Stein J, Turan TN, Virani SS, Wong ND, Woo D, and Turner MB. Heart disease and stroke statistics--2013 update: a report from the American Heart Association. *Circulation* 127: e6-e245, 2013.

29. **Goirand F, Solar M, Athea Y, Viollet B, Mateo P, Fortin D, Leclerc J, Hoerter J, Ventura-Clapier R, and Garnier A**. Activation of AMP kinase alpha1 subunit induces aortic vasorelaxation in mice. *J Physiol* 581: 1163-1171, 2007.

30. **Goransson O, McBride A, Hawley SA, Ross FA, Shpiro N, Foretz M, Viollet B, Hardie DG, and Sakamoto K**. Mechanism of action of A-769662, a valuable tool for activation of AMP-activated protein kinase. *The Journal of biological chemistry* 282: 32549-32560, 2007.

31. **Grosse R, Copeland JW, Newsome TP, Way M, and Treisman R**. A role for VASP in RhoA-Diaphanous signalling to actin dynamics and SRF activity. *The EMBO journal* 22: 3050-3061, 2003.

32. **Han JH, Ahn YH, Choi KY, and Hong SH**. Involvement of AMP-activated protein kinase and p38 mitogen-activated protein kinase in 8-Cl-cAMP-induced growth inhibition. *J Cell Physiol* 218: 104-112, 2009.

33. **Handa N, Takagi T, Saijo S, Kishishita S, Takaya D, Toyama M, Terada T, Shirouzu M, Suzuki A, Lee S, Yamauchi T, Okada-Iwabu M, Iwabu M, Kadowaki T, Minokoshi Y, and Yokoyama S**. Structural basis for compound C inhibition of the human AMP-activated protein kinase alpha2 subunit kinase domain. *Acta Crystallogr D Biol Crystallogr* 67: 480-487, 2011.

34. **Hao H, Gabbiani G, and Bochaton-Piallat ML**. Arterial smooth muscle cell heterogeneity: implications for atherosclerosis and restenosis development. *Arteriosclerosis, thrombosis, and vascular biology* 23: 1510-1520, 2003.

35. **Hardie DG**. AMP-activated protein kinase: an energy sensor that regulates all aspects of cell function. *Genes Dev* 25: 1895-1908, 2011.

36. **Hardie DG**. AMP-activated/SNF1 protein kinases: conserved guardians of cellular energy. *Nat Rev Mol Cell Biol* 8: 774-785, 2007.

37. **Hawley SA, Ross FA, Chevtzoff C, Green KA, Evans A, Fogarty S, Towler MC, Brown LJ, Ogunbayo OA, Evans AM, and Hardie DG**. Use of cells expressing gamma subunit variants to identify diverse mechanisms of AMPK activation. *Cell Metab* 11: 554-565, 2010.

38. **Hervy M, Hoffman L, and Beckerle MC**. From the membrane to the nucleus and back again: bifunctional focal adhesion proteins. *Curr Opin Cell Biol* 18: 524-532, 2006.

39. **Hewer RC, Sala-Newby GB, Wu YJ, Newby AC, and Bond M**. PKA and Epac synergistically inhibit smooth muscle cell proliferation. *Journal of molecular and cellular cardiology* 50: 87-98, 2011.

40. **Hneino M, Bouazza L, Bricca G, Li JY, and Langlois D**. Density-dependent shift of transforming growth factor-beta-1 from inhibition to stimulation of vascular smooth muscle cell growth is based on unconventional regulation of proliferation, apoptosis and contact inhibition. *J Vasc Res* 46: 85-97, 2009.

41. **Hu Y, Hu X, Boumsell L, and Ivashkiv LB**. IFN-gamma and STAT1 arrest monocyte migration and modulate RAC/CDC42 pathways. *Journal of immunology* 180: 8057-8065, 2008.

42. **Hurley RL, Barre LK, Wood SD, Anderson KA, Kemp BE, Means AR, and Witters LA**. Regulation of AMP-activated protein kinase by multisite phosphorylation in response to agents that elevate cellular cAMP. *J Biol Chem* 281: 36662-36672, 2006.

43. **Igata M, Motoshima H, Tsuruzoe K, Kojima K, Matsumura T, Kondo T, Taguchi T, Nakamaru K, Yano M, Kukidome D, Matsumoto K, Toyonaga T, Asano T, Nishikawa T, and Araki E**. Adenosine monophosphate-activated protein kinase suppresses vascular smooth muscle cell proliferation through the inhibition of cell cycle progression. *Circ Res* 97: 837-844, 2005.

44. **Insull W, Jr.** The pathology of atherosclerosis: plaque development and plaque responses to medical treatment. *Am J Med* 122: S3-S14, 2009.

45. **Janssens V, and Goris J**. Protein phosphatase 2A: a highly regulated family of serine/threonine phosphatases implicated in cell growth and signalling. *The Biochemical journal* 353: 417-439, 2001.

46. **Johnson C, and Galis ZS**. Matrix metalloproteinase-2 and -9 differentially regulate smooth muscle cell migration and cell-mediated collagen organization. *Arteriosclerosis, thrombosis, and vascular biology* 24: 54-60, 2004.

47. **Joshi CN, Martin DN, Fox JC, Mendelev NN, Brown TA, and Tulis DA**. The soluble guanylate cyclase stimulator BAY 41-2272 inhibits vascular smooth muscle growth through the cAMP-dependent protein kinase and cGMP-dependent protein

kinase pathways. *The Journal of pharmacology and experimental therapeutics* 339: 394-402, 2011.

48. **Joshi CN, Martin DN, Fox JC, Mendelev NN, Brown TA, and Tulis DA**. The Soluble Guanylate Cyclase Stimulator BAY 41-2272 Inhibits Vascular Smooth Muscle Growth through the PKA and PKG Pathways. *The Journal of pharmacology and experimental therapeutics* 2011.

49. **Joshi CN, Martin DN, Shaver P, Madamanchi C, Muller-Borer BJ, and Tulis DA**. Control of vascular smooth muscle cell growth by connexin 43. *Front Physiol* 3: 220, 2012.

50. **Kawaguchi T, Takenoshita M, Kabashima T, and Uyeda K**. Glucose and cAMP regulate the L-type pyruvate kinase gene by phosphorylation/dephosphorylation of the carbohydrate response element binding protein. *P Natl Acad Sci USA* 98: 13710-13715, 2001.

51. **Kemp BE, Stapleton D, Campbell DJ, Chen ZP, Murthy S, Walter M, Gupta A, Adams JJ, Katsis F, van Denderen B, Jennings IG, Iseli T, Michell BJ, and Witters LA**. AMP-activated protein kinase, super metabolic regulator. *Biochem Soc Trans* 31: 162-168, 2003.

52. **Kim JE, Song SE, Kim YW, Kim JY, Park SC, Park YK, Baek SH, Lee IK, and Park SY**. Adiponectin inhibits palmitate-induced apoptosis through suppression of reactive oxygen species in endothelial cells: involvement of cAMP/protein kinase A and AMP-activated protein kinase. *J Endocrinol* 207: 35-44, 2010.

53. **Koshman YE, Kim T, Chu M, Engman SJ, Iyengar R, Robia SL, and Samarel AM**. FRNK inhibition of focal adhesion kinase-dependent signaling and migration in

vascular smooth muscle cells. *Arteriosclerosis, thrombosis, and vascular biology* 30: 2226-2233, 2010.

54. **Laslett LJ, Alagona P, Jr., Clark BA, 3rd, Drozda JP, Jr., Saldivar F, Wilson SR, Poe C, and Hart M**. The worldwide environment of cardiovascular disease: prevalence, diagnosis, therapy, and policy issues: a report from the American College of Cardiology. *J Am Coll Cardiol* 60: S1-49, 2012.

55. **Lee EJ, Kim WJ, and Moon SK**. Cordycepin suppresses TNF-alpha-induced invasion, migration and matrix metalloproteinase-9 expression in human bladder cancer cells. *Phytother Res* 24: 1755-1761, 2010.

56. **Li HX, Han M, Bernier M, Zheng B, Sun SG, Su M, Zhang R, Fu JR, and Wen JK**. Kruppel-like factor 4 promotes differentiation by transforming growth factor-beta receptor-mediated Smad and p38 MAPK signaling in vascular smooth muscle cells. *The Journal of biological chemistry* 285: 17846-17856, 2010.

57. **Li J, Li P, Zhang Y, Li GB, Zhou YG, Yang K, and Dai SS**. c-Ski inhibits the proliferation of vascular smooth muscle cells via suppressing Smad3 signaling but stimulating p38 pathway. *Cellular signalling* 25: 159-167, 2013.

58. **Lin YY, Kiihl S, Suhail Y, Liu SY, Chou YH, Kuang Z, Lu JY, Khor CN, Lin CL, Bader JS, Irizarry R, and Boeke JD**. Functional dissection of lysine deacetylases reveals that HDAC1 and p300 regulate AMPK. *Nature* 482: 251-255, 2012.

59. **Liu Y, Dolence J, Ren J, Rao M, and Sreejayan N**. Inhibitory effect of dehydrozingerone on vascular smooth muscle cell function. *Journal of cardiovascular pharmacology* 52: 422-429, 2008.

60. **Lucchi S, Calebiro D, de Filippis T, Grassi ES, Borghi MO, and Persani L**. 8-Chloro-cyclic AMP and protein kinase A I-selective cyclic AMP analogs inhibit cancer cell growth through different mechanisms. *PLoS One* 6: e20785, 2011.

61. **Luo Z, Zang M, and Guo W**. AMPK as a metabolic tumor suppressor: control of metabolism and cell growth. *Future Oncol* 6: 457-470, 2010.

62. **Majesky MW**. Neointima formation after acute vascular injury. Role of counteradhesive extracellular matrix proteins. *Tex Heart Inst J* 21: 78-85, 1994.

63. **Mendelev NN, Williams VS, and Tulis DA**. Antigrowth properties of BAY 41-2272 in vascular smooth muscle cells. *Journal of cardiovascular pharmacology* 53: 121-131, 2009.

64. **Mihaylova MM, and Shaw RJ**. The AMPK signalling pathway coordinates cell growth, autophagy and metabolism. *Nat Cell Biol* 13: 1016-1023, 2011.

65. **Miranda L, Carpentier S, Platek A, Hussain N, Gueuning MA, Vertommen D, Ozkan Y, Sid B, Hue L, Courtoy PJ, Rider MH, and Horman S**. AMP-activated protein kinase induces actin cytoskeleton reorganization in epithelial cells. *Biochem Bioph Res Co* 396: 656-661, 2010.

66. **Momcilovic M, Hong SP, and Carlson M**. Mammalian TAK1 activates Snf1 protein kinase in yeast and phosphorylates AMP-activated protein kinase in vitro. *The Journal of biological chemistry* 281: 25336-25343, 2006.

67. **Nagata D, Takeda R, Sata M, Satonaka H, Suzuki E, Nagano T, and Hirata Y**. AMP-activated protein kinase inhibits angiotensin II-stimulated vascular smooth muscle cell proliferation. *Circulation* 110: 444-451, 2004.

68. **Newby AC**. Matrix metalloproteinases regulate migration, proliferation, and death of vascular smooth muscle cells by degrading matrix and non-matrix substrates. *Cardiovasc Res* 69: 614-624, 2006.

69. **Ning J, Xi G, and Clemmons DR**. Suppression of AMPK activation via S485 phosphorylation by IGF-I during hyperglycemia is mediated by AKT activation in vascular smooth muscle cells. *Endocrinology* 152: 3143-3154, 2011.

70. **Owens GK, Geisterfer AA, Yang YW, and Komoriya A**. Transforming growth factor-beta-induced growth inhibition and cellular hypertrophy in cultured vascular smooth muscle cells. *J Cell Biol* 107: 771-780, 1988.

71. **Owens GK, Kumar MS, and Wamhoff BR**. Molecular regulation of vascular smooth muscle cell differentiation in development and disease. *Physiol Rev* 84: 767-801, 2004.

72. **Pastula C, Johnson I, Beechem JM, and Patton WF**. Development of fluorescence-based selective assays for serine/threonine and tyrosine phosphatases. *Comb Chem High Throughput Screen* 6: 341-346, 2003.

73. **Peyton KJ, Liu XM, Yu Y, Yates B, and Durante W**. Activation of AMP-activated protein kinase inhibits the proliferation of human endothelial cells. *The Journal of pharmacology and experimental therapeutics* 342: 827-834, 2012.

74. **Peyton KJ, Yu Y, Yates B, Shebib AR, Liu XM, Wang H, and Durante W**. Compound C inhibits vascular smooth muscle cell proliferation and migration in an AMP-activated protein kinase-independent fashion. *The Journal of pharmacology and experimental therapeutics* 338: 476-484, 2011.

75. **Polyak K, Kato JY, Solomon MJ, Sherr CJ, Massague J, Roberts JM, and Koff A**. p27Kip1, a cyclin-Cdk inhibitor, links transforming growth factor-beta and contact inhibition to cell cycle arrest. *Genes Dev* 8: 9-22, 1994.

76. **Raffetto JD, and Khalil RA**. Matrix metalloproteinases and their inhibitors in vascular remodeling and vascular disease. *Biochemical pharmacology* 75: 346-359, 2008.

77. **Raines EW, and Ross R**. Smooth muscle cells and the pathogenesis of the lesions of atherosclerosis. *Br Heart J* 69: S30-37, 1993.

78. **Reardon C, and McKay DM**. TGF-beta suppresses IFN-gamma-STAT1-dependent gene transcription by enhancing STAT1-PIAS1 interactions in epithelia but not monocytes/macrophages. *Journal of immunology* 178: 4284-4295, 2007.

79. **Rensen SS, Doevendans PA, and van Eys GJ**. Regulation and characteristics of vascular smooth muscle cell phenotypic diversity. *Neth Heart J* 15: 100-108, 2007.

80. **Richter EA, Nielsen JN, Jorgensen SB, Frosig C, and Wojtaszewski JF**. Signalling to glucose transport in skeletal muscle during exercise. *Acta Physiol Scand* 178: 329-335, 2003.

81. **Roger VL, Go AS, Lloyd-Jones DM, Benjamin EJ, Berry JD, Borden WB, Bravata DM, Dai S, Ford ES, Fox CS, Fullerton HJ, Gillespie C, Hailpern SM, Heit JA, Howard VJ, Kissela BM, Kittner SJ, Lackland DT, Lichtman JH, Lisabeth LD, Makuc DM, Marcus GM, Marelli A, Matchar DB, Moy CS, Mozaffarian D, Mussolino ME, Nichol G, Paynter NP, Soliman EZ, Sorlie PD, Sotoodehnia N, Turan TN, Virani SS, Wong ND, Woo D, and Turner MB**. Heart Disease and Stroke Statistics--2012

Update: A Report From the American Heart Association. *Circulation* 125: e2-e220, 2012.

82. **Ross R**. The pathogenesis of atherosclerosis: a perspective for the 1990s. *Nature* 362: 801-809, 1993.

83. **Rossoni LV, Wareing M, Wenceslau CF, Al-Abri M, Cobb C, and Austin C**. Acute simvastatin increases endothelial nitric oxide synthase phosphorylation via AMP-activated protein kinase and reduces contractility of isolated rat mesenteric resistance arteries. *Clin Sci (Lond)* 121: 449-458, 2011.

84. **Rubin LJ, Magliola L, Feng X, Jones AW, and Hale CC**. Metabolic activation of AMP kinase in vascular smooth muscle. *J Appl Physiol* 98: 296-306, 2005.

85. **Ruiz-Ortega M, Rodriguez-Vita J, Sanchez-Lopez E, Carvajal G, and Egido J**. TGF-beta signaling in vascular fibrosis. *Cardiovasc Res* 74: 196-206, 2007.

86. **Samarakoon R, Higgins SP, Higgins CE, and Higgins PJ**. TGF-beta1-induced plasminogen activator inhibitor-1 expression in vascular smooth muscle cells requires pp60(c-src)/EGFR(Y845) and Rho/ROCK signaling. *Journal of molecular and cellular cardiology* 44: 527-538, 2008.

87. **Sanders MJ, Grondin PO, Hegarty BD, Snowden MA, and Carling D**. Investigating the mechanism for AMP activation of the AMP-activated protein kinase cascade. *Biochem J* 403: 139-148, 2007.

88. **Santibanez JF, Quintanilla M, and Bernabeu C**. TGF-beta/TGF-beta receptor system and its role in physiological and pathological conditions. *Clin Sci (Lond)* 121: 233-251, 2011.

89. **Schaller MD**. Cellular functions of FAK kinases: insight into molecular mechanisms and novel functions. *J Cell Sci* 123: 1007-1013, 2010.

90. **Schirenbeck A, Arasada R, Bretschneider T, Stradal TE, Schleicher M, and Faix J**. The bundling activity of vasodilator-stimulated phosphoprotein is required for filopodium formation. *P Natl Acad Sci USA* 103: 7694-7699, 2006.

91. **Schlegel N, and Waschke J**. VASP is involved in cAMP-mediated Rac 1 activation in microvascular endothelial cells. *American journal of physiology Cell physiology* 296: C453-462, 2009.

92. **Scott JW, van Denderen BJ, Jorgensen SB, Honeyman JE, Steinberg GR, Oakhill JS, Iseli TJ, Koay A, Gooley PR, Stapleton D, and Kemp BE**. Thienopyridone drugs are selective activators of AMP-activated protein kinase beta1-containing complexes. *Chem Biol* 15: 1220-1230, 2008.

93. **Serrels B, Serrels A, Brunton VG, Holt M, McLean GW, Gray CH, Jones GE, and Frame MC**. Focal adhesion kinase controls actin assembly via a FERM-mediated interaction with the Arp2/3 complex. *Nat Cell Biol* 9: 1046-1056, 2007.

94. **Shen J, Smith RA, Stoll VS, Edalji R, Jakob C, Walter K, Gramling E, Dorwin S, Bartley D, Gunasekera A, Yang J, Holzman T, and Johnson RW**. Characterization of protein kinase A phosphorylation: multi-technique approach to phosphate mapping. *Anal Biochem* 324: 204-218, 2004.

95. **Shirwany NA, and Zou MH**. AMPK in cardiovascular health and disease. *Acta Pharmacol Sin* 31: 1075-1084, 2010.

96. **Shoji S, Ericsson LH, Walsh KA, Fischer EH, and Titani K**. Amino acid sequence of the catalytic subunit of bovine type II adenosine cyclic 3',5'-phosphate dependent protein kinase. *Biochemistry* 22: 3702-3709, 1983.

97. **Song P, Wang S, He C, Liang B, Viollet B, and Zou MH**. AMPKalpha2 deletion exacerbates neointima formation by upregulating Skp2 in vascular smooth muscle cells. *Circulation Research* 109: 1230-1239, 2011.

98. **Steinberg RA, Cauthron RD, Symcox MM, and Shuntoh H**. Autoactivation of catalytic (C alpha) subunit of cyclic AMP-dependent protein kinase by phosphorylation of threonine 197. *Mol Cell Biol* 13: 2332-2341, 1993.

99. **Stone JD NA, and Tulis DA**. Inhibition of vascular smooth muscle growth via signaling crosstalk between AMP-activated protein kinase and cAMP-dependent protein kinase. *Front Physio* 3: 409, 2012.

100. **Stone JD, Narine A, Shaver PR, Fox JC, Vuncannon JR, and Tulis DA**. AMP-activated protein kinase inhibits vascular smooth muscle cell proliferation and migration and vascular remodeling following injury. *American journal of physiology Heart and circulatory physiology* 304: H369-381, 2013.

101. **Stone JD, Narine A, and Tulis DA**. Inhibition of vascular smooth muscle growth via signaling crosstalk between AMP-activated protein kinase and cAMP-dependent protein kinase. *Front Physiol* 3: 409, 2012.

102. **Stricker SA, Swiderek L, and Nguyen T**. Stimulators of AMP-activated kinase (AMPK) inhibit seawater- but not cAMP-induced oocyte maturation in a marine worm: Implications for interactions between cAMP and AMPK signaling. *Mol Reprod Dev* 77: 497-510, 2010.

103. **Sung JY, and Choi HC**. Aspirin-induced AMP-activated protein kinase activation regulates the proliferation of vascular smooth muscle cells from spontaneously hypertensive rats. *Biochem Bioph Res Co* 408: 312-317, 2011.

104. **Suwanabol PA, Seedial SM, Shi X, Zhang F, Yamanouchi D, Roenneburg D, Liu B, and Kent KC**. Transforming growth factor-beta increases vascular smooth muscle cell proliferation through the Smad3 and extracellular signal-regulated kinase mitogen-activated protein kinases pathways. *Journal of vascular surgery* 56: 446-454, 2012.

105. **Suwanabol PA, Seedial SM, Zhang F, Shi X, Si Y, Liu B, and Kent KC**. TGF-beta and Smad3 modulate PI3K/Akt signaling pathway in vascular smooth muscle cells. *American journal of physiology Heart and circulatory physiology* 302: H2211-2219, 2012.

106. **Tang YC, Williams BR, Siegel JJ, and Amon A**. Identification of aneuploidy-selective antiproliferation compounds. *Cell* 144: 499-512, 2011.

107. **Tomar A, and Schlaepfer DD**. Focal adhesion kinase: switching between GAPs and GEFs in the regulation of cell motility. *Curr Opin Cell Biol* 21: 676-683, 2009.

108. **Tsai S, Hollenbeck ST, Ryer EJ, Edlin R, Yamanouchi D, Kundi R, Wang C, Liu B, and Kent KC**. TGF-beta through Smad3 signaling stimulates vascular smooth muscle cell proliferation and neointimal formation. *American journal of physiology Heart and circulatory physiology* 297: H540-549, 2009.

109. **Tulis DA**. Histological and morphometric analyses for rat carotid balloon injury model. *Methods Mol Med* 139: 31-66, 2007.

110. **Tulis DA**. Novel therapies for cyclic GMP control of vascular smooth muscle growth. *Am J Ther* 15: 551-564, 2008.

111. **Tulis DA**. Rat carotid artery balloon injury model. *Methods Mol Med* 139: 1-30, 2007.

112. **Tulis DA, Bohl Masters KS, Lipke EA, Schiesser RL, Evans AJ, Peyton KJ, Durante W, West JL, and Schafer AI**. YC-1-mediated vascular protection through inhibition of smooth muscle cell proliferation and platelet function. *Biochem Biophys Res Commun* 291: 1014-1021, 2002.

113. **Tulis DA, Durante W, Peyton KJ, Chapman GB, Evans AJ, and Schafer AI**. YC-1, a benzyl indazole derivative, stimulates vascular cGMP and inhibits neointima formation. *Biochem Bioph Res Co* 279: 646-652, 2000.

114. **Tulis DA, Durante W, Peyton KJ, Evans AJ, and Schafer AI**. Heme oxygenase-1 attenuates vascular remodeling following balloon injury in rat carotid arteries. *Atherosclerosis* 155: 113-122, 2001.

115. **Tulis DA, Keswani AN, Peyton KJ, Wang H, Schafer AI, and Durante W**. Local administration of carbon monoxide inhibits neointima formation in balloon injured rat carotid arteries. *Cell Mol Biol (Noisy-le-grand)* 51: 441-446, 2005.

116. **Tulis DA, Mnjoyan ZH, Schiesser RL, Shelat HS, Evans AJ, Zoldhelyi P, and Fujise K**. Adenoviral gene transfer of fortilin attenuates neointima formation through suppression of vascular smooth muscle cell proliferation and migration. *Circulation* 107: 98-105, 2003.

117. **Valero MS, Pereboom D, Barcelo-Batllory S, Brines L, Garay RP, and Alda JO**. Protein kinase A signalling is involved in the relaxant responses to the selective

beta-oestrogen receptor agonist diarylpropionitrile in rat aortic smooth muscle in vitro. *J Pharm Pharmacol* 63: 222-229, 2011.

118. **Wang M, Monticone RE, and Lakatta EG**. Arterial aging: a journey into subclinical arterial disease. *Curr Opin Nephrol Hypertens* 19: 201-207, 2010.

119. **Watt MJ, Holmes AG, Pinnamaneni SK, Garnham AP, Steinberg GR, Kemp BE, and Febbraio MA**. Regulation of HSL serine phosphorylation in skeletal muscle and adipose tissue. *Am J Physiol Endocrinol Metab* 290: E500-508, 2006.

120. **Witters LA, Nordlund AC, and Marshall L**. Regulation of intracellular acetyl-CoA carboxylase by ATP depletors mimics the action of the 5'-AMP-activated protein kinase. *Biochem Bioph Res Co* 181: 1486-1492, 1991.

121. **Woods A, Vertommen D, Neumann D, Turk R, Bayliss J, Schlattner U, Wallimann T, Carling D, and Rider MH**. Identification of phosphorylation sites in AMP-activated protein kinase (AMPK) for upstream AMPK kinases and study of their roles by site-directed mutagenesis. *The Journal of biological chemistry* 278: 28434-28442, 2003.

122. **Woods AJ, Kantidakis T, Sabe H, Critchley DR, and Norman JC**. Interaction of paxillin with poly(A)-binding protein 1 and its role in focal adhesion turnover and cell migration. *Mol Cell Biol* 25: 3763-3773, 2005.

123. **Worth DC, Hodivala-Dilke K, Robinson SD, King SJ, Morton PE, Gertler FB, Humphries MJ, and Parsons M**. Alpha v beta3 integrin spatially regulates VASP and RIAM to control adhesion dynamics and migration. *J Cell Biol* 189: 369-383, 2010.

124. **Yang XP, Thomas DP, Zhang XC, Culver BW, Alexander BM, Murdoch WJ, Rao MNA, Tulis DA, Ren J, and Sreejayan N**. Curcumin inhibits platelet-derived

growth factor-stimulated vascular smooth muscle cell function and injury-induced neointima formation. *Arterioscl Throm Vas* 26: 85-90, 2006.

125. **Yokote K, Kobayashi K, and Saito Y**. The role of Smad3-dependent TGF-beta signal in vascular response to injury. *Trends Cardiovasc Med* 16: 240-245, 2006.

126. **Yu HW, Liu QF, and Liu GN**. Positive regulation of the Egr-1/osteopontin positive feedback loop in rat vascular smooth muscle cells by TGF-beta, ERK, JNK, and p38 MAPK signaling. *Biochem Bioph Res Co* 396: 451-456, 2010.

127. **Zhang S, Liu Y, Guo S, Zhang J, Chu X, Jiang C, and Zhu D**. Vasoactive intestinal polypeptide relaxes isolated rat pulmonary artery rings through two distinct mechanisms. *J Physiol Sci* 60: 389-397, 2010.

128. **Zhang X, Jiang G, Cai Y, Monkley SJ, Critchley DR, and Sheetz MP**. Talin depletion reveals independence of initial cell spreading from integrin activation and traction. *Nat Cell Biol* 10: 1062-1068, 2008.

129. **Zhuang S, Nguyen GT, Chen Y, Gudi T, Eigenthaler M, Jarchau T, Walter U, Boss GR, and Pilz RB**. Vasodilator-stimulated phosphoprotein activation of serum-response element-dependent transcription occurs downstream of RhoA and is inhibited by cGMP-dependent protein kinase phosphorylation. *The Journal of biological chemistry* 279: 10397-10407, 2004.